



**NUMERICAL SIMULATION ON THE EFFECT OF MIXING THE LPG,  
HYDROGEN, AND DIESEL FUEL ON THE COMBUSTION  
CHARACTERISTIC AND EMISSION LEVELS IN A DIESEL ENGINE**

**By**

**RADHWAN ALI ABD ALREDA**

**Thesis Submitted to the School of Graduate Studies, Universiti Putra Malaysia,  
in Fulfillment of the Requirements for the Degree of Master of Science**

**Jan 2017**

## **COPYRIGHT**

All Material contained within the thesis, including without limitation text, logos, icon, photographs and all other artwork, is copyright material of Universiti Putra Malaysia unless otherwise stated. Use may be made of any material contained within the thesis for non-commercial purposes from the copyright holder. Commercial use of material may only be made with the express, prior, written permission of Universiti Putra Malaysia.

Copyright © Universiti Putra Malaysia

## **DEDICATION**

**To my parents whose support and understanding helped to make this possible**

Abstract of thesis presented to the Senate of Universiti Putra Malaysia in fulfillment of the requirement for the degree of Master of Science

**NUMERICAL SIMULATION ON THE EFFECT OF MIXING THE LPG,  
HYDROGEN, AND DIESEL FUEL ON THE COMBUSTION  
CHARACTERISTIC AND EMISSION LEVELS IN A DIESEL ENGINE**

By

**RADHWAN ALI ABD ALREDA**

**Jan 2017**

**Chairman: Associate Professor Nuraini Abdul Aziz, PhD**

**Faculty: Engineering**

Towards the effort of reducing pollutant emissions, especially nitrogen oxides, and smoke, from the diesel engine direct injection (DI), engineers have proposed various solutions; one of these solutions is the use of alternative gaseous fuel. The utilization of the alternative fuels like liquefied petroleum gas (LPG), hydrogen (H<sub>2</sub>), etc., is a promising approach in decreasing the dependence on petroleum fuels and reducing emission from a diesel engine. However, diesel-H<sub>2</sub> and diesel-LPG dual fuel engine produced many of the unwanted effects such as rapid burning rate, increase diffusivity, and high emission levels. Therefore, researchers started focusing on tri-fuel engines. Hence, LPG addition to the diesel-H<sub>2</sub> operation has the ability to make hydrogen combustion smoother and stable which can prevent imperfect combustion, also lowers the combustion temperature of hydrogen so as to repress NO<sub>x</sub> emission. The mixture of LPG and H<sub>2</sub> may be a potential solution for higher energy and lower emission level.

In the present study, the usage of ANSYS design modular was chosen to create the entire computational domain of the engine and for Computational Fluid Dynamic (CFD) the FLUENT approach was used for Ricardo Hydra diesel engine, a single cylinder engine that operates using the direct injection method. A two-dimensional CFD code was used in the study in order to evaluate the emissions and combustion characteristics of a diesel engine, diesel-LPG, diesel-H<sub>2</sub> under dual-fuel, and diesel-LPG-H<sub>2</sub> under tri-fuel operations, with different air-fuel ratios ( $\lambda$ ) such as 1.2, 1.6, 2, and 2.4. Moreover, torque (20.18 Nm), intake temperature (298 K), and engine speed (2000 rpm) were taken constantly to an atmospheric condition. However, the results for the peak pressure showed an increase when gaseous fuels were added at levels of excess air (1.2, 1.6, and 2). On the other hand, given a ( $\lambda$ ) value of 2.4 for excess air; there is an increase in peak pressure through the addition of hydrogen's limit value, like 50L-50H and 60L-40H. Conversely, a decrease is observed under diesel-H<sub>2</sub> diesel operations and that may be because of the low value of fuels in the air compared with other cases. In addition, the results showed an increase in peak temperature when gaseous fuels (LPG and H<sub>2</sub>) were added at all values of excess air compared with diesel-H<sub>2</sub> for dual mode and diesel-50L-50H for tri-mode. Diesel-LPG-H<sub>2</sub> operations produce lower CO/CO<sub>2</sub> emissions compared to diesel-LPG operation. It also produces lower NO emission compared to diesel-H<sub>2</sub> operation for every value of excess air. Reduced CO/CO<sub>2</sub> emissions were observed at high hydrogen fraction for LPG (50L-50H) for all values of excess air. Consequently, the low hydrogen fraction for LPG (90L-10H) has the capacity to curb uncontrolled hydrogen combustion and limit the increase of NO emission further.

Abstrak tesis yang dikemukakan kepada Senat Universiti Putra Malaysia sebagai memenuhi keperluan untuk ijazah Master Sains

**SIMULASI BERANGKA BAGI KESAN CAMPURAN BAHAN API LPG,  
HIDROGEN DAN DIESEL PADA CIRI PEMBAKARAN DAN KADAR  
PELEPASAN DI DALAM ENJIN DIESEL**

Oleh

**RADHWAN ALI ABD ALREDA**

**Jan 2017**

**Pengerusi: Profesor Madya Nuraini Abdul Aziz, PhD**

**Fakulti: Kejuruteraan**

Ke arah usaha mengurangkan pelepasan bahan pencemar, terutamanya nitrogen oksida dan asap daripada enjin diesel pencucuhan terus, para jurutera telah menyarankan pelbagai penyelesaian; salah satunya adalah penggunaan bahan api alternatif. Penggunaan bahan api alternatif seperti gas petroleum cair (LPG), hidrogen ( $H_2$ ) dan lain-lain, adalah satu pendekatan yang menggalakkan bagi mengurangkan kebergantungan kepada bahan api petroleum dan mengurangkan pelepasan daripada enjin diesel. Walau bagaimanapun, enjin bahan api duaan diesel- $H_2$  dan diesel-LPG memberikan banyak kesan yang tidak diinginkan seperti kadar pembakaran yang cepat, peningkatan daya keresapan dan paras pelepasan yang tinggi. Oleh itu, para penyelidik mula memberi tumpuan kepada enjin tiga bahan api. Justeru, penambahan LPG ke dalam operasi diesel- $H_2$  berupaya membakar hidrogen dengan lebih lancar dan stabil di mana ia boleh menghalang pembakaran tidak sempurna dan juga menurunkan suhu pembakaran hidrogen bagi mengekang pelepasan  $NO_x$ . Campuran LPG dan  $H_2$  berpotensi menjadi penyelesaian untuk menjana tenaga yang lebih tinggi dan paras pelepasan yang lebih rendah.

Dalam kajian ini, penggunaan perisian reka bentuk modular Ansys telah dipilih untuk menghasilkan keseluruhan domain pengiraan bagi enjin manakala bagi Pengiraan Dinamik Bendalir, kod FLUENT telah digunakan pada enjin diesel Ricardo Hydra, enjin satu silinder tunggal yang beroperasi menggunakan kaedah pencucuhan terus. Kod Pengiraan Dinamik Bendalir dua dimensi telah digunakan di dalam kajian ini untuk menilai pelepasan dan ciri-ciri pembakaran daripada operasi enjin diesel, diesel-LPG, diesel-H<sub>2</sub> di bawah bahan api duaan, dan diesel-LPG-H<sub>2</sub> di bawah operasi tiga bahan api, dengan nisbah udara-bahan api ( $\lambda$ ) yang berbeza iaitu 1.2, 1.6, 2, dan 2.4. Tambahan pula, daya kilas (20.18 Nm), suhu pengambilan (298 K), dan kelajuan enjin (2000 rpm) sentiasa ditetapkan pada keadaan atmosfera. Walau bagaimanapun, keputusan bagi tekanan puncak menunjukkan peningkatan apabila bahan api dimasukkan pada paras udara lebihan (1.2, 1.6, and 2). Sementara itu, bagi udara lebihan pada nilai 2.4, terdapat peningkatan pada tekanan puncak melalui penambahan nilai had H<sub>2</sub>, seperti 50L-50H dan 60L-40H. Sebaliknya, penurunan dapat dilihat ketika operasi diesel- H<sub>2</sub> dan hal ini mungkin disebabkan oleh jumlah bahan api di dalam udara yang rendah berbanding dengan kes-kes lain. Di samping itu, keputusan kajian menunjukkan peningkatan suhu puncak apabila bahan api (LPG and H<sub>2</sub>) dimasukkan bagi seluruh nilai udara lebihan, berbanding diesel-H<sub>2</sub> bagi dua mod dan diesel-50L-50H bagi tiga mod. Operasi diesel-LPG-H<sub>2</sub> menghasilkan pelepasan CO/CO<sub>2</sub> yang lebih rendah berbanding operasi LPG-diesel. Pada setiap nilai udara lebihan, diesel-LPG-H<sub>2</sub> turut menghasilkan pelepasan NO yang lebih rendah berbanding operasi diesel-H<sub>2</sub>. Penurunan pelepasan CO/CO<sub>2</sub> dapat diperhatikan pada pecahan H<sub>2</sub> yang tinggi bagi LPG pada semua nilai udara lebihan. Oleh itu, LPG dengan pecahan H<sub>2</sub> yang rendah (90L-10H) berupaya mengawal

pembakaran  $H_2$  yang tidak terkawal dan mengehendkan peningkatan lebih banyak pelepasan NO.



## **ACKNOWLEDGEMENTS**

In the Name of Allah, Most Gracious, Most Merciful, all praise and thanks are due to Allah, and peace and blessings are upon his Messenger. I would like to express the most sincere appreciation to those who made this work possible; supervisory members, and friends.

Firstly, I would like to express my great gratitude to my respected supervisor Associate Professor Dr. Nuraini Abdul Aziz for her invaluable advice and comments, constant encouragement, guidance, support, and patience all the way through my study work. I could not have imagined having a better supervisor for my Master study. Also special thanks to my supervisory committee member, Dr. Abdul Aziz Bin Hairuddin, for his encouragement and helpful advice.

Finally, I should not forget my dear wife who supported me by her wide heart and her pretty patience, as well as my brothers and sisters who have supported me to complete this thesis.

I certify that a Thesis Examination Committee has met on dd<sup>th</sup>mm 2017 to conduct the final examination of Radhwan Ali Abd Al-Reda on his thesis entitled “Numerical Simulation on the Effect of Mixing LPG, Hydrogen, and Diesel Fuel on the Combustion Characteristic and Emission Levels in a Diesel Engine” in accordance with Universities and University Colleges Act 1971 and the Constitution of the Universiti Putra Malaysia [P.U.(A) 106] 15 March 1998. The Committee recommends that the candidate is awarded the Master of Science.

Members of the Thesis Examination Committee were as follows:

**xxx, PhD**

Professor

Faculty of Engineering

Universiti Putra Malaysia

(Chairman)

**xxx, PhD**

Professor

Faculty of Engineering

Universiti Putra Malaysia

(Internal Examiner)

**xxx, PhD**

Professor

Faculty of Engineering

Universiti Putra Malaysia

(Internal Examiner)

**xxx, PhD**

Professor

Faculty of Engineering

Universiti Kebangsaan Malaysia

(External Examiner)

---

**ZULKARNAIN ZAINAL, PhD**

Professor and Deputy Dean

School of Graduate Studies

Universiti Putra Malaysia

Date:

This thesis submitted to the Senate of Universiti Putra Malaysia and has been accepted as fulfilment of the requirement for the degree of Master of Science. The members of the Supervisory Committee were as follows:

**Nuraini Abdul Aziz, PhD**

Associate Professor

Faculty of Engineering

Universiti Putra Malaysia

(Chairman)

**Abdul Aziz Bin Hairuddin, PhD**

Senior Lecturer

Faculty of Engineering

Universiti Putra Malaysia

(Member)

---

**BUJANG BIN KIM HUAT, PhD**

Professor and Dean

School of Graduate Studies

Universiti Putra Malaysia

Date:

## **Declaration by graduate student**

I hereby confirm that:

- this thesis is my original work;
- quotations, illustrations, and citations have been duly referenced;
- this thesis has not been submitted previously or concurrently for any other degree at any other institutions;
- intellectual property from the thesis and copyright of thesis are fully-owned by Universiti Putra Malaysia, as according to the Universiti Putra Malaysia (Research) Rules 2012;
- written permission must be obtained from supervisor and the office of Deputy Vice-Chancellor (Research and Innovation) before thesis is published (in the form of written, printed or in electronic form) including books, journals, modules, proceedings, popular writings, seminar papers, manuscripts, posters, reports, lecture notes, learning modules or any other materials as stated in the Universiti Putra Malaysia (Research) Rules 2012;
- there is no plagiarism or data falsification/fabrication in the thesis, and scholarly integrity is upheld as according to the Universiti Putra Malaysia (Graduate Studies) Rules 2003 (Revision 2012-2013) and the Universiti Putra Malaysia (Research) Rules 2012. The thesis has undergone plagiarism detection software.

Signature: \_\_\_\_\_ Date: \_\_\_\_\_

Name and Matric No: Radhwan Ali Abd Alreda (GS42865)

## **Declaration by Members of Supervisory Committee**

This is to confirm that:

- The research conducted and the writing of this thesis was under our supervision;
- Supervision responsibilities as stated in the Universiti Putra Malaysia (Graduate Studies) Rules 2003 (Revision 2012-2013) were adhered to.

Signature: \_\_\_\_\_  
Name of  
Chairman of  
Supervisory  
Committee: Associate Prof. Dr. Nuraini Abdul Aziz

Signature: \_\_\_\_\_  
Name of  
Member of  
Supervisory  
Committee: Abdul Aziz Bin Hairuddin, PhD

## TABLE OF CONTENTS

	<b>Page</b>
<b>ABSTRACT</b>	i
<b>ABSTRAK</b>	iii
<b>ACKNOWLEDGEMENTS</b>	vi
<b>APPROVAL</b>	vi
<b>DECLARATION</b>	viii
<b>LIST OF TABLES</b>	xiii
<b>LIST OF FIGURES</b>	xiv
<b>LIST OF ABBREVIATIONS</b>	xvii
<b>CHAPTER</b>	<b>1</b>
<b>1 INTRODUCTION</b>	<b>1</b>
1.1 Background	1
1.2 Problem Statement	4
1.3 Research Objectives	5
1.4 Hypothesis	5
1.5 Scope of Study	5
1.6 Thesis Layout	6
<b>2 LITERATURE REVIEW</b>	<b>8</b>
2.1 Overview	8
2.2 Alternative Fuels	8
2.2.1 Hydrogen (H <sub>2</sub> )	8
2.2.2 Liquid Petroleum Gas (LPG)	9
2.3 Emission and Performance	14
2.3.1 Effect of LPG addition on Performance	14
2.3.2 Fuel Consumption	16
2.3.3 Particular Matter (PM)	17
2.3.4 Nitrogen Oxides (NO <sub>x</sub> )	19
2.3.5 Unburned Hydrocarbons	21
2.3.6 Carbon Monoxide	22
2.4 Effect of addition LPG, Hydrogen, and Diesel blend	24
2.5 Previous Numerical Simulation Studies	26
2.5.1 Turbulence Modeling	27
2.5.2 Ignition Delay (Autoignition) Modeling	28
2.5.3 Atomization Models	30
2.5.4 Emissions of Dual Fuel Engine	31
2.6 Summary	34
<b>3 METHODOLOGY</b>	<b>36</b>
3.1 Overview	36
3.2 Data and Initial Condition	37
3.3 Design of Research Flows Chart	41
3.4 Grid Generation	42
3.4.1 Initial Grid Generation	42

3.4.2	Moving Dynamic Mesh	43
3.5	Boundary Condition and Fluid Properties	45
3.6	Numerical Methods	46
3.6.1	Equation of Motion	46
3.6.2	Fluent Solver	48
3.6.3	Discretization	49
3.6.4	Pressure Interpolation Schemes	50
3.6.5	Pressure-Velocity Coupling	50
3.6.6	The Under Relaxation Factors	51
3.6.7	Iteration Residual and Time Steps	51
3.6.8	Phenomena Simulated	52
3.7	Chemical Reaction Modeling	53
3.7.1	The Finite-Rate/Eddy-Dissipation Model	53
<b>4</b>	<b>RESULTS AND DISCUSSION</b>	<b>55</b>
4.1	Overview	55
4.2	Mesh Independent Test	55
4.3	Validation Model	57
4.4	Verification of Emissions	58
4.5	The Effect of LPG and Hydrogen Percentage Variation	59
4.5.1	Combustion Characteristics	59
4.5.2	Emissions	72
4.6	Summary	94
<b>5</b>	<b>CONCLUSION AND RECOMMENDATIONS</b>	<b>96</b>
5.1	Conclusions	96
5.2	Recommendation for Future Research	98
	<b>REFERENCES</b>	<b>99</b>
	<b>APPENDICES</b>	<b>108</b>
	<b>BIODATA OF STUDENT</b>	<b>111</b>
	<b>LIST OF PUBLICATIONS</b>	<b>112</b>

## LIST OF TABLES

<b>Table</b>	<b>Page</b>
3.1: Engine Specification (Wannatong et al., 2007)	38
3.2: Test Cases	38
3.3: Percentage Variation of LPG and Hydrogen	39
3.4: The Specifications of Diesel Fuel (Wannatong et al., 2007)	46
4.1-a: The development of average temperature under 1.2 excess air and different ratio of gaseous fuel	68
4.1-b: The development of average temperature under 1.6 exceeds air and different ratio of gaseous fuel	69
4.1-c: The development of average temperature under 2 excess air different ratio of gaseous fuel	70
4.1-d: The development of average temperature under 2.4 excess air different ratio of gaseous fuel	71
4.2-a: The development of NO mass fraction of pollutant under 1.2 excess air and different ratio of gaseous fuel	75
4.2-b: The development of NO mass fraction of pollutant under 1.6 excess air and different ratio of gaseous fuel	77
4.2-c: The development of NO mass fraction of pollutant under 2 excess air and different ratio of gaseous fuel	78
4.2-d: The development of NO mass fraction of pollutant under 2.4 excess air and different ratio of gaseous fuel	80
4.3-a: The development of CO mass fraction under 1.2 excess air and different ratio of gaseous fuel	84
4.3-b: The development of CO mass fraction under 1.6 excess air and different ratio of gaseous fuel	85
4.3-c: The development of CO mass fraction under 2 excess air and different ratio of gaseous fuel	86
4.3-d: The development of CO mass fraction under 2.4 excess air and different ratio of gaseous fuel	87



4.4-a:	The development of CO <sub>2</sub> mass fraction under 1.2 excess air and different ratio of gaseous fuel	91
4.4-b:	The development of CO <sub>2</sub> mass fraction under 1.6 excess air and different ratio of gaseous fuel	92
4.4-c:	The development of CO <sub>2</sub> mass fraction under 2 excess air different ratio of gaseous fuel	93
4.4-d:	The development of CO <sub>2</sub> mass fraction under 2.4 excess air different ratio of gaseous fuel	94
A.1:	Gaseous Fuel Properties	110
A.2:	Mass Fraction of LPG, H <sub>2</sub> , O <sub>2</sub> , and N <sub>2</sub>	111

## LIST OF FIGURES

Figure		page
2.1:	LPG diesel dual fuel engine (Ogawa et al., 2001)	13
2.2:	Variation of fuel conversion efficiency vs. engine load for LPG blends (Saleh, 2008)	15
2.3:	Variations of BTE vs. load (Rosha et al., 2014)	16
2.4:	Specific energy consumption (g/kWh) vs. load (PFI LPG-diesel) (Jian et al., 2001)	17
2.5:	Smoke emissions of diesel and two different LPG-diesel blends vs. BMEP and engine speed (Donghui et al., 2005)	19
2.6:	Smoke emissions for different fuel blends and engine speed vs. load (Qi et al., 2007)	19
2.7:	Variation of NO <sub>x</sub> concentration with engine load for LPG blends (Saleh, 2008)	20
2.8:	Variation of nitrogen oxide under Diesel and blended fuels operation vs. load at 1500 and 2000 r/min engine speed (Qi et al., 2007)	21
2.9:	HC emissions (ppm) vs. engine speed and loads for different diesel /LPG blends and net diesel (Donghui et al., 2005)	22
2.10:	Variation of CO concentration with engine load for LPG blends (Saleh, 2008)	23
2.11:	CO emissions (ppm) vs. engine speed and loads for different diesel /LPG blends and net diesel (Donghui et al., 2005)	24
2.12:	Comparison of brake thermal efficiency for the cases II, III and IV at 80% load condition (Lata et al., 2012)	25
2.13:	Unburnt HC (g/kW h) vs. diesel + gaseous fuels substitution (%) (Lata et al., 2012)	25
2.14:	Variation of NO <sub>x</sub> emissions with relative air-fuel ratio (Choi et al., 2005)	26
2.15:	In-cylinder pressure for Z=87% by k- $\epsilon$ standard and k- $\epsilon$ RNG (Ghiji, 2011)	28
2.16:	In-cylinder pressure curves under different ratio of gaseous addition (Alrazen et al., 2015)	29

2.17:	In-cylinder pressures by varying the $B_i$ constant (Abagnale et al., 2014)	31
2.18:	Emission characteristics of diesel and methanol blends (Soni and Gupta, 2016)	32
2.19:	Comparison between predicted CO, NO <sub>x</sub> and UHC emissions at part and full load (Mousavi et al., 2016)	33
2.20:	NO emission with various diesel content (Mansor et al., 2017)	33
3.1:	Steps of CFD analysis	37
3.2:	Computational approach flow chart	41
3.3:	The Geometry and Mesh at TDC	42
3.4:	Computational geometry with defined zones	43
3.5:	Layering and Re-meshing methods tested for computational model	44
4.1:	(a) Fine sector meshes (20921 cells) and (b) medium (10980 cells) at (TDC) used in 2D-CFD simulations	56
4.2:	In-cylinder pressure for typical grid dependency test	56
4.3:	Validation of 2D simulation for diesel fuel in-cylinder pressure at 2000 rpm engine operation mode	58
4.4:	Verification of the NO <sub>x</sub> emission under diesel-H <sub>2</sub> dual fuel engine operation	59
4.5:	Effect of different ratio of gaseous fuel on peak in-cylinder pressure	60
4.6-a:	In-cylinder pressure curves at 1.2 excess air and different ratio of gaseous fuel	61
4.6-b:	In-cylinder pressure curves at 1.6 excess air and different ratio of gaseous fuel	62
4.6-c:	In-cylinder pressure curves at 2 excess air and different ratio of gaseous fuel	63
4.6-d:	In-cylinder pressure curves at 2.4 excess air and different ratio of gaseous fuel	64
4.7:	Effect of different ratio of gaseous fuel on peak in-cylinder temperature	65
4.8-a:	Temperature curves under 1.2 excess air and different ratio of gaseous fuel	68
4.8-b:	Temperature curves under 1.6 excess air and different ratio of gaseous fuel	69

4.8-c:	Temperature curves under 2 excess air and different ratio of gaseous fuel	70
4.8-d:	Temperature curves under 2.4 excess air and different ratio of gaseous fuel	71
4.9:	Effect of different ratio of gaseous fuel on peak NO emissions	72
4.10-a:	NO emissions curves under 1.2 excess air and different ratio of gaseous fuel	75
4.10-b:	NO emissions curves under 1.6 excess air and different ratio of gaseous fuel	76
4.10-c:	NO emission curves under 2 excess air and different ratio of gaseous fuel	78
4.10-d:	NO emission curves under 2.4 excess air and different ratio of gaseous fuel	79
4.11:	Effect of different ratio of gaseous fuel on peak CO emissions	81
4.12-a:	CO emissions curves under 1.2 excess air and different ratio of gaseous fuel	84
4.12-b:	CO emissions curves under 1.6 excess air and different ratio of gaseous fuel	85
4.12-c:	CO emissions curves under 2 excess air and different ratio of gaseous fuel	86
4.12-d:	CO emissions curves under 2.4 excess air and different ratio of gaseous fuel	87
4.13:	Effect of different ratio of gaseous fuel on peak CO <sub>2</sub> emissions	88
4.14-a:	CO <sub>2</sub> emissions curves under 1.2 excess air and different ratio of gaseous fuel	90
4.14-b:	CO <sub>2</sub> emissions curves under 1.6 excess air and different ratio of gaseous fuel	91
4.14-c:	CO <sub>2</sub> emissions curves under 2 excess air and different ratio of gaseous fuel	92
4.14-d:	CO <sub>2</sub> emissions curves under 2.4 excess air and different ratio of gaseous fuel	93

## LIST OF ABBREVIATIONS

BTE	Brake Thermal Efficiency
AFR <sub>st</sub>	Stoichiometric Air to Fuel Ratio
A/F	Air Fuel Ratio
BDC	Bottom Dead Center
2D	2-Dimensional
BSEC	Brake Specific Energy Consumption
EGR	Exhaust Gas Recirculation
CFD	Computational Fluid Dynamics
CAD	Crank Angle Degree
CI	Compression Ignition
SI	Spark Ignition
LPG	Liquefied Petroleum Gas
CO <sub>2</sub>	Carbon Dioxide
CNG	Compressed Natural Gas
CO	Carbon Monoxide
PM	Particulate Matter
C <sub>3</sub> H <sub>8</sub>	Propane
H <sub>2</sub>	Hydrogen
EVC	Exhaust Valve Close
EVO	Exhaust Valve Open
IC	Internal Combustion
HC	Hydrocarbons
MDM	Moving Dynamic Mesh
IVC	Intake Valve Close

IVO	Intake Valve Open
TAB	Taylor Analogy Breakup
DPM	Discrete Phase Model
DI	Direct Injection
OCC	Omega Combustion Chamber
NO <sub>x</sub>	Nitrogen Oxides
NO	Nitric Oxide
N <sub>2</sub> O	Nitrous Oxide
NO <sub>2</sub>	Nitrogen Dioxide
TDC	Top Dead Center
NG	Natural Gas
PISO	Pressure-Implicit with Splitting of Operators
RNG	Re-Normalized Group
$\lambda$	Excess Air ( $1/\phi$ air-fuel ratio)
$\dot{m}$	Mass Flow Rate
X	Mass Fraction of Fuels

## CHAPTER 1

### INTRODUCTION

#### 1.1 Background

The use of gaseous fuels for internal combustion engines have long been suggested as a potential way to maintain engine efficiency and performance while reducing emissions (Xu et al., 2010). These days, studies on various alternative fuels for diesel engines have been conducted with the goal of reducing diesel fuel consumption as well as particulate and nitrogen oxide (NO<sub>x</sub>) emissions. Therefore, Liquefied petroleum gas (LPG) has been suggested as one of the most suited alternative fuels that work not only as a petroleum fuel replacement but also as an alternative that is able to lower smoke, NO<sub>x</sub> and particulate matter emissions (Jothi et al., 2007). Therefore, development of LPG vehicles is being undertaken in order to come up with a vehicle that is economical and results in lower pollution levels. This interest has led several researchers works on the utilization of LPG mixtures with a number of new fuels in diesel engines. Vijayabalan and Nagarajan, (2009) modified a vertical, single cylinder air-cooled diesel engine so that it can take LPG in dual fuel mode. They then studied the engine's emission, performance, and combustion characteristics. LPG was prepared to combine with air before being compressed and ignited using a minimal pilot spray of diesel. The resulting of dual fuel engine exhibited reduced amounts of oxides of nitrogen and smoke given at the whole load condition range. However, because of poor ignition, it showed higher carbon monoxide and hydrocarbon emissions with poor brake thermal efficiency under lower load conditions. To improve the lower load performances, a glow plug was introduced inside the combustion chamber. There was a 3% improvement in the brake thermal efficiency and carbon

monoxide, hydrocarbon, and smoke emissions were reduced by 50%, 69%, and 9%, respectively, under lower load condition. However, the NO<sub>x</sub> emission was unaffected by the glow plug's presence. Ganesan (2002) modified a normal diesel engine in order for it to operate in dual fuel mode using diesel as a pilot fuel and LPG as the primary fuel. The experiments were conducted to observe the engine's combustion parameters, brake thermal efficiency, and emission for various diesel substitutions. The higher combustion level resulted in an increase in brake thermal efficiency from 35% for the diesel mode to up to 37% in dual fuel mode under a full load state. It was also observed that in the dual fuel mode, the NO<sub>x</sub> ranks decrease was up to 60% under a full load state. The ignition delay period increase by two degrees of crank angle while there was a decrease in the peak pressure under light diesel and high load substitutions conditions.

Additionally, due to its availability and emission considerations, hydrogen has been suggested as another good alternative fuel for internal combustion engines. Hence, hydrogen has the capacity to improve engine efficiency while reducing emissions (Saravanan et al., 2008). Hydrogen's combustion characteristics differ from hydrocarbon fuels since it has a wider flammability range, rapid combustion, and higher adiabatic flame temperature. Hydrogen is considered a clean fuel since it does not produce dangerous exhaust gasses like unburned hydrocarbon, particulate matter, and carbon monoxide (CO) and it does not release greenhouse gasses such as carbon dioxide (CO<sub>2</sub>) (Mansour et al., 2001). Thus, the interest for diesel-H<sub>2</sub> dual-fuel engines has considerably increased in recent years (Bose and Banerjee, 2012). Gatts et al., (2010) studied the combustion efficiency of hydrogen by examining the amount of unburned hydrogen that was observable through the exhaust gas. These studies revealed that hydrogen combustion efficiency depended on the engine load. When



operating under high load states, hydrogen has to be added in order to achieve high efficiencies for both hydrogen and diesel fuels. Liew et al., (2012); Lilik et al., (2010) demonstrated that HC/CO/CO<sub>2</sub>/PM emissions were decreased in an almost linear pattern when hydrogen addition was increased. This also indicated that decreases in particle and carbon-based gaseous emissions were affected by the amount of hydrogen being added. Under low to middle load states, there was a decrease in NO<sub>x</sub> emission. However, at high load state, NO<sub>x</sub> emission increased because of hydrogen's fast burning level that resulted in higher combustion temperatures and enhanced NO<sub>x</sub> formation (Ghazal, 2013b). Miyamoto et al., (2011) suggested that thermal efficiency was affected by factors such as engine load, speed, and the amount of hydrogen that was added.

However, the works mentioned above only conducted studies on the use of either LPG or H<sub>2</sub> as a secondary fuel, researchers started focusing on tri-fuel engines. Recently, Lata and Misra, (2011); Lata et al., (2012) conducted some experimental and theoretical investigations to evaluate the performance of a dual fuel engine that used a mixture of LPG-H<sub>2</sub> as the main fuel and the diesel fuel as a pilot fuel. As a result, these studies revealed that efficiency could be improved at low load condition states in a dual fuel operation as well as the emissions improved when hydrogen and LPG are mixed to serve as the secondary fuel. On the other hand, the mixture of LPG and H<sub>2</sub> may be a potential solution for higher energy and lower emission level.

This study will compare the emissions features and combustion characteristics. As well as, different fuel configuration in diesel engines using normal diesel fuel, diesel-LPG, diesel-H<sub>2</sub> dual fuel, and diesel-LPG-H<sub>2</sub> tri-fuel under different gasses substations and different excess of air.

## 1.2 Problem Statement

Diesel engines are the most popular engines as it has high energy power, durability, and low CO emission (Stavinoha et al., 2000). However, the main problem with most of the vehicles nowadays is the emission of Nitrogen Oxides ( $\text{NO}_x$ ) which can be controlled by different methods such as exhaust gas recirculation and use of alternative gasses fuels (Renald and Somasundaram, 2012). Therefore, using alternative gasses fuels for the modified diesel engine are receiving more interest from many scientists due to many reasons including the national concerns of the liquid fuels limited resources, the environment advantage and the needs to use a reliable, durable, and efficient engine (Elnajjar et al., 2011). However, diesel- $\text{H}_2$  and diesel-LPG dual fuel engine produced many unwanted effects such as rapid burning rate, increased diffusivity, and high emission levels (Lata et al., 2012; Miao et al., 2014). Therefore, researchers started focusing on tri-fuel engines. Thus, the mixture of LPG and  $\text{H}_2$  may be a potential solution for high energy and low emission level (Aravind et al., 2015; Miao et al., 2014). Since hydrogen has wide flammability limits while the LPG has low flame propagation speed and narrow flammability limits (Lata et al., 2011). As a result, hydrogen enrichment enhances the process of LPG combustion such as enhance the efficiency and reduced the emissions. As well as, the advantage with LPG presence is to improve hydrogen combustion by avoiding uncontrolled combustion, such as the sharp increase of peak in-cylinder pressure and temperature. It seems that LPG and  $\text{H}_2$  are complementary with each other on reducing  $\text{CO}_2/\text{CO}$  emissions and enhanced the engine efficiency (Miao et al., 2014). Consequently, better performance engine could be obtained when  $\text{H}_2$  is added with LPG to make a secondary fuel for diesel dual fuel engine (Lata et al., 2012).

### **1.3 Research Objectives**

The aim of the current study is to simulate diesel, dual and tri-fuel diesel engine consists of LPG, hydrogen, and diesel. Consequently, the specific objectives are as follow:

- 1- Examine the combustion characteristics and emissions of a compression ignition engine under different gasses fuel substations and different excess air.
- 2- Evaluate the best ratio of a gasses fuel under dual and tri-fuel conditions, give the best reduction in the emissions.

### **1.4 Hypothesis**

- The commercial CFD code can predict accurate results to simulate the phenomena inside a dual fuel engine in comparison with published experimental data (Wannatong et al., 2007).
- RNG k- $\epsilon$  turbulence model can give more accurate results than Standard k- $\epsilon$  turbulence model.
- The mixture of LPG with hydrogen is expected to enhance the lean-burn characteristics in addition to decreasing the real engine's emission (CO and CO<sub>2</sub>), but the probability including higher NO<sub>x</sub> emission will be involving concern (Lata et al., 2012).

In this study, a two Dimensional simulation for the dual and tri-fuel engine has been performed by commercial computational fluid dynamic (CFD) approach. The achieved results from the simulations have been compared with the experimental data to validate the computer simulation against the diesel engine test. This study aims to prove that a computational fluid dynamic (CFD) analysis can be used to simulate 2-D fluid flow in diesel dual Fuel Engine.

## **1.5 Scope of Study**

The focus of the present study was on the effect of the different value of excess air ( $\lambda$ ) and the different mixing ratio of gaseous fuel substitutions namely LPG, hydrogen with normal diesel fuel on combustion characteristics and emissions in the dual and tri-fuel engine. These two parameters are considered for overcoming the high emission levels from a diesel engine and improving the efficiency by mixing the gaseous fuel in a diesel engine. The scope of this study is to examine the engine characteristics (in-cylinder pressure and temperature) as well as the emissions ( $\text{NO}_x$ , CO, and  $\text{CO}_2$ ) under diesel, dual and tri-fuel engine. Also, an effort has been done to illustrate the distribution and formation region for in-cylinder temperature and emissions at various crank angle degree in the combustion chamber of the engine with two-dimensional analysis for better understanding the behavior of gaseous distribution in the combustion chamber. This study is limited to the numerical analysis of normal diesel, dual and tri-fuel engine under different gasses fuel substitutions and a different value of excess air in a constant engine speed, pressure, and temperature to examine the engine characteristics and emissions.

## **1.6 Thesis Layout**

This thesis has been systematized into five chapters; the thesis begins with the introduction in Chapter 1 which includes a background of dual fuel engine. Then, it is followed by the problem statement. After that, the objective and scope of the study are presented.

Chapter 2 explains benefits for using alternative fuels as well as explains the combustion process of dual fuel engine and the effect of addition LPG and hydrogen

on performance, combustion, and emission. Then, the previous numerical simulation studies and their results have been considered.

Chapter 3 illuminates the methodology that utilized includes an explanation of the grid generation for the diesel engine by using the ANSYS design modular that generated the needed mesh from moving dynamic mesh model (MDM), defines the boundary condition, and sets the solver variables in the software fluent.

Chapter 4 illustrates the results, which has attained from CFD simulation and the corresponding discussions.

Chapter 5 presents the conclusion of this research and the recommendation for future studies.

## CHAPTER 2

### LITERATURE REVIEW

#### 2.1 Overview

The energy amount in the world is affected by various factors like the increase in per capita energy consumption, economic growth, and the increase of world population. Furthermore, this increase in energy consumption raises two major problems; increasing energy prices due to the limitations of energy sources and environmental pollution due to intensive use of energy (Ugurlu and Oztuna, 2015). Motor vehicles utilize a large part of the global energy consumed. These motor vehicles operate mainly by diesel and gasoline fuel obtained from crude oil that is a formula of energy with limited reserves and that need to be resolved since they might lead to difficulties all around the world in future (Agarwal, 2007; Yamik, 2002). Therefore, using gaseous fuel along with the liquid diesel in CI engine is one of the ways to resolve this issue (Xu et al., 2010). Thus, the utilization of alternative gas fuels like liquefied petroleum gas (LPG), natural gas (NG), hydrogen (H<sub>2</sub>), etc. is a promising approach in decreasing the dependence on liquid fuels and decreasing the emission pollutants from a diesel engine (Lim et al., 2015; Selim et al., 2009). The aim of this review chapter is to make an overview of the effect of alternative fuels enrichment such as LPG and H<sub>2</sub> in diesel engines on emissions and performance.

#### 2.2 Alternative Fuels

High emissions, such as nitric oxides, hydrocarbons, carbon monoxide, and carbon dioxide, have been produced from the engine operated by using petroleum and this problem is still faced by researchers (Akansu et al., 2007). The environment is polluted

through these emissions. Alternative fuel is one of new technologies to decrease the emissions in the CI engine. Natural gas, methanol, and propane had been used in 2000 as alternative fuels for automobiles (Ferguson and Kirkpatrick, 2015; Zhou et al., 2014). Due to their clean burning nature and their increasing utilization in the automobile industry, alternative fuels might be termed as future fuels. Therefore, LPG, H<sub>2</sub>, and mixtures of LPG and H<sub>2</sub> were taken into consideration as alternative fuels in latest years in order to limit the pollution of vehicles (Aravind et al., 2015; Lata and Misra, 2012; Lata et al., 2012; Miao et al., 2014).

### **2.2.1 Hydrogen (H<sub>2</sub>)**

Hydrogen is one of the most renewable promising fuels since it is naturally available on the earth and can be produced from fossil or non-fossil sources (Najjar, 2013; Yang et al., 2015). Hydrogen is considered being the exceptional additive candidate to be blended into diesel in order to enhance the performance of the engine. Furthermore, faster combustion approximates constant volume leading to an extension in the efficiency of the engine (Ghazal, 2013; Yang et al., 2015). However, the significant shortcomings of using hydrogen as a fuel are excessive in-cylinder peak temperatures and pressure, higher emissions (NO<sub>x</sub>), combustion knocking, and high self-ignition temperature (Adnan et al., 2012; Ghazal, 2013). In contrast with diesel, hydrogen can be consumed as the only fuel in an SI engine; however, it cannot be employed in a CI engine due to the fact of its higher ignition point (Saravanan and Nagarajan, 2008). Therefore, H<sub>2</sub> used in diesel is modified as primary fuel and diesel as pilot fuel. Due to safety reasons, the usage of hydrogen in IC engine requires more attention. Because of the combustion characteristics of hydrogen are altered from those of hydrocarbon fuels which include rapid combustion and a wide range of flammability (Mansour et al., 2001).

## **A. The Effect of Hydrogen-Hydrocarbon Mixtures**

Recently, hydrogen-hydrocarbon mixtures have received more attention as alternative fuels for IC engine. Therefore, the addition of hydrogen to regular hydrocarbon fuels was suggested as a technique to improve the performance and the emissions from IC engine (Choudhuri and Gollahalli, 2003). Therefore, numerous researchers have suggested hydrogen addition to normal diesel fuel and another hydrocarbon such as LPG, NG, etc., in the internal combustion compression-ignition engine as a method to improve the performance of diesel engines (Lata et al., 2012). This is because the H<sub>2</sub> reduces the period of combustion and rises the H/C ratio of the whole fuel and that led to reducing the emissions such as carbon monoxide. Since hydrogen's high speed in terms of flame propagation( Antunes et al., 2009; Yasiry and Shahad, 2016). The small quantities of hydrogen fuel injection to a diesel engine can decrease the heterogeneity of a diesel fuel spray. Subsequently, this allows improving the combustible mixture to be premixed with air with more uniformity (Szwaja et al., 2009).

### **2.2.2. Liquid Petroleum Gas (LPG)**

LPG is a gas that is odorless and colorless and mainly consists of butane and propane or a combination of both in different ratios as a mixture. It is possible to store LPG as a mixture or separately. They exist as the gas at a normal atmospheric pressure and room temperature (Demirbas, 2002). The LPG standard is not universally observed. The propane concentration is as low as 50% and as high as 100% at particular locations. There is a significant difference in the usage of LPG as an automotive fuel from one country to another depending on the availability and cost of the fuel relative to alternative fuels particularly diesel and petrol. Having knowledge about the liquid petroleum gas' composition has great importance in the analysis of the differing



compositions that have a significant impact on the combustion process and to improve the exhaust emission quality while maintaining high thermal efficiency (Saleh, 2008).

#### **A. Advantages and Disadvantages of using LPG in Diesel Engine**

Significantly less nitrogen oxides (NO<sub>x</sub>), and less particulate matter is emitted by LPG in comparison to a diesel engine (Thomas Renald and Somasundaram, 2012).

However, LPG has its own set of advantages along with the disadvantages.

##### **▪ Advantages of using LPG Fuel in Vehicles:**

1. LPG is an economical fuel which is almost twice less in term of the price compared to the diesel and petrol (Katinas and Savickas, 2012; Ugurlu and Oztuna, 2015).
2. LPG has a high calorific value and good anti-knock properties since it has a high octane rating (Chaichan, 2011).
3. Entering the combustion chamber in the gas phase completely, LPG does not cause the dilution of the engine oil and leaves no residue. Therefore, it results in lower maintenance costs (Karamangil, 2007).
4. A clean combustion is provided by these two characteristics. Initially, LPG fuels are hydrogen-rich and they enter into the cylinders in the gas phase. Therefore, lower NO<sub>x</sub>, HC, and CO emission are emitted by vehicles that utilize LPG in comparison with diesel-fueled vehicles (Díaz et al., 2000; Klausmeier and Billick, 1993).
5. Sufficient numbers of LPG filling stations can be found in various countries (Katinas and Savickas, 2012).

▪ **Disadvantages of LPG Fuel:**

1. The conversion of vehicles to LPG needs a certain cost (Chaichan, 2011).
2. In faulty LPG system installations, the fuel consumption and exhaust emissions increase (Ugurlu and Oztuna, 2015).
3. Because LPG is an explosive and flammable gas, it poses a danger in accidents, although the rates are low (Ugurlu and Oztuna, 2015).

Despite the disadvantages of LPG, its advantages are more significant. However, the modification of the diesel engine to operate on diesel-LPG (dual-fuel engine) is illustrated, provided, and discussed in the following section.

**B. Diesel Engine Modifications**

Configuring diesel engines to run on diesel-LPG dual fuel engine can be done with simple methods. In these engines, the LPG is mixed in the air intake whereas in an ordinary diesel fuel it is injected through an injection system, with a specific degree of diesel supplied; however, at a decreased rate (Ergenç and Koca, 2014; Goldsworthy, 2012). Engine modifications are necessary in order for the engine to work in dual mode through the attachment of an LPG line to the intake manifold beside an evaporator (Sproat et al., 2006). Through the regulating valve, the gaseous fuel flows into the gas mixer which is placed on and connected to the intake manifold (Bora et al., 2013; Paykani, 2011; Rao et al., 2010). LPG is supplied to the engine with accompanying electronic or mechanical controls for different engine speeds and loads. The engine output and combustion process differ based on the engine type and the type of gaseous fuel supply system (port injection or direct injection). The LPG's mass flow rate is in proportion to the difference of the pressure between a gas mixer and the evaporator where the pressure is retained and kept almost equal to the atmospheric

pressure. However, in LPG dual fuel engines, it is very crucial to control the pilot diesel and primary LPG's flow rate at various operating conditions of the engine. Therefore, the Performance improvement and smoke emission reduction might not be affected by lower LPG content. Though, much higher LPG content is likely to rapidly enhance the in-cylinder pressure and damage the engine (Jian et al., 2001).

Numerous revision have been carried out in the diesel-LPG dual fuel engines by various researchers, such as the adjustment of single cylinder (Murthy et al., 2012; Rao et al., 2011) and multi-cylinder (Stewart et al., 2007) diesel engines in which the LPG is supplied in the dual fuel mode by manifold injection (Raslavičius et al., 2014; Wattanavichien, 2011) and manifold induction (Kaleemuddin and Rao, 2009; Murthy et al., 2012). It was found that the combustion, performance and emission characteristics of diesel-LPG dual fuel engine depend on the type of the engine, LPG fuel supply system, and engine operating conditions.

### **C. LPG-Diesel Dual Fuel Operation**

The entire internal combustion reciprocating engines use the same basic process to operate. Firstly, a combustible mixture is compressed in a small volume between the head of a piston and its surrounding cylinder. Then the mixture is ignited and the piston is pushed through the cylinder by the force that results from the combustion. Two ignition methods are used in reciprocating IC engines which are spark ignition (SI) and compression ignition (CI). The compression ignition (CI) method is the current operation method of the diesel engine where the intake air is compressed alone and the fuel is injected and introduced directly at high pressure at the end of the stroke of the compressed air that is in the combustion chamber resulting in an easy ignition through its ignition temperature. However, concepts of both spark ignition and compression ignition

principles are used in diesel-LPG dual fuel engine in burning the mixture of liquid pilot fuel and primary gaseous (LPG) fuel (Chatlatanagulchai et al., 2010; Ramos et al., 2012). In diesel-LPG dual fuel engine, the LPG/air mixture is drawn into the cylinder from the intake manifold, the same way as the spark-ignited engine; and to increase the pressure and temperature, the mixture is compressed. The ignition of the mixture occurs at the end of the compression stroke by means of injecting small amounts of pilot diesel fuel as illustrated in Figure 2.1. This pilot diesel fuel injection operates as an ignition source. The LPG gas-air mixture within the injected diesel spray's vicinity ignites at different places and establishes some flame-fronts. This results in the rapid and smooth start of the combustion. It is worth noting that the combustion begins in the way similar to the CI in a dual-fuel engine; however, it propagates through flame a front that is in a way similar to SI engine. The engine's power output is usually controlled by altering the quantity of primary LPG gaseous fuel that is added to the inlet manifold. The amount of diesel fuel used will differ based on the design parameters and operating conditions of the engine. Generally, the pilot diesel quantity required for ignition is 10% to 20% of operation on the diesel fuel alone at normal working loads (Pal and Tiwari, 2013; Sahoo et al., 2009).

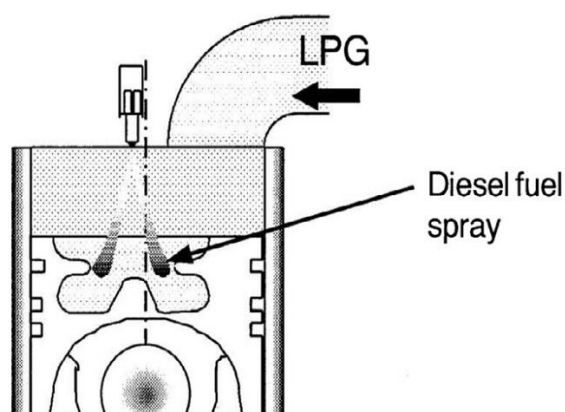


**Figure 2.1: LPG diesel dual fuel engine (Ogawa et al., 2001)**

## **2.3 Emissions and Performance**

Using gaseous fuels together with diesel in compression-ignition engines is thought to be a proper alternative for the existing stationary, maritime, and automotive engines. It is believed that economic and environmental advantages can be provided through this application (Ashok et al., 2015). As a result, the impacts of using diesel-gaseous fuel in dual-fuel engines have been widely examined in various studies. The studies were carried out on carrying test engines with different gaseous fuel types as well as different operating points. These studies evaluate the performance as well as the engine-out emission like particulate matters, nitrogen oxides, unburned hydrocarbons, and carbon monoxide.

### **2.3.1 Effect of LPG addition on Performance**

High thermal efficiency can be provided by dual fuel that operates with LPG, which is almost comparable to that of the same engines, which operate on diesel fuel at higher loads. Furthermore, engine emissions and performance deteriorate at low loads in a dual-fuel mode operation. The most important reason for the poor performance at low loads is the induction of significantly lean LPG-air mixtures in a dual-fuel engine case. These lean mixtures ignite with difficulty and burn slowly at low loads. The flame propagation is incomplete in these mixtures and the bulk of gas fresh air mixture remains unburnt which leads to high HC emission and worse brake thermal efficiency (Pirouzpanah et al., 2007; Poonia et al., 2011).

Moreover, a number of experimental and theoretical investigations were conducted to study an diesel-LPG dual-fuel engine's performance at different LPG compositions, like propane to butane ratio (Elnajjar et al., 2013a; Elnajjar et al., 2013b; Lee et al., 2013; Leermakers et al., 2011; Saleh, 2008). Saleh (2008) investigated five different LPG fuel

compositions to understand the impact of LPG-fuel composition on the exhaust emissions and performance of the engine in a twin cylinder dual-fuel engine. Figure 2.2 shows the comparison between the impacts of different engine loads on the thermal conversion efficiency of the pure propane (fuel #1) and different LPG blends in dual fuel operation. It can be observed that the efficiency enhances with an increase in the load for all the different LPG blends. The behavior of three LPG mixtures was very similar, and the thermal conversion efficiency of pure propane (fuel #1), (fuel #2 of 10% butane), and fuel (#3 of 30% butane) do not have noticeable or obvious difference at full load; however, the thermal conversion efficiency of ( fuel #3 ) was 3% lower than that of the pure propane at 25% load. In comparison to Fuel #1, fuel #4 of 50% butane, and fuel #5 of 70% butane had lower thermal conversion efficiency at full load by almost 2% and 3% respectively. Rosha et al., (2014) conduct that the thermal efficiency for diesel-LPG at low load was lower than diesel fuel at same load by 11%. Conversely, the efficiency at high load for the diesel-LPG was more than diesel by 29%. On the other hand, at part loads, the efficiency was increased in the case of the EGR-operated engine due to re-burning of hydrocarbons that enter the combustion chamber as illustrated in Figure 2.3.

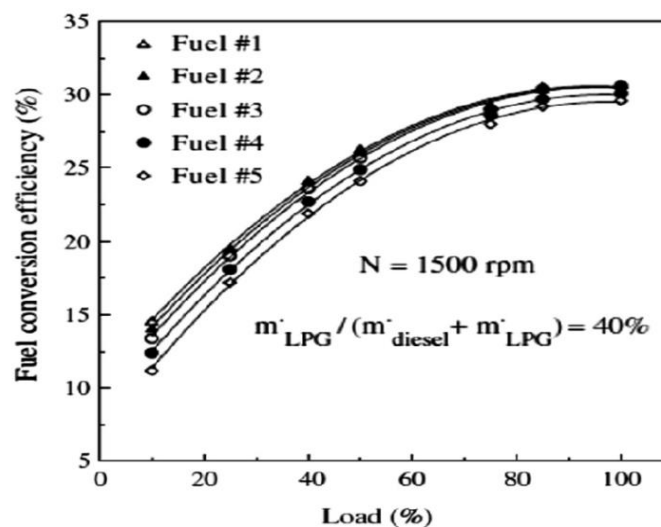


**Figure 2.2: Variation of fuel conversion efficiency vs. engine load for LPG blends (Saleh, 2008)**

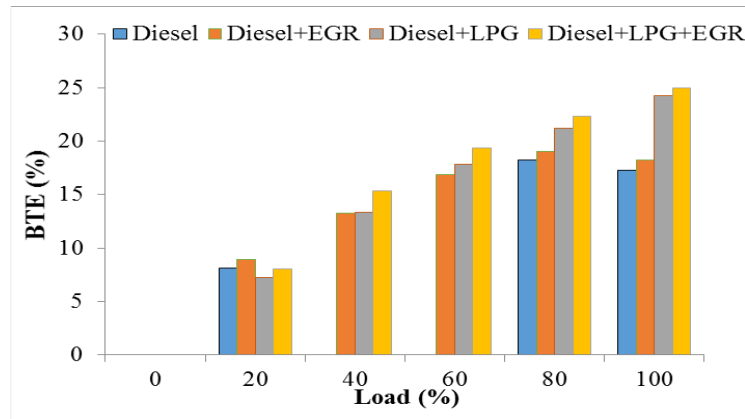


**Figure 2.3: Variations of BTE vs. load (Rosha et al., 2014)**

### 2.3.2 Fuel Consumption

Here, the effect of a dual-fuel operation with a comparison to conventional diesel combustion on fuel consumption is compared. Dual-fuel combustion tends to result in increased carbon monoxide and unburned hydrocarbon emissions. This is a direct implication of dual-fuel operation's worst combustion efficiency, which leads to the increase of fuel consumption. Amarendar et al., (2008) conducted the experiments on a conventional diesel engine operating in a dual-fuel mode using diesel- LPG and found that the brake specific fuel consumption was 30% lower than diesel fuel operation. This could be due to better mixing of air and LPG and improved combustion efficiency. Saleh (2008) performed that the dual fuel combustion using diesel-LPG (PFI) did not have significantly effect on the engine's consumption. Generally, at low loads, there is a slight increase in particular energy consumption in comparison to the conventional diesel operation.

Figure 2.4, illustrate the impact of engine load on specific energy consumption for normal diesel operation and dual-fuel operation. There is a decrease in specific energy consumption at higher loads for dual fuel than normal diesel operation. Thus, a complete gaseous fuel utilization is realized as a result of the more rapid combustion process and

higher temperature. Therefore, this leads to a reduction of specific energy combustion that is similar to or slightly better than normal diesel operation (Jian et al., 2001; Poonia et al., 1999a). Qi et al., (2007) discovered that comparable outcomes can be attained by using directly injected diesel-LPG blends where there is an increase in the fuel consumption of the dual-fuel operation at low loads in comparison to the diesel operation since the combustion is delayed into the expansion stroke because of the reduced cetane number of the blended fuel which prolongs the delay in ignition. On the other hand, at high loads of the LPG content of fuel blend, the fuel economy increases since the fuel economy is similar to that of the conventional diesel operation.

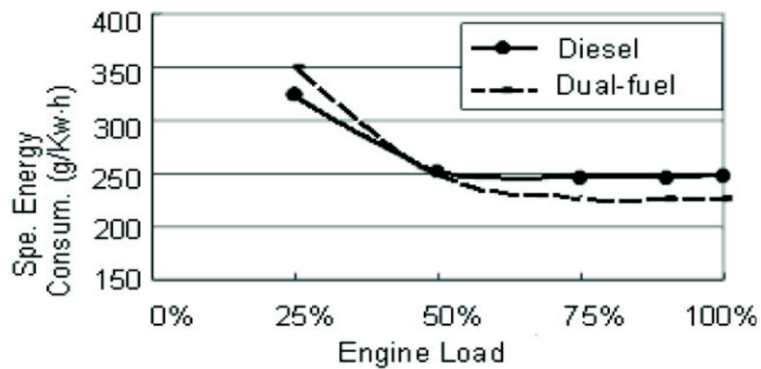


**Figure 2.4: Specific energy consumption (g/kWh) vs. load (PFI LPG-diesel) (Jian et al., 2001)**

### 2.3.3 Particulate Matter (PM)

Particulate Matter (PM), also known as smoke or soot, which compression ignition engines emit, is mainly generated as a result of the hydrocarbon fuels' incomplete combustion. A mechanism model which was designed for PM was presented by Kayes and Hochgreb (1999) where they named liquid fuel nucleation that stems from the port fuel to inject as the reason for PM formation. PM is significantly affected by the A/F ratio and likewise, the PM amount in the exhaust gas emissions increased by the burning of the liquid fuel (Kayes and Hochgreb, 1999). This study conducted on the usage of dual fuel



engine which is fueled with directly injected diesel-LPG blend reveals that when the LPG fraction increases, the smoke emission reduces, and this is illustrated in Figure 2.5 and 2.6. In Figure 2.5, 10% and 30% LPG content in the fuel blend are represented respectively and the LPG content of the fuel is represented by “z” in Figure 2.6. In addition, these Figures show the comparison with normal diesel operation and the most notable decrease of particulate matter emission occur at high loads ( $\geq 70\%$ ). Since LPG evaporates with greater ease because of its lower boiling temperature and due to the pressure drop. The injected blend of diesel-LPG content evaporates immediately, thereby enhancing the spray’s gas disturbance. This process is known as “flash boiling” and smaller droplets of blended fuel (in comparison to a conventional diesel injection) are formed in the combustion chamber as the result. Therefore, lower particulate matter emissions result from the smaller droplets (Alam et al., 2001; Donghui et al., 2005; Qi et al., 2007). In comparing the soot emissions of normal diesel combustion and dual-fuel combustion with different diesel/LPG ratios, a reduction in soot emission can be found with an increase of the LPG content. Nearly 70% soot emission reduction is realized in a specific case where 42% LPG is added. Moreover, it has been mentioned that soot emissions will not be significantly improved with a further increase in the amount of LPG content (Jian et al., 2001).

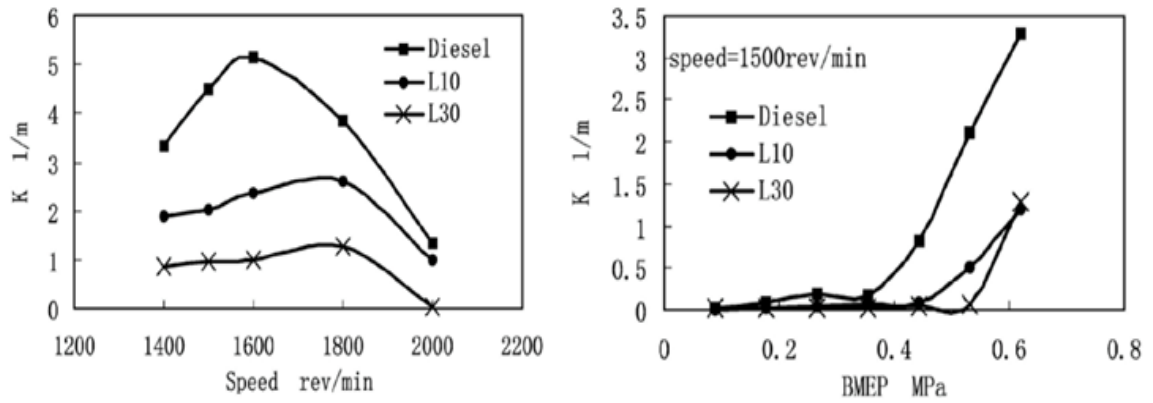


Figure 2.5: Smoke emissions of diesel and two different LPG-diesel blends vs. BMEP and engine speed (Donghui et al., 2005)

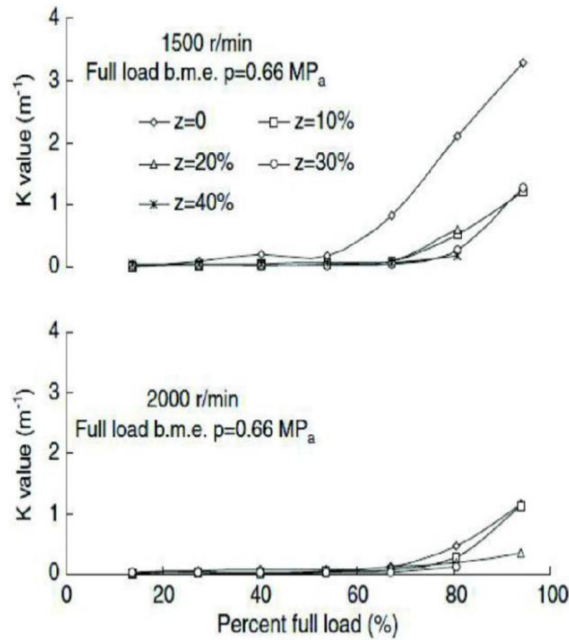
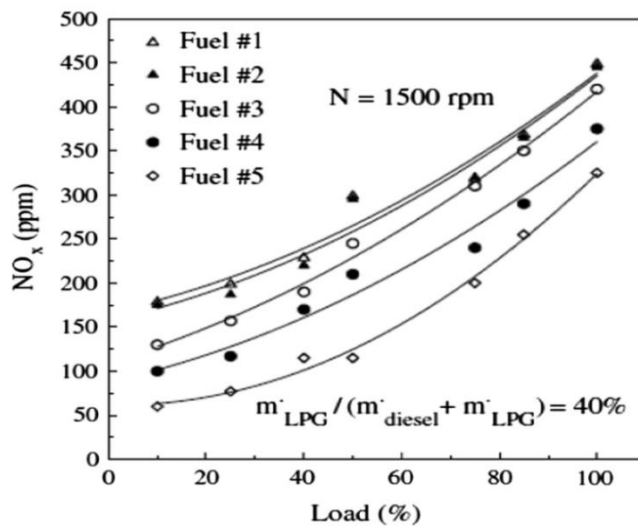


Figure 2.6: Smoke emissions for different fuel blends and engine speed vs. load (Qi et al., 2007)

### 2.3.4 Nitrogen Oxides (NO<sub>x</sub>)

The majority of the Nitrogen oxides (NO<sub>x</sub>) which is generated in coal combustion is nitrogen dioxide (NO<sub>2</sub>), and nitric oxide (NO) normally named in combination as (NO<sub>x</sub>). NO<sub>x</sub> generated through the combustion mostly consists of NO (90–95%) along with smaller quantities of NO<sub>2</sub> (5%-10%). The amount of formed N<sub>2</sub>O is significantly low

(“Oilgae-Glossary,” 2014). Normally, the maximum quantities of the NO<sub>x</sub> found are determined through the peak temperature in the combustion process where the peak temperature relies on other parameters such as the initial temperature of the fuel-air mixture, equivalence ratio, and the fuel composition (Hairuddin et al., 2014; Kuo et al., 2005). Saleh (2008) conduct the effect of different LPG blends on NO<sub>x</sub> emissions in comparison with pure propane in dual fuel operation is illustrated in Figure 2.7. The emission of NO<sub>x</sub> increased for the entire LPG blends with an increase in the engine load. On the other hand, the increase in the percentage of butane is shown to correspond with NO<sub>x</sub> emission reduction. NO<sub>x</sub> with fuel #2 of 10% butane, fuel #3 of 30% butane, fuel #4 of 50% butane and fuel #5 of 70% butane was lower by almost 1%, 6.7%, 16.7% and 27.8%, respectively at full load than that with tested fuel #1 (pure propane). Generally, high NO<sub>x</sub> levels are formed as a result of high temperatures and high oxygen amounts; conditions which do not occur in the combustion chamber with enhancing the percentage of butane.



**Figure 2.7: Variation of NO<sub>x</sub> concentration with engine load for LPG blends (Saleh, 2008)**

Additionally, Qi et al., (2007) conducted an experimental by using diesel-LPG dual fuel engine and compared with normal diesel engine at different engine speed (1500, 2000 rpm) and the result shows that the  $\text{NO}_x$  concentration decreased with increased the LPG concentration in diesel fuel as illustrate in Figure 2.8 and that because of increase the heat of evaporation of the diesel-LPG blended and as a result decrease the temperature of the cylinder gases due to the fuel evaporation. As well, the increase of engine speed under blended fuel operation results in a further decrease of  $\text{NO}_x$  values compared to diesel fuel operation.

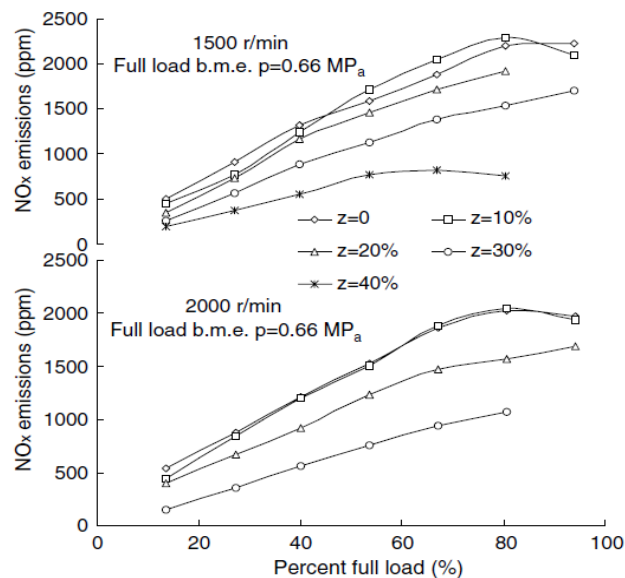


**Figure 2.8: Variation of nitrogen oxide under Diesel and blended fuels operation vs. load at 1500 and 2000 r/min engine speed (Qi et al., 2007)**

### 2.3.5 Unburned Hydrocarbons

Unburned Hydrocarbon (UHC) is a significance of incomplete combustion produced by low temperatures (Bression et al., 2008; Ganesh et al., 2008; Yap et al., 2006) during the combustion process which results in fuel deposition in crevices and boundary layers (Hairuddin et al., 2014). UHC is originated from the cylinder wall which continues a thin

layer of oil as the piston is going down, that accumulates and amasses in the crevice area and any other cold region of the combustion wall (Heywood, 1988; Komninos, 2009). Donghui et al., (2005) investigated and observed various diesel/LPG ratios which are shown in Figure 2.9. However, this Figure shows operating under low loads and high ratios of diesel/LPG leads to increased UHC emissions because of the crevices mechanisms and the lower charge temperature. Moreover, greater levels of UHC will be emitted when the diesel/LPG ratio is enhanced at high loads probably because of higher temperatures that result in a more thorough combustion of the air-fuel blend (Donghui et al., 2005; Qi et al., 2007).

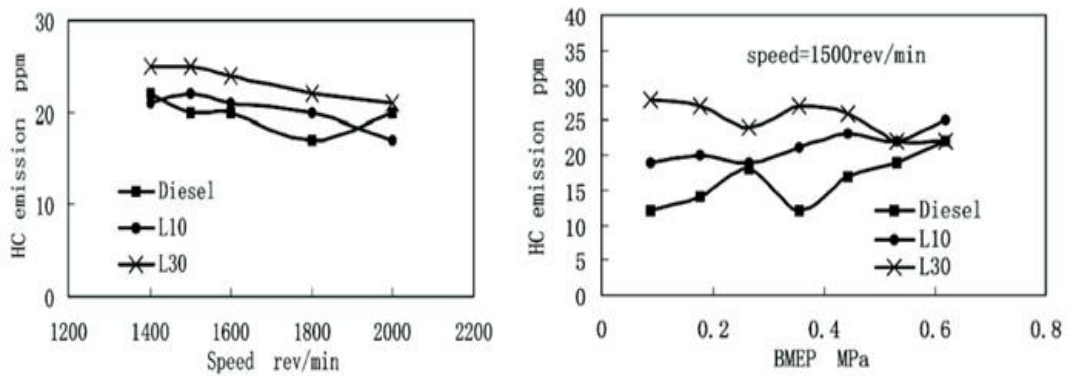


**Figure 2.9: HC emissions (ppm) vs. engine speed and loads for different diesel /LPG blends and net diesel (Donghui et al., 2005)**

### 2.3.6 Carbon Monoxide (CO)

The emission of CO is normally controlled by the fuel-air equivalence ratio (Heywood, 1988; Stone, 1999). Furthermore, CO emissions originate from the significantly cold boundary and crevices layers where complete consumption is not possible (due to the coldness) (Aceves et al., 2001; Hairuddin et al., 2014). The oxidation of CO is dominated by the reaction of carbon monoxide and OH radical as  $\text{CO} + \text{OH} = \text{CO}_2 + \text{H}$ , the result of which also contains hydrogen radicals. In a similar way, the CO to  $\text{CO}_2$  conversion happens with an increase in the OH radicals' concentration during the process of combustion (Kuo et al., 2005). The combustion's low temperature eventually results in the

decrease of the combustion efficiency due to lower oxidation activities of hydrocarbons and the lower rate of conversion of CO to CO<sub>2</sub> (Alkidas, 2007; Sjöberg and Dec, 2005). However, the impact of different LPG mixtures on the mission of CO under various loadings related to the pure propane (fuel #1) was observed by Saleh (2008) in the dual-fuel operation which is illustrated in Figure 2.10. As expected, the fuel#3 30%, fuel#4 50%, and fuel#5 70% increase of the butane in the LPG composition resulted in the highest CO emissions. Therefore, with an increase in the percentage of the butane, the CO emissions were expected to increase in comparison to pure propane gas because of its lower flame speeds and flame temperature, and longer ignition delays (Saleh, 2008).

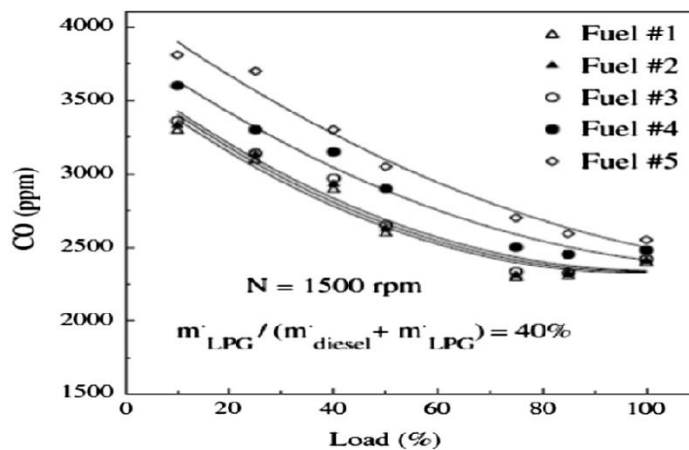


**Figure 2.10: Variation of CO concentration with engine load for LPG blends (Saleh, 2008)**

Figure 2.11 illustrated a comparison between diesel and mixtures that contain 10% and 30% LPG is conducted to determine the CO emission. As a result, a small increase in CO emission is noticed at low loads which enhance with an increase in the quantity of LPG because of the low charge temperature. On the other hand, at high loads, there is a decrease in CO emission when the LPG amount increases; this reduction in CO emission is significant compared to the levels in normal diesel operation. Due to LPG's flash-boiling in the mixture, the fuel mixture mixes better with the air, and higher temperatures

will result from high loads. Therefore, the complete combustion is attained and on the other hand, the CO emission formation does not appear to be significantly affected by the engine speed (Donghui et al., 2005; Qi et al., 2007).

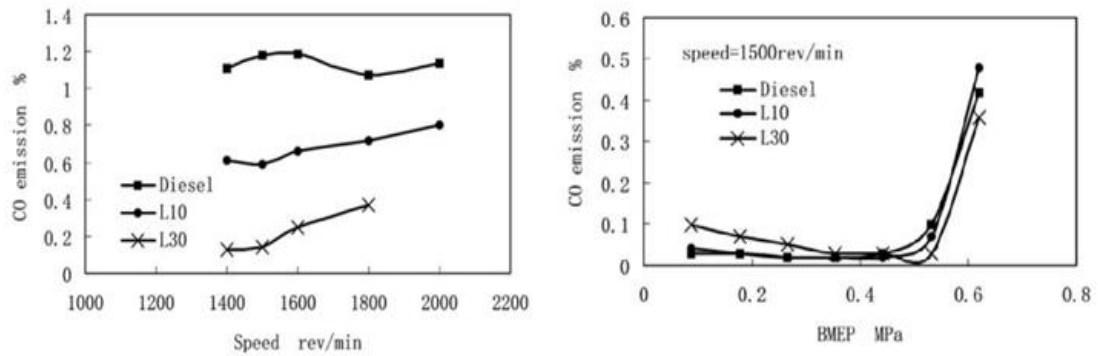


**Figure 2.11: CO emissions (ppm) vs. engine speed and loads for different diesel /LPG blends and net diesel (Donghui et al., 2005)**

#### 2.4 Effect of addition LPG, Hydrogen, and Diesel blend

A study on a four-cylinder diesel engine in a dual-fuel mode with diesel as the pilot fuel and the addition of H<sub>2</sub> and LPG as the primary gaseous fuel has been carried out by Lata (2011, 2012); Lata and Misra (2010, 2011). To determine the emission, combustion, and performance characteristics. It was found that the mixture combination of the LPG-H<sub>2</sub> ratio (70:30) increased the brake thermal efficiency as compared to diesel cases at 80% load conditions as shown in Figure 2.12. Since LPG flame has the tendency of becoming unstable whereas hydrogen-air flame has the tendency of becoming stable. Therefore, hydrogen fraction results in flame stabilization.

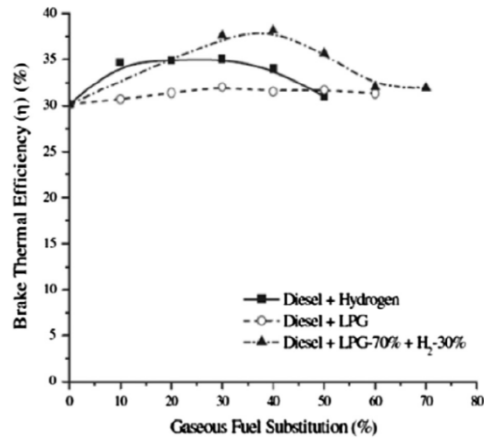


**Figure 2.12: Comparison of brake thermal efficiency for the cases II, III and IV at 80% load condition (Lata et al., 2012)**

Figure 2.13 (a) and (b) illustrates the variation of UHC at load conditions of 10% and 80%. The UHC emissions increased when LPG-H<sub>2</sub> at 10% low load compared with diesel mode and this might be because of the decrease in the amount of pilot fuel, which is the cause of the gaseous fuel's poor ignition, as well as the inducted mixture, is too lean to burn. On the other hand, a lower UHC emission can observe in LPG-H<sub>2</sub> in 80% high load as compared to diesel mode since the faster and better combustion rate, which results in a complete combustion, thereby, lower UHC emissions.

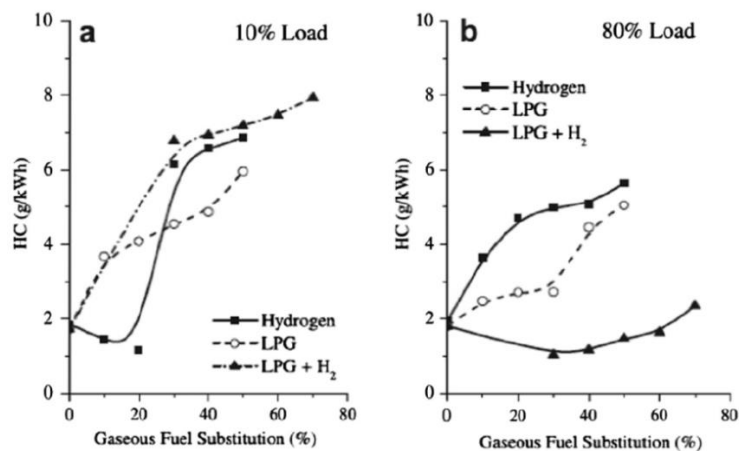


**Figure 2.13: Unburnt HC (g/kW h) vs. diesel + gaseous fuels substitution (%) (Lata et al., 2012)**



Additionally, a comparison between H<sub>2</sub> and LPG was carried out by Choi et al., (2005). Different H<sub>2</sub> amounts (0%, 10%, and 20%) at 1400 rpm were used to examine the impact of NO<sub>x</sub> emission. NO<sub>x</sub> emissions were reported to be the highest at addition of 20% H<sub>2</sub> results in an almost 20% increase in the NO<sub>x</sub> emission amount and this is in contrast with pure LPG combustion since higher emissions of NO<sub>x</sub> resulting from the addition of H<sub>2</sub>, depend on the flame temperature of the H<sub>2</sub> fuel and the maximum temperature of the cylinder (which are higher in comparison to LPG combustion). However, due to the 10% addition of H<sub>2</sub>, the NO<sub>x</sub> emission amounts will be high in comparison to the pure LPG fuel as illustrated in Figure 2.14.

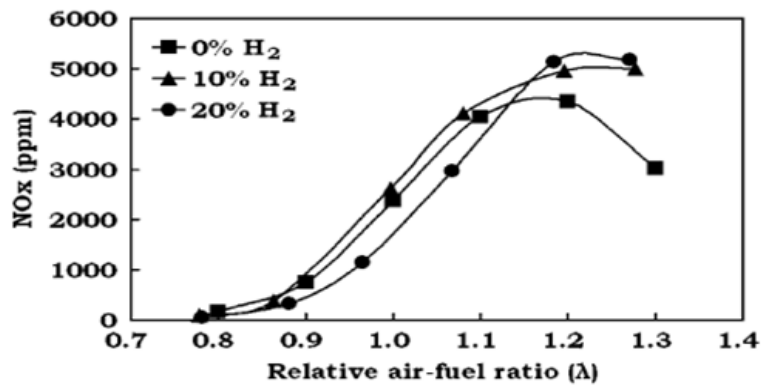


**Figure 2.14: Variation of NO<sub>x</sub> emissions with relative air–fuel ratio (Choi et al., 2005)**

## 2.5 Previous Numerical Simulation Studies

This part of the literature review is conducted the utilized of (CFD) computational fluid dynamics methods. Since, the CFD simulation is one of the best tools to investigate complex in-cylinder movements of engines (Mousavi et al., 2016). CFD code has the ability to resolve the governing flow equations in order to create detailed explanations of the chemical reacting flows and the turbulent velocity fields. On the

other hand, it is safer to utilize CFD method before moving to experimental analysis because of almost no manufacturing danger involved in it (Soni and Gupta, 2016).

### **2.5.1 Turbulence Modeling**

The main key in internal combustion engines is the turbulence modeling. In order to improve engine performance and to decrease emissions, turbulence modeling is necessary for more understanding of the phenomena of spray, mixing, and combustion in an engine. The model of turbulence is based on the calculation of the turbulence kinetic energy  $k$  and the turbulence dissipation function  $\varepsilon$  (Lim et al., 2015). Subsequently, the equation of turbulence models apply with the computational work on a diesel engine is the RNG  $k$ - $\varepsilon$  model in order to model turbulence phenomena. However, several researchers have stated that  $k$ - $\varepsilon$  (RNG) model is the most suitable model for the simulation engine (Jafarmadar, 2014; Mousavi et al., 2016; Ng et al., 2013), and therefore this model was applied for this study.

Ng et al., (2013) examined the emissions formation and combustion characteristics processes of biodiesel fuels in a diesel engine by utilizing the (RNG)  $k$ - $\varepsilon$  model Renormalization Group, thus giving more accurate result for engine simulation. Mousavi et al., (2016) conduct a numerical examination on emission and combustion characteristics of a dual fuel engine by using KIVA-3V code and applied for turbulence modeling the RNG  $K$ - $\varepsilon$  turbulent flow. Kaario et al., (2002) implemented a simulation by utilizing the fluid dynamic STAR-CD feature and implementing the standard  $k$ - $\varepsilon$  model and also an adjusted version of the  $k$ - $\varepsilon$  RNG turbulence model. The combustion models of a diesel engine with three direct injections was performed and examined with respects to combustion performance. The results confirmed that the

turbulence RNG  $k-\varepsilon$  model demonstrated more understanding with the experimental details. Ghiji, (2011) conduct a simulation on Ricardo Hydra diesel engine-single cylinder which utilized a two-dimensional CFD approach to examine the performance of the  $k-\varepsilon$  RNG and the  $k-\varepsilon$  standard turbulence models and compared with experimental work. The comparison between these two models shows that the RNG  $k-\varepsilon$  turbulence model is more precise than the  $k-\varepsilon$  standard turbulence model specially at a higher mixing ratio of gases fuel for expecting in cylinder pressure during the engine cycle. The agreement with experimental ignition delay values was better for RNG  $k-\varepsilon$  turbulence model than standard  $k-\varepsilon$  turbulence model over a different range of mixing ratios and temperatures as illustrated in Figure 2.15.

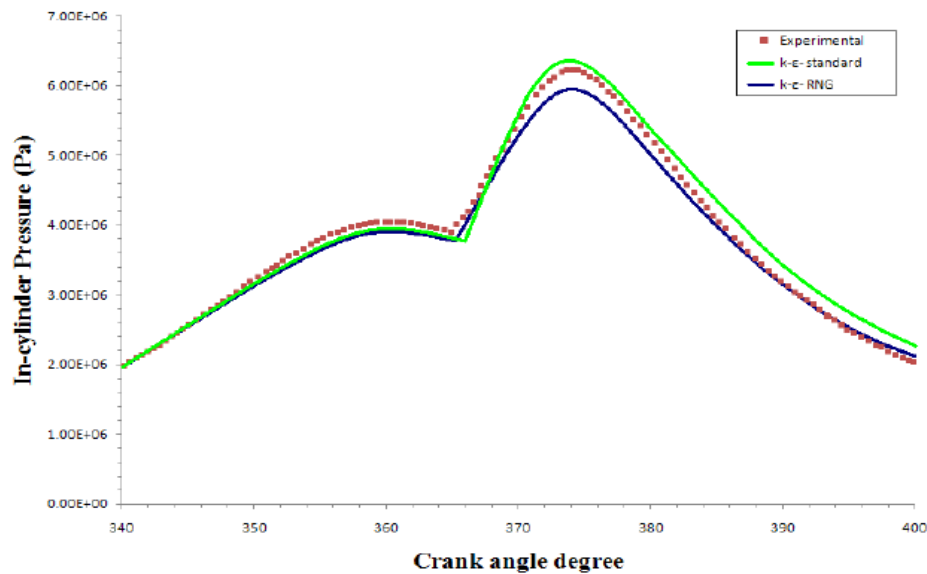


**Figure 2.15: In-cylinder pressure for  $Z=87\%$  by  $k-\varepsilon$  standard and  $k-\varepsilon$  RNG (Ghiji, 2011)**

### 2.5.2 Ignition Delay (Autoignition) Modeling

In diesel engines, the ignition delay is defined per the time once the fuels are injected into the combustion chamber and when the pressure starts to rise due to the fuel

released energy. However, in dual fuel engine, the ignition delay has been obviously noted when diesel fuel combined with a hydrocarbon such as CNG and LPG. Alrazen et al.,( 2015) conducted a numerical simulation on single cylinder direct injection by combining diesel fuel with natural gas using fluent software and the result illustrated that was obvious ignition delay for diesel-CNG as shown in Figure 2.16. Xu et al., (2014) investigated methanol-diesel dual fuel engine and they stated that with rising in the methanol fraction, the ignition delay is affected by the coupling of the methanol and diesel fuel chemical reactions and by alterations in the in-cylinder temperature. Lata and Misra, (2011) conduct that in a dual fuel diesel engine the ignition delay affected by the kind of gaseous fuels and their concentration in the cylinder charge. On the other hand, the autoignition methods in the Fluent method is suitable with any volumetric combustion model. The autoignition techniques are basically transient hence are not offered with steady simulations. This design is classified in relatives of single autoignition model equation (Shell Model) and correlations are applied to consideration for complex chemical kinetics (Fluent, 2006).

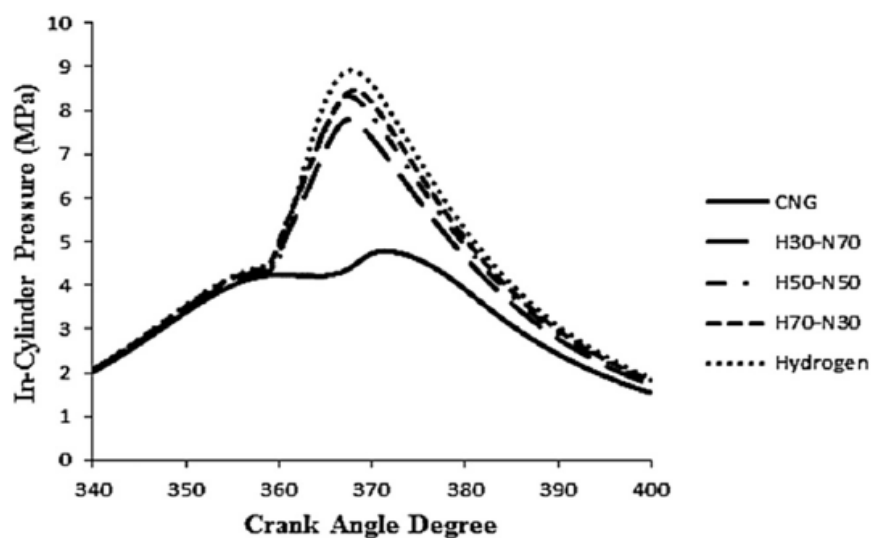


**Figure 2.16: In-cylinder pressure curves under different ratio of gaseous addition (Alrazen et al., 2015)**

### 2.5.3 Atomization Models

The discrete phase model DPM is described as the diesel fuel spray (Fluent, 2006). This involved both primary and secondary atomization, the primary atomization type is utilized to offer the initial particle state in the case of suitable nozzle parameters in order to precisely mimic the spray from the nozzle. The secondary atomization types are utilized to characterize the effect of spray breakup, coalescence, collision and dynamic drag downstream of the nozzle (Fluent, 2006). The Fluent software approach involved the Taylor Analogy Breakup (TAB) model and the Wave breakup model. The TAB model is suggested for sprays through low speed in the regular atmosphere. The Wave model is the most common model utilized in the condition of high-speed fuel injection applications (Jafarmadar, 2014; Mousavi et al., 2016; Ng et al., 2013; Soni and Gupta, 2016). Ng et al., (2013) conducted a simulation of biodiesel combustion in a light-duty diesel engine. Subsequently, for modeling the spray breakup event, Wave model is implemented with the values of model constants, B1 and B0 retained at 10 and 0.61, respectively. Consequently, the selection of existing B1 value is basically to produce reasonably good prediction on the ignition delay period, as well as the timings and magnitudes of peak pressure. Moreover, the Fluent, (2006) guide conduct that the value for B0, is 0.61 for a spray of diesel while B1 is the breakup up time constant is based on wall impingement consequences and to the initial disturbance level in the approach of a breakup and the suggested values are  $B1 = (10-60)$ . As well, the influence of the B1 constant Wave model was performed by Abagnale et al., (2014) on the in-cylinder pressure to examine as shown in Figure 2.17. The best constant value B1 to match the data of experimental is in the range of 5-7, although the ignition start seems to be clearly advanced.

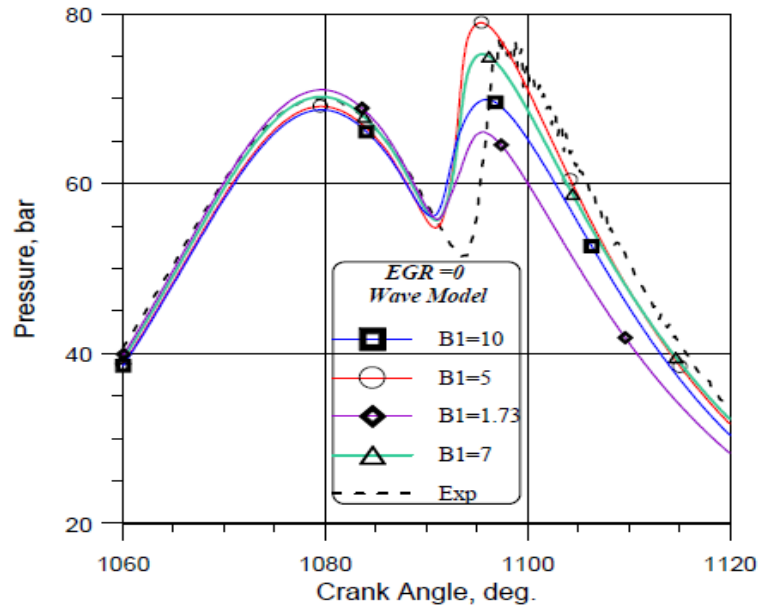


**Figure 2.17: In-cylinder pressures by varying the  $B_1$  constant (Abagnale et al., 2014)**

#### 2.5.4 Emissions of Dual Fuel Engine

This section discusses the emissions of dual fuel engines using numerical simulation. Dual fuel engines are more attractive due to lower emission levels in comparison with conventional diesel engines (Mousavi et al., 2016). Therefore, several researchers have contemplated decreasing the emission especially focusing on the decrease of  $\text{NO}_x$  and soot emission (Mousavi et al., 2016; Zhu et al., 2010). Soni and Gupta, (2016) implemented a numerical simulation by utilizing CFD approach to attain minimum potential emissions from methanol-diesel blend by the application of initial swirl, water emulsion methods, and EGR percentage. As a result, high amount of methanol in the diesel fuel leads to low  $\text{NO}_x$  emissions from diesel dual fuel engine. The rise in methanol up to 30% has attained a maximum decrease of 58%, 27% and 65% in CO, NO, and HC emission respectively compared to normal diesel fuel. However, higher methanol-diesel blend caused to increase the soot emissions

because of low combustion temperature of the D+M30 blend as shown in Figure 2.18.

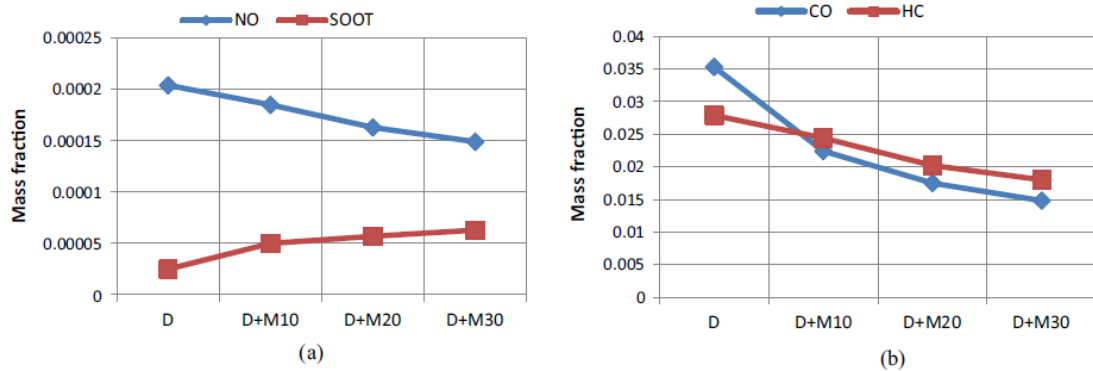
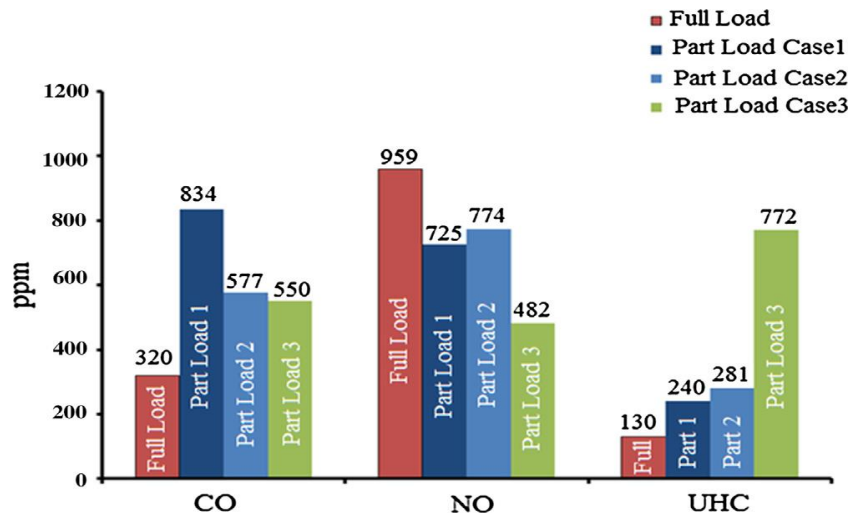


**Figure 2.18: Emission characteristics of diesel and methanol blends (Soni and Gupta, 2016)**

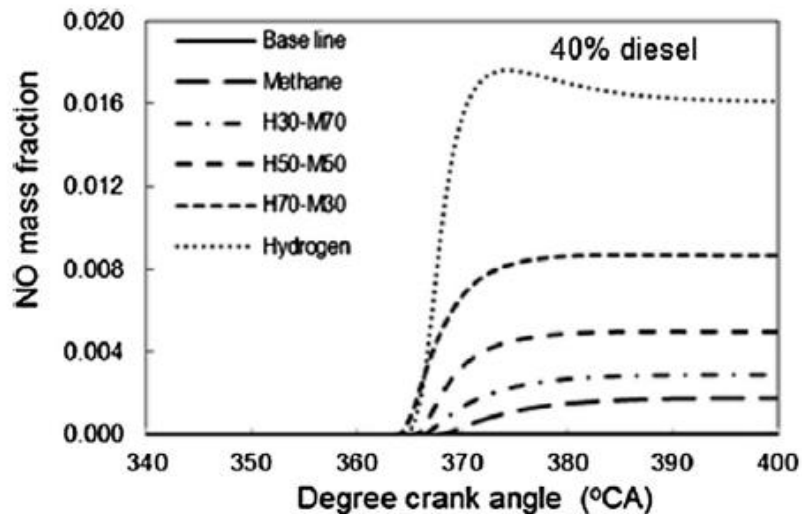
Another study by Mousavi et al., (2016) performed a numerical investigation on emission and combustion characteristics of a dual fuel engine by utilizing KIVA-3V code at full and part loads. However, at part loads, UHC and CO emissions are higher in contrast with the condition of the full load. Additionally, at part loads, the NO emissions are lower in contrast with full load condition as presented in Figure 2.19. Thus, the mixture of the air and methane is very lean and the rate of combustion of the lean mixture is slow and causes to incomplete combustion at part load. Therefore, less fuel will be burned at part load condition on contrast with a full load.

Mansor et al., (2017) examined the NO<sub>x</sub> emission of different diesel contents with hydrogen and methane (H<sub>2</sub>/CH<sub>4</sub>) blend in a direct injection compression ignition engine by using ANSYS FLUENT approach. Subsequently, for diesel-CH<sub>4</sub> operation, NO emission is slightly increased in comparison to diesel fuel operation. Since the decrease of NO emission is a result of increasing methane fraction in the mixture. Higher hydrogen presence in the mixture results in higher NO emission and

its peak values occur with the diesel-H<sub>2</sub> operation. Due to higher flame temperature as shown in Figure 2.20. In contrast, increasing diesel content suppresses NO formation due to the low combustion temperature of diesel while increasing hydrogen content inhibits NO formation due to higher flame temperature.



2.19: Comparison between predicted CO, NO<sub>x</sub> and UHC emissions at part and full load (Mousavi et al., 2016)



2.20: NO emission with various diesel content (Mansor et al., 2017)



## 2.6 Summary

The experiments and numerical simulations as conducted by different researchers have been reviewed in this chapter. The literature revealed that the employment of LPG and hydrogen gaseous fuel in the diesel engine as the dual-fuel operation is among the effective and prominent measures of overcoming fossil fuel and exhaust emissions. The following conclusions are made based on the present study on a diesel-LPG dual fuel engine.

- Diesel-LPG dual fuel engines have issues like poor brake thermal efficiency at low load, the brake thermal efficiency increases at higher load conditions.
- Generally, there is a slight increase in the specific energy consumption in diesel dual fuel operation at low loads, and yet, the specific energy consumption decreases at higher loads since the gaseous fuel is almost completely utilized because of faster proceeding combustion and higher temperatures.
- The most significant PM emission reduction in comparison to normal diesel operation is observed at high loads. This because the process is known as “flash boiling” and leads to smaller droplets of blended fuel in the combustion chamber in comparison to a conventional diesel injection. The smaller droplets lead to better mixing and as a result, reduction in particulate matter emissions.
- The oxygen availability and combustion temperatures mainly influence NO formation. As well, the increase in the percentage of butane is shown to correspond with NO<sub>x</sub> emission reduction compared with pure propane.
- The majority of carbon monoxide and unburned hydrocarbon emissions are due to incomplete combustion. Unburned fuel in crevices volumes is one of

the main sources of gaseous fuels' incomplete combustion and poor flame propagation.

- The brake thermal efficiency will be enhanced at high loads with the utilization of LPG and hydrogen as secondary fuel whereas reverse effects are produced at low conditions.
- At higher load condition,  $\text{NO}_x$  and unburnt hydrocarbon will decrease with the use of an LPG and hydrogen mixture as secondary fuel.
- The (RNG)  $k-\varepsilon$  model was employed by the most computational works on diesel engines. Hence, it is the best turbulence model method for engine simulation. The Wave model is the most common model utilized in the condition of high-speed fuel injection applications with the values of model constants, B1 and B0 retained at 10 and 0.61.
- At part loads, the mixture of the air and the gaseous blend is very lean, slow and causes to incomplete combustion and led to increasing the UHC and CO emissions and decreased NO emissions in contrast with the condition of the full load.

## CHAPTER 3

### METHODOLOGY

#### 3.1 Overview

The fluent software is a modern commercial CFD code and therefore can offer more complex tools such as turbulence modeling, injection configuration, and moving dynamic mesh that could be utilized for simulation. Additionally, the visualization methods in this software can be employed to plot and describe the flow characteristics more efficiently.

The considerable three-dimensional CFD analysis of the entire process is the most precise design of analysis, but this application needs a significant quantity of computational effort for its modeling. The engine system associates with components that move such as pistons and valves. Thus, the mesh must be updated at each time step based on the motion of these components. This type of moving dynamic mesh is expensive and valuable due to the severe demands of mesh quality which is necessary in order to simulate accurately by using CFD solvers. Besides that, it also takes up a high (computational memory-RAM) and high amount of time by using the three-dimensional mesh (Ghiji, 2011).

Therefore, the 2-dimensional approaches are applied as a simplification for the (3-D analysis) procedure to simulate the intake, compression, combustion and expansion procedure of the diesel, dual and tri-fuel combustion in this study. The direct injection of diesel pilot fuel, the evaporation of the fuel droplet and the combustion are simulated. Utilizing the wall film modeling functions of the fluent software is design

the interaction of fuel spray with the piston surface. Figure 3.1 shows the specific process of the CFD simulation as mentioned above.

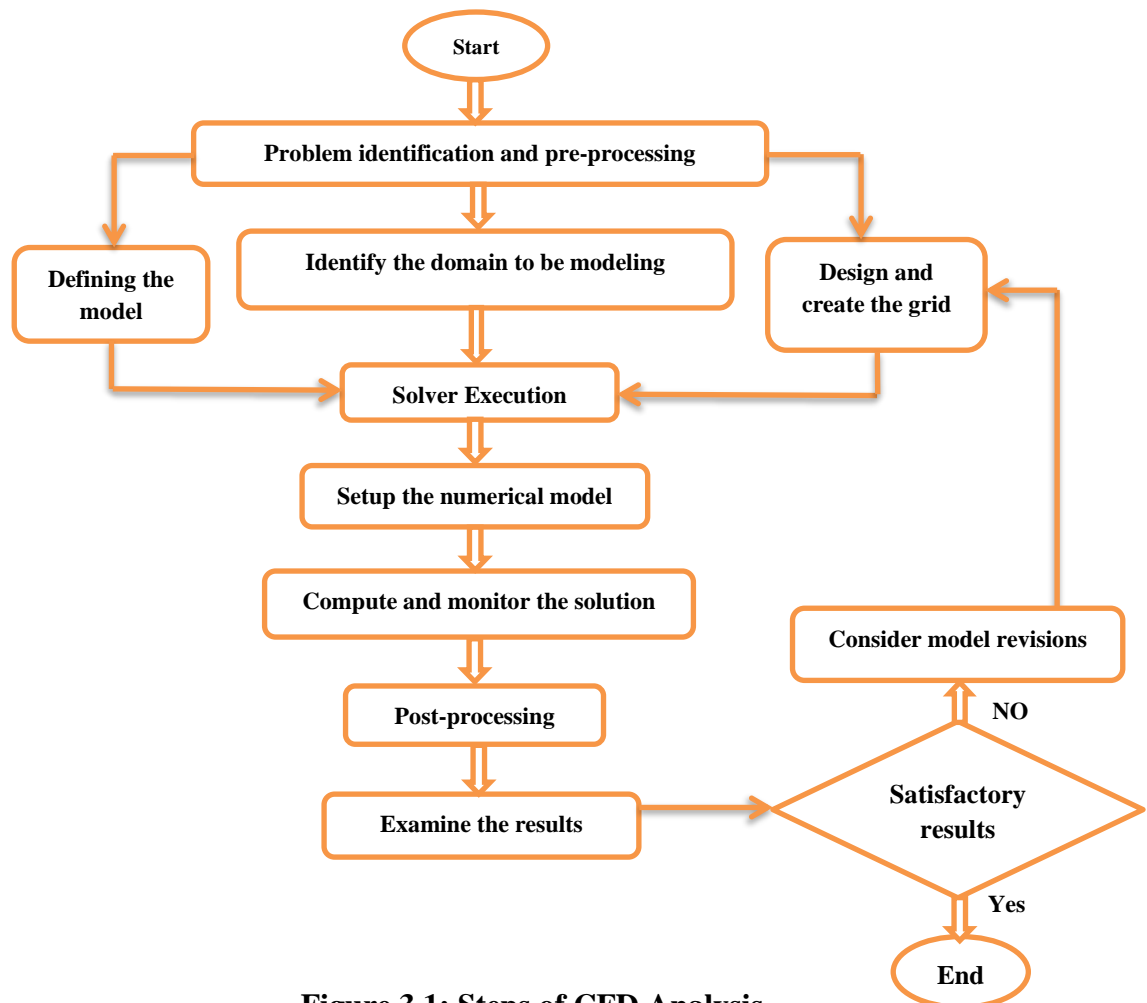


**Figure 3.1: Steps of CFD Analysis**

### 3.2 Data and Initial Condition

The engine simulation of this research is following from the study which has been performed by Wannatong et al., (2007). The details of the engine Specification are shown in Table 3.1. In the current study, the engine was run under diesel, dual and tri-fuel processes with different of excess air ( $\lambda$ ) values, which include 1.2, 1.6, 2, and 2.4 as demonstrated in Table 3.2. Moreover, intake temperature (298K), the torque of the engine is (20.18 Nm), and engine speed (2000 rpm) were taken consistently at an

atmospheric condition. Liquid petroleum gas (LPG) was assumed to be 100% propane (Anbarasu and Karthikeyan, 2014; Saleh 2008; Surawski et al., 2014).

**Table 3.1: Engine Specification (Wannatong et al., 2007)**

Subjects	Description
Model	Ricardo Hydra
Engine Type	DI diesel
Number of cylinders	1
Number of valves	2
Swept volume (Liter)	0.45
Bore (mm)	80.26
Stroke (mm)	88.9
Compression ratio	20.36:1
Combustion chamber shape	bowl in piston
Connecting rod length (mm)	158
Injector operating pressure (bar)	250
Valve timings	IVO 8° bTDC / IVC 42° aBDC EVO 60° bBDC / EVC 12° aTDC

**Table 3.2: Test Cases**

Cases	Primary fuel	Secondary fuel	Excess air ( $\lambda$ )
Diesel	Diesel	-----	1.2, 1.6, 2, 2.4
Diesel 30%-LPG70%	Diesel	LPG	1.2, 1.6, 2, 2.4
Diesel 50%-H <sub>2</sub> 50%	Diesel	H <sub>2</sub>	1.2, 1.6, 2, 2.4
Diesel 30%-(LPG+ H <sub>2</sub> ) 70%	Diesel	LPG+H <sub>2</sub>	1.2, 1.6, 2, 2.4

In this work, the fuel operation was utilized with different substitutions such as diesel fuel, diesel-LPG, diesel-H<sub>2</sub> under dual fuel operation, and diesel-LPG-H<sub>2</sub> under tri-fuel operation. Diesel-LPG (30%,70% ), diesel-H<sub>2</sub> ( 50%, 50% ) and diesel-LPG-H<sub>2</sub> (30%, 70%) were designed for the mixture percent of LPG to H<sub>2</sub> which are 90:10,

60:40, 50:50 respectively as a mass fraction in FLUENT and present in Table 3.3, based on (Lata et al., 2011), and were utilized in the simulation. Because of the knocking, the maximum amount supplement has limited to the LPG and H<sub>2</sub> up to 70%, 50% respectively (Lata et al., 2012; Saravanan et al., 2008). Therefore, the amount of diesel was utilized 30 percent by mass of total fuel at diesel mode and the other 70 percent was substituted by the LPG and H<sub>2</sub> in the case of tri-fuel operation as stated above. In addition, since the engine was operating under the same conditions, the input power is applied to be the same for dual, tri and diesel models.

**Table 3.3: Percentage Variation of LPG and Hydrogen**

<b>Cases</b>	<b>LPG</b>	<b>Hydrogen</b>
90L-10H	90%	10%
60L-40H	60%	40%
50L-50H	50%	50%

However, different procedures can be utilized to include the gaseous fuel into a diesel engine to comprehend the dual fuel and tri-fuel procedure. These procedures contain the carburetion, continuous manifold induction, direct injection and timing-controlled manifold/port injection (Saravanan and Nagarajan, 2009).

In this study, the port injection approach of gaseous is the best common mixture formation and is utilized in a variety of variants that differ in multiple aspects including air-fuel ratio, and part-load control (Verhelst and Wallner, 2009). Consequently, the gaseous fuels were identified with air as a mass fraction in FLUENT. This study assumed that the fresh air into the cylinder was consisting of N<sub>2</sub> and O<sub>2</sub> and their mass fraction were 76.8% and 23.2% respectively (Yang et al.,

2015), then to provide the mass fraction of hydrogen, LPG, and air, the next formula is utilized:

$$X_{h2} = \frac{\dot{m}_{h2}}{\dot{m}_{h2} + \dot{m}_{LPG} + \dot{m}_{air}} \quad (3.1)$$

Where,  $\dot{m}$  is the mass flow rate of gaseous, and  $\dot{m}_{LPG}$ , was determined and identified by Papagiannakis et al., (2010):

$$\dot{m}_{lpg} = \frac{\dot{m}_{mix} - \lambda * AFR_{Dst} * \dot{m}_D}{\lambda * AFR_{LPG} + 1} \quad (3.2)$$

$$\dot{m}_{max} = \dot{m}_{LPG} + \dot{m}_{air} \quad (3.3)$$

Consequently,  $\dot{m}_{air}$  can be computed here by:

$$\dot{m}_{air} = \lambda * AFR_{Dst} * \dot{m}_D + \lambda * AFR_{st.gaseous} * \dot{m}_{gaseous} \quad (3.4)$$

Where ( $\lambda$ ) is the excess air and  $AFR_{st.gaseous}$  matching to the stoichiometric air-fuel ratio for gaseous fuels (by mass) which can be achieved from Appendix A, Table A.1, and  $AFR_{Dst}$ , matching to stoichiometric air/fuel ratio for diesel. The mass fraction of hydrogen, LPG, O<sub>2</sub>, and N<sub>2</sub> can be settled in the same technique and the results are shown in Appendix B.

### 3.3 Design of Research Flows Chart

The subsequent chart indicates the procedures which have to be taken sequentially to get the suitable computation results.

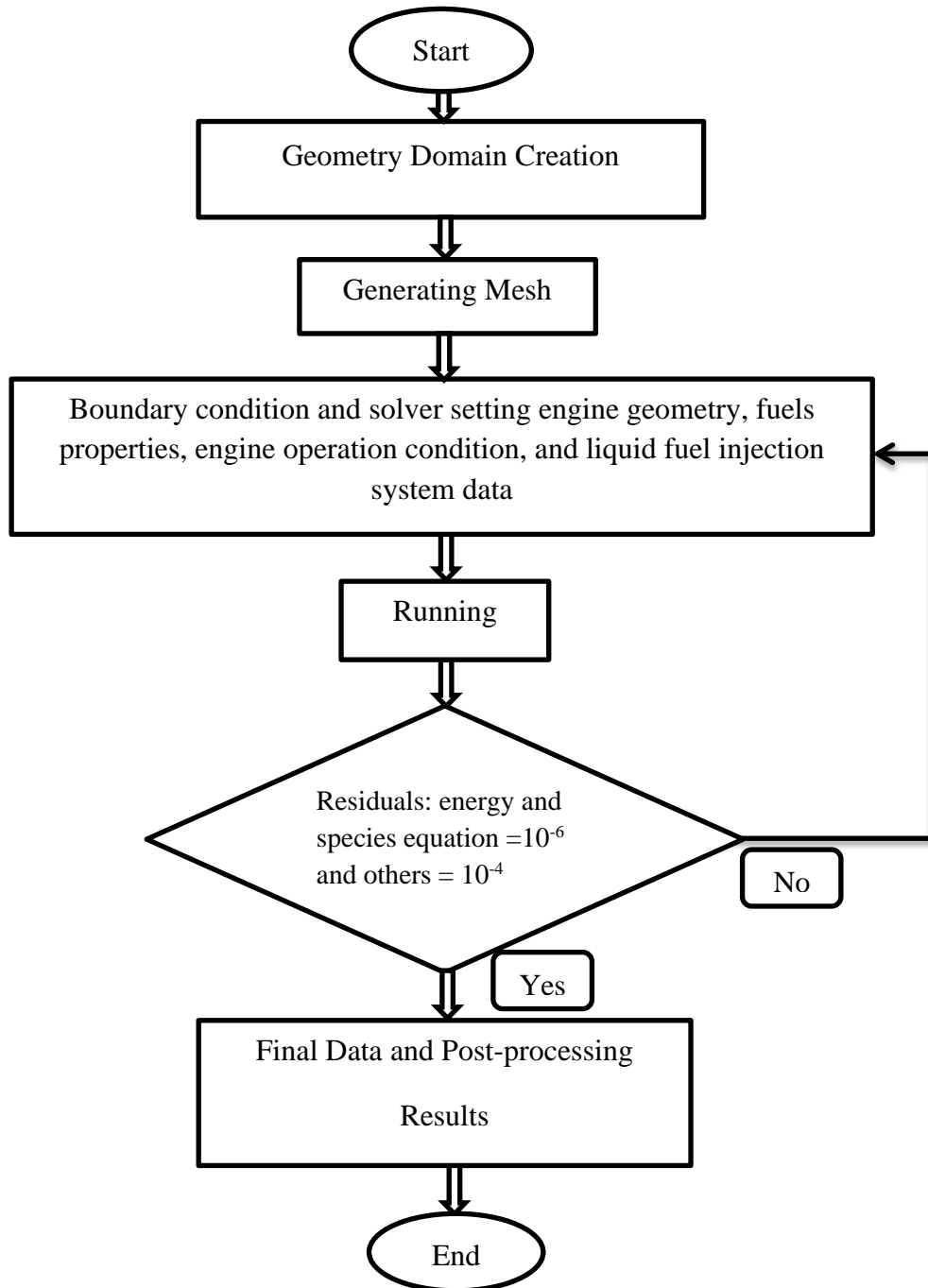


**Figure 3.2: Computational approach flow chart**



### 3.4 Grid Generation

#### 3.4.1 Initial Grid Generation

According to the very little gap between a piston and the head of the cylinder of the Ricardo Hydra engine direct injection (Wannatong et al., 2007), it is a difficult mission to generate a design for the moving mesh in that area. The geometric construction of the two-dimensional simulation designs can be implemented in the earlier stage of the ANSYS design modular as shown in Figure 3.3, including both quadrilateral and triangular elements. It is significant to implement these features in order to offer the necessary conditions for the moving valves and deforming zone like the combustion chamber (Fluent, 2006).

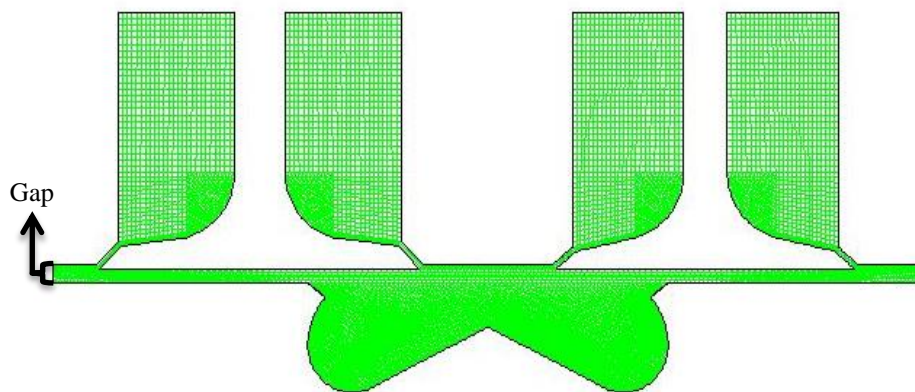


**Figure 3.3: The Geometry and Mesh at TDC**

As observed from Figure 3.4, the two-dimensional geometry has four regions namely the piston bowl (dynamic zone), inlet (stationary zone), valve layering zone, and the inlet-layering zone.

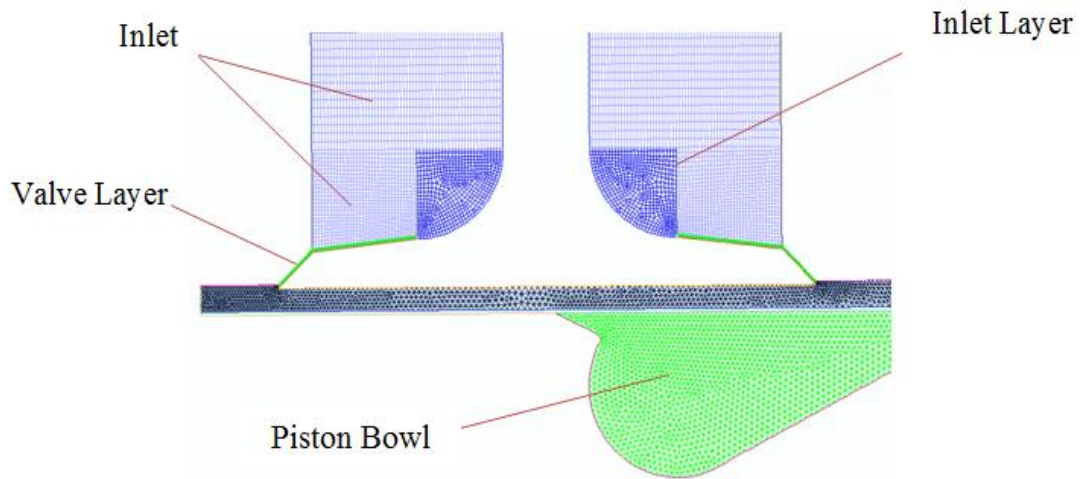


**Figure 3.4: Computational geometry with defined zones**

### 3.4.2 Moving Dynamic Mesh

The moving Dynamic Mesh (MDM) model can be applied to model the flows that the shape of the domain is changing respecting to the time due to the motion on the boundaries of the domain. The volume mesh update is performed automatically for each time step based on the new positions of the boundaries. Two different types of meshes were created for moving parts (one piston and two valves). This is because of the complex geometry of piston bowl and also to avoid creating negative volumes at the same time as valves and piston move up and down. As well as, because of a large movement of piston and valves in this zone, a type of mesh must be utilized to be able to sweep when piston and valves go up and again generate mesh when they go down. For this part, triangular elements are used because of this kind of mesh has the ability to expand and contract while valves are moving. Therefore, there are three methods for updating the meshes of a moving boundary project:

- ❖ Smoothing
- ❖ Layering
- ❖ Re-meshing

The smoothing technique was applied for triangular cells. As well as, in this method, it is possible for the components to expand and contract in addition to that it is not different between the numbers of the layer. Therefore, this is a valuable technique and can be used in moving boundary simulations. Furthermore, the layering method is suitable when there is a case of quadrilateral cells and large movements. However, the re-meshing technique generates new layers with the exist of triangular cells and this technique consuming a lot of time, expensive, and employed on the complicated geometric.

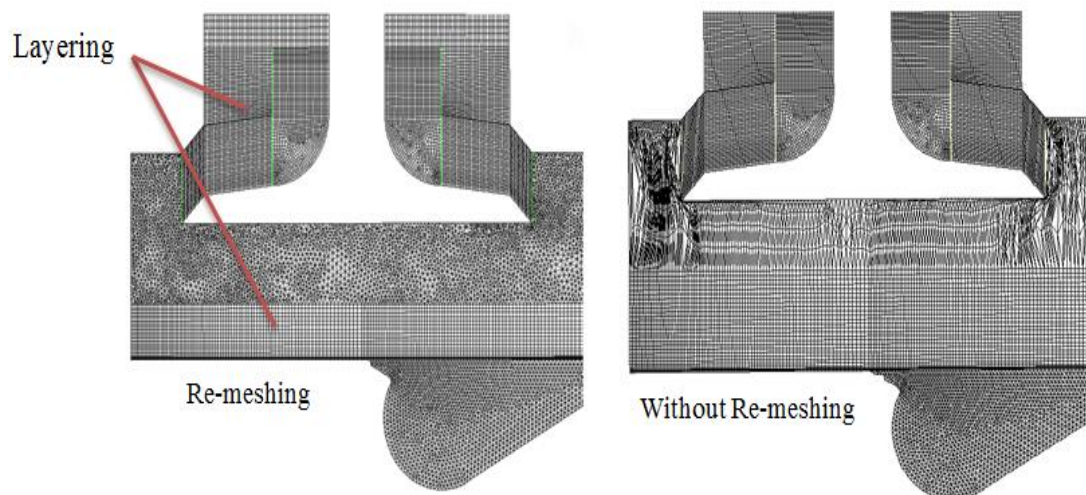


**Figure 3.5 Layering and Re-meshing methods tested for computational model**

In addition, the maximum cell skewness sets by software for re-meshing and smoothing technique in Moving Dynamic Mesh (MDM) was set to 0.7 that is satisfactory for 2D simulations (Fluent, 2006). This technique used to get a high-quality mesh and to reduction the required time needed for meshing significantly.

Therefore, to decrease the computational period through the engine cycle, sub-domains of intake and exhaust ports were removed from the computations when the intake and exhaust valves were closed. Additionally, the grid quality is suitable for the utilization of the standard wall features ( $11.225 < y^+ < 60$ ) (Fluent, 2006).

### **3.5 Boundary Condition and Fluid Properties**

An essential step in the setup of the model is to describe the materials and their physical characteristics. The boundary conditions are decided on the basis of an experiment Wannatong et al., (2007). In addition, the air properties are required for analyses are obtained from the fluent database. During the engine speed of 2000 rpm and at 343 degrees crank angle before TDC the diesel fuel begins to inject up to 360 crank angle degrees. Kerosene ( $C_{12}H_{23}$ ) is selected to diesel fuel from the fluent database and its specifications are shown in Table 3.4. The ends of the exhaust and intake pipes are open to the atmosphere. Therefore, the static pressure at these ends is set at the atmospheric pressure. As proposed by experiment Wannatong et al., (2007) the pressure boundary condition for the intake and outlet pipe is used and which has a value of (atmospheric pressure = 101325 Pa).

The gas is considered to be an ideal gas with viscosity and specific heat varying as a function of temperature. The cylinder head and the block and has a thickness (15mm) and are made from steel and the temperature assumed to be at (358K) of steel with a natural convection coefficient of  $10 \text{ W/m}^2\text{K}$  according to (Ghiji, 2011).

**Table 3.4: The Specifications of Diesel Fuel (Wannatong et al., 2007)**

<b>Diesel Fuel</b>	<b>Value</b>
Specific gravity at 15.6/15.6C	0.827
Calculated cetane index	57.8
Viscosity at 40C (cSt)	3.096
Sulfur Content (%wt)	0.043
Net Heating Value (J/g)	42.636

### **3.6 Numerical Methods**

#### **3.6.1 Equation of Motion**

The divergence and conservative kind of equations that manages the two-dimensional flow of the fluid and transfer of heat fluid can be defined (Fluent, 2006) as:

##### **A. Mass Conservation Equation**

The mass conservation equation in fluid flow equation as a state by (Abdullah et al., 2008):

$$\frac{\partial \rho}{\partial t} + \nabla \cdot (\rho u) = 0 \quad (3.5)$$

Where:

$\rho$  = fluid density

$u$  = velocity

## B. Momentum Conservation Equation

Conservation of momentum is described by (Abdullah et al., 2008) as:

$$\rho \frac{\partial u}{\partial t} + \rho(U \cdot \nabla)u = -\nabla P + \nabla \cdot \{\mu[\nabla U + (\nabla U)]^T + \lambda(\nabla \cdot U)\} + \rho g \quad (3.6)$$

Where:

$\rho$ = fluid density

$u$ = velocity

$T$ = temperature

$\lambda$  = bulk viscosity

$p$ = static pressure

$\rho g$  = gravitational body force

## C. Energy Conservation Equation

Energy conservation equation is expressed by (Abdullah et al., 2008) as:

$$\rho c_v \frac{\partial T}{\partial t} + \rho c_v (u \cdot \nabla)T = -P(\nabla \cdot u) + \nabla \cdot (k \nabla T) + \lambda(\nabla \cdot u)^2 + \nabla u \cdot \{\mu[\nabla u + (\nabla u)^T]\} \quad (3.7)$$

Where:

$c_v$  = heat capacity at constant volume

$\rho$  = density

$T$  = temperature

$u$  = velocity

$P$  = pressure

$K$  = thermal conductivity coefficient

$\lambda$  = bulk viscosity

$\mu$  = dynamic viscosity

## D. Equation of Perfect Gas

The defined of a perfect gas, the equation is described by (Jemni et al., 2011):

$$P = \rho RT$$

Where:

$\rho$  = Fluid density

P = static pressure

T = temperature

R= universal gas constant = 8.314 (J/ mol K).

### 3.6.2 Fluent Solver

Two numerical methods the fluent can provide:

- **Pressure-Based Solver**
- **Density-Based Solver**

**Pressure-Based Method** was majorly applied for low-speed incompressible flows; although the **Density-Based approach** was applied for high-speed compressible flows. These two methods were expanded and reformulated these days for performance and solving for a wide range of flow condition beyond their conventional or serious objective. The pressure-based solver is chosen for this study because it needs less memory and supports flexibility in the procedure of solution. The pressure-based solver contains a solution algorithm. Such as, Segregated algorithm and coupled algorithm are two pressure-based solver algorithms obtainable in Fluent. The discretized equations of the segregated algorithm only requisite to be stored one time, On the other hand, a coupled system of equations including the pressure-based continuity equation and momentum equations can solve by pressure-based coupled algorithm. While the discrete system of all pressure-based continuity equations and

momentum of the segregated algorithm needs to be stored in the memory when solving for the pressure field and velocity, the memory necessity requirements 1.5-2 more times (Fluent, 2006). Due to this, the segregated algorithm is selected to be utilizing in this study.

### **3.6.3 Discretization**

In order to turn a universal scalar transport equation to an algebraic equation that can be fixed numerically. Fluent uses a control-volume-based approach that including the transport equation. The equation of transport is about every control volume, producing a discrete equation that defines the conservation law on a control-volume foundation.

#### **a) Spatial Discretization**

The upwind schemes used by fluent for example, first order upwind, second-order upwind, power law, third order-MUSCL and quick. By using these schemes the first-order upwind can evaluation the flow when aligned to the grid. The second order scheme conversely can expect flows that are no aligned to the grid, however, it growths discretization numerical errors. Consequently, in this study employed second order upwind methods depending on its excellent solving capability (Abdullah et al., 2008).

#### **b) Temporal Discretization**

The governing equations must be discretized in both space and time for the transient simulations to work. In the situation of equations based mostly on the time, spatial discretization is similar to the steady-state situation. The two methods in temporal discretization are:



1. Implicit time integration: this equation can be solved constantly at each time level and therefore it has the advantage of being unconditionally steady in respects to the time step size.
2. Explicit time integration: this technique is most suitable in the case of the density based explicit solver. It is also identified as “global time stepping.”

Therefore, pressure-based solver and implicit technique are utilized for this study comparable with previous researchers (Abdullah et al., 2008; Shojaeefard et al., 2008).

### **3.6.4 Pressure Interpolation Schemes**

The second-order upwind is suggested for compressible flows Fluent, (2006) and this scheme utilized by many previous researchers such as (Abdullah et al., 2008). Therefore, second order scheme is using for solving the momentum, energy, continuity, and k- $\epsilon$  equations for this study.

### **3.6.5 Pressure-Velocity Coupling**

Four pressure velocity algorithms options the Fluent can provide such as SIMPLEC, SIMPLE, PISO, and Coupled. These schemes are based on predictor-corrector approach techniques excepting “coupled” scheme. Except Coupled uses the pressure-based coupled and all others algorithms utilized the pressure based segregated algorithm (Fluent, 2006).

For this research, (PISO) pressure-implicit with Splitting of Operators pressure-velocity coupling scheme is used for the connection between velocity and pressure as employed by Abdullah et al., (2008).

### 3.6.6 The Under Relaxation Factors

From the fluent and due to the nonlinearity of the equation, it is required to manage the change of the value of the variable  $\phi$ . The modification can be the mechanism by the under-relaxation scheme, which decreases the change of  $\phi$  created through every iteration. The old value,  $\phi_{old}$ , can determine the new value of the variable,  $\phi$ , inside the cell, the computed modification in,  $\phi$ ,  $\Delta \phi$ , and,  $\alpha$ ; the under-relaxation factor follows (Fluent, 2006):

$$\phi = \phi_{old} + \alpha \Delta \phi \quad (3.10)$$

Where:

$\phi$  = value of the variable

$\phi_{old}$  = old value of the variable

$\Delta \phi$  = the computed change in  $\phi$

$\alpha$  = under relaxation factor

Meanwhile, convergence difficulties were met with defaulting values, especially when the exhaust valve opens to release high pressure from the cylinder to the low-pressure manifold, the under-relaxation factors for momentum and pressure were changed from 0.7 and 0.3 to 0.5 and 0.2, respectively (Ghiji, 2011).

### 3.6.7 Iteration Residual and Time Steps

The residual convergence value that was used in this study for energy equation is  $10^{-6}$  in addition to the residual convergence value for the remaining equation is  $10^{-4}$  which is sufficient for scientific researchers (Fluent, 2006). Smaller residual values do not alteration much of the results calculated, but they need considerable more computation time. For obtaining an independent solution for the time step size, it was recognized that small sufficient time step has to be set such that a single step does not rotate the interface a distance better than the smallest cell size. Therefore, the applied time step

was significantly small, typically of 0.25 degree of crank angle and the solution is run for 300 iterations at every time step relating to Ghiji (2011). Fluent iterates on the current time step solution till acceptable residual decrease is achieved, or the greatest number of iteration per time step is attained. When it advances to the next step time, the cell and divider zones will consequently, be moved because of the predetermined translational profiles. RNG-K- $\epsilon$  needed about four days to simulate intake, compression, combustion, and expansion strokes with 300 iterations per each time step. It was noticed that the range of iterations for all the residual values was below  $10^{-6}$  for the species and energy equation and the value was  $10^{-4}$  for other equation for each time step values. Therefore, the rising of iterations per each time step didn't alteration responses.

### **3.6.8 Phenomena Simulated**

#### **A. NO<sub>x</sub> Modeling**

The fluent software offers NO<sub>x</sub> model and that can help to understand the basics of NO<sub>x</sub> and gives methods to mechanism it. The diesel engine produces a significant emission of Nitrogen Oxides NO<sub>x</sub>. The NO<sub>x</sub> concentration does not have much influence on the flow field. Since the time required is much longer for NO<sub>x</sub> reactions than the time needed for the main flow field approximations. There are two recognized methods definite by (Jayashankara and Ganesan, 2010) that form of Nitric Oxide through the combustion process of thermal NO<sub>x</sub> and prompt NO<sub>x</sub>

#### **1. Thermal NO<sub>x</sub>**

At high temperatures, the thermal NO<sub>x</sub> is produced by the atmospheric reaction of nitrogen and oxygen. In other words, it is produced by the oxidation of atmospheric nitrogen. In the case of the thermal NO, the reactions are generally identified to be

these recommended by Zeldovich mechanisms. However, the thermal of nitrogen is requirements considerably high temperatures to break the stringent of N<sub>2</sub> bond; therefore, the formation of NO<sub>x</sub> wants higher temperatures.



## 2. Prompt NO<sub>x</sub>

Prompt NO<sub>x</sub> produced when hydrocarbon fragment and molecular nitrogen react. It has a low dependency on temperature and a lifetime is only a few microseconds. The part of NO<sub>x</sub> emission in diesel engines from this can be considerable due to rich combination and the closeness of the fuel spray to the combustion chamber.

## 3.7 Chemical Reaction Modeling

The concern of the mathematical forming of the turbulent combustion is the issue of the turbulent flow modeling in addition to chemical kinetics and moreover the link among chemical reactions and flow. The inhomogeneous composition that is a result of the link among turbulence, as well as chemical reactions, is quite well established.

### 3.7.1 The Finite-Rate/Eddy-Dissipation Model

In FLUENT, the mixing and transport of chemical species are simulated by solving the equations of conservation which include diffusion, convection and reaction sources of every individual species. Reactions occurring was used to model multi-chemical reactions. Finite-Rate/Eddy-Dissipation model was used to simulate the turbulent species transport combustion (Abagnale et al., 2014; Mansor et al., 2017). This model determines the mixing rate, the Arrhenius rate and the smaller of the two.

• **Arrhenius rate equation**

$$\dot{R}_{i,r} = \Gamma (\ddot{v}_{i,r} - \dot{v}_{i,r}) (\prod_{i=1}^N [C_{i,r}]^{\hat{n}_{i,r}} - k_{b,r} \prod_{i=1}^N [C_{i,r}]^{\dot{v}_{i,r}}) \quad (3.14)$$

$\Gamma$  Describes are the net influence of third bodies on reaction rate. This expression is defined as:

$$\Gamma = \sum_i^N Y_{i,r} C_i \quad (3.15)$$

Where the third body efficiency is  $Y_{i,r}$ .

$$k_{i,r} = A_r T^{\beta_r} e^{-E_r/RT} \quad (3.16)$$

Where:

$A_r$  = Pre-exponential factor (consistent units)

$\Gamma$  = temperature exponent (dimensionless)

$E_r$  = activation energy for the reaction (J/kg mol)

$R$  = universal gas constant (J/kgmol – K)

• **The mixing rate equations**

$$R_{i,r} = \dot{v}_{i,r} M_{w,i} A \rho^{\frac{\varepsilon \min}{k}} \left( \frac{Y_R}{\dot{v}_{R,r} M_{w,R}} \right) \quad (3.17)$$

$$R_{i,r} = \dot{v}_{i,r} M_{w,i} A B \rho^{\frac{\varepsilon}{k}} \left( \frac{\sum_p Y_p}{\sum_j^N \dot{v}_{j,r} M_{w,j}} \right) \quad (3.18)$$

Where:

$R_{i,r}$  = the net rate of production of species i due to reaction r

$Y_p$  = the mass fraction of any product species, p

$Y_R$  = the mass fraction of a particular reaction, R

$\frac{\varepsilon}{k}$  = large eddy mixing time scale

$A$  = an empirical constant equal to 4.0

$B$  = an empirical constant equal to 0.5

## CHAPTER 4

### RESULTS AND DISCUSSION

#### 4.1 Overview

A two-dimensional method was employed in this study by using the numerical analysis. Firstly, the effects of a number of cells on the expected result were verified. Then the results were validated with experimental results, which is necessary to ensure that acceptable accuracy is attained. In the following section, combustion characteristics of the engine have been examined include in-cylinder pressure and temperature. In the last section of this chapter, results of emissions were computed for example NO<sub>x</sub>, CO, and CO<sub>2</sub> emissions. However, graphs related to in-cylinder pressure, temperature, NO<sub>x</sub>, CO, and CO<sub>2</sub> based on different ratios of the gaseous mixture, and various excess air ( $\lambda$ ) against crank angle degree are existing in this chapter. The speed of the engine, torque, and mixing ratio of gaseous fuel was constant. The existing results in this chapter are based on simulations, which have been done by Fluent Commercial Software.

#### 4.2 Mesh Independent Test

Initially, the independence mesh test was prepared for the (OCC) bowl. As described in Figure 4.1, two measurement meshes had been created, specifically medium and fine, which have 10980 and 20921 cells, respectively, the quality of mesh dependent on these numbers of cells. At an engine speed of 2000 rpm, the simulation was done for each mesh in order to illustration the independence. Figure 4.2 indications the expected in-cylinder pressure against crank angle graph. the results obvious that there is no significant difference between the fine and medium meshes. Indeed, the refined

computational mesh raised the cost of the CPU via three times and meanwhile was not given beneficial for the CFD simulation (Mansor et al., 2017). Therefore, taking the computational time into account, the medium mesh was chosen as the most appropriate for this study.

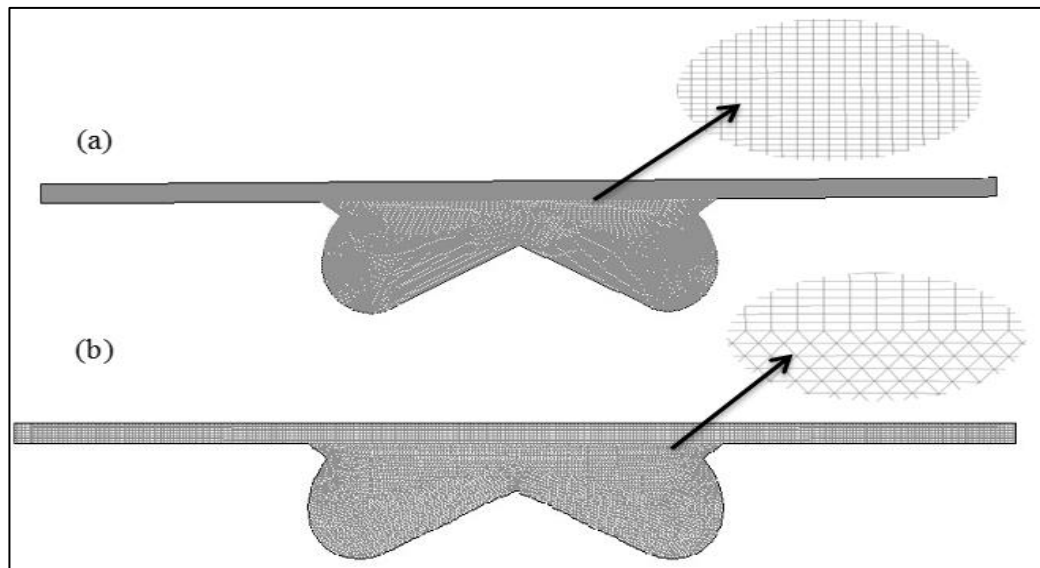


**Figure 4.1:** (a) Fine sector meshes (20921 cells) and (b) medium (10980 cells) at (TDC) used in 2D-CFD simulations

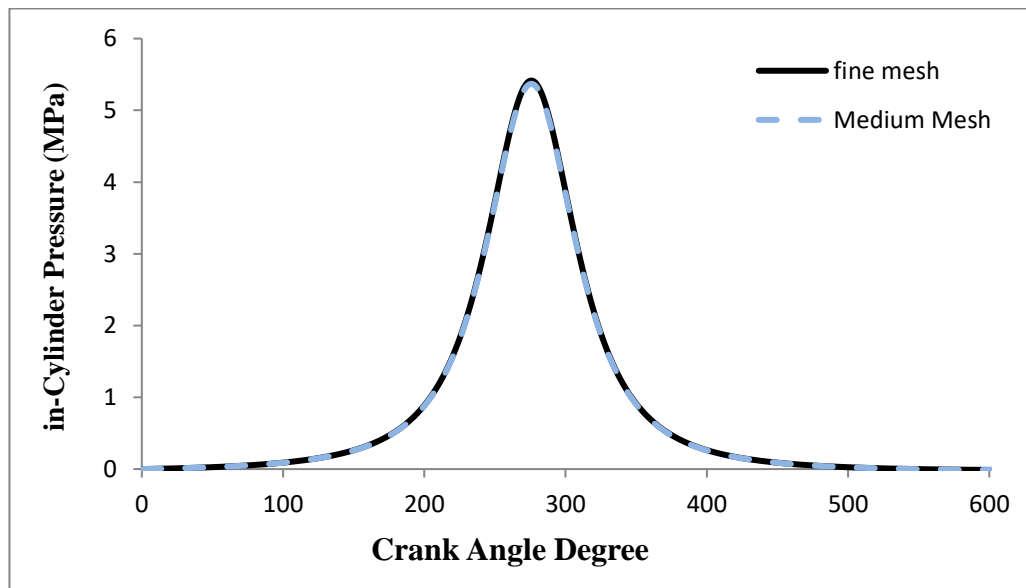


**Figure 4.2:** In-cylinder pressure for typical grid dependency test

### 4.3 Validation Model

For validation, an engine model single cylinder was construct and simulated. Engine specification and further engine information which were utilized from the engine specifications of (Wannatong et al., 2007) were imported under conditions particularly the engine speed (2000 rpm), temperature (330 K), and 100% diesel fuel. A 2D model of the engine has been constructed and validated by having it compared with an experimental data, for the diesel mode operation. Moreover, to validate the simulation, the in-cylinder pressure rate was compared with the experimental results (Wannatong et al., 2007). The in-cylinder pressure validation in this study is presented in Figure 4.3.

In general, there is a good agreement between experimental data and numerical results especially at ignition and peak pressure times in most of the points. From 340 to 375 CA, the in-cylinder pressure curves obtainable a good experimental estimation while from 380 to 400 CA it was predicted slightly by simulation. Since the maximum pressure at 385 CA reached 4 MPa for simulation and for experimental it reached 3.8 MPa with less than (5% error). These minor discrepancies between experimental and computed data indicate that significant chemistry pathways and physical phenomena within the combustion chamber and possibly, because of the properties of diesel fuel, which had been changed to  $C_{12}H_{23}$ .



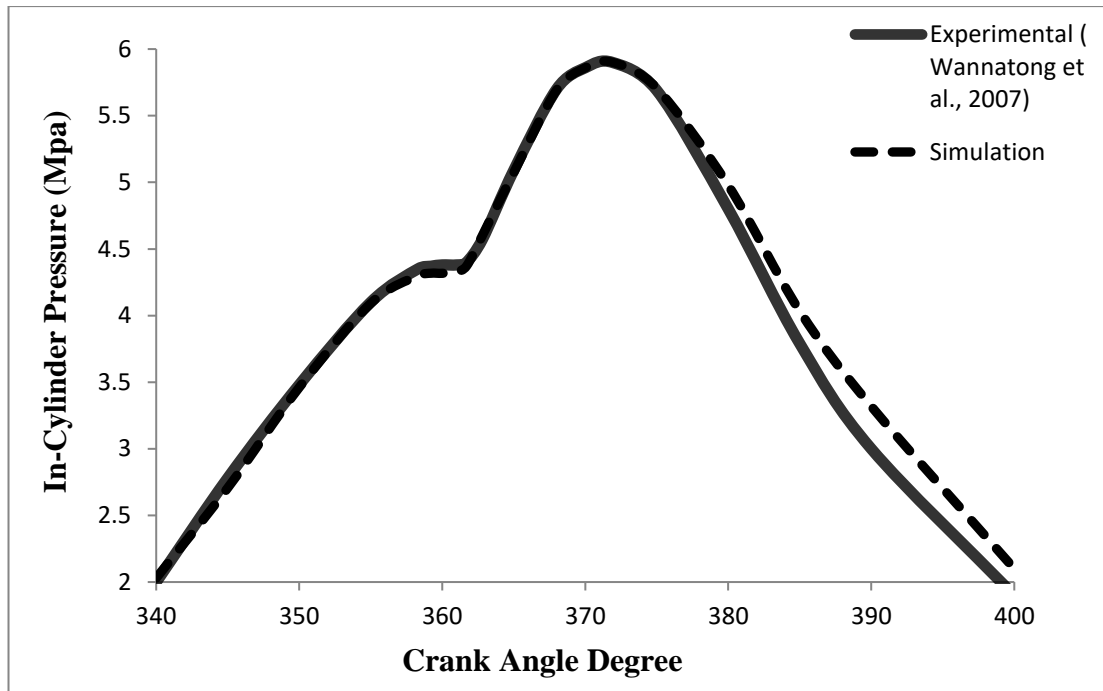


**Figure 4.3: Validation of 2D simulation for diesel fuel in-cylinder pressure at 2000-rpm engine operation mode**

#### 4.4 Verification of Emissions

To verify the accuracy of the emission result from CFD approach. The verification was applied on the  $\text{NO}_x$  emission at the same conditions mainly for the engine speed (2000 rpm), temperature (330 K), and diesel-hydrogen fuel mixture. Furthermore, 50:50 % for the mixture percent of diesel and hydrogen respectively and utilized in the simulation and it has been compared with previous work done by (Alrazen et al., 2015). The verification of  $\text{NO}_x$  emission in this investigation is shown in Figure 4.4. Generally, the simulation data appears to obtain a good agreement with the data of previous work in most of the point.

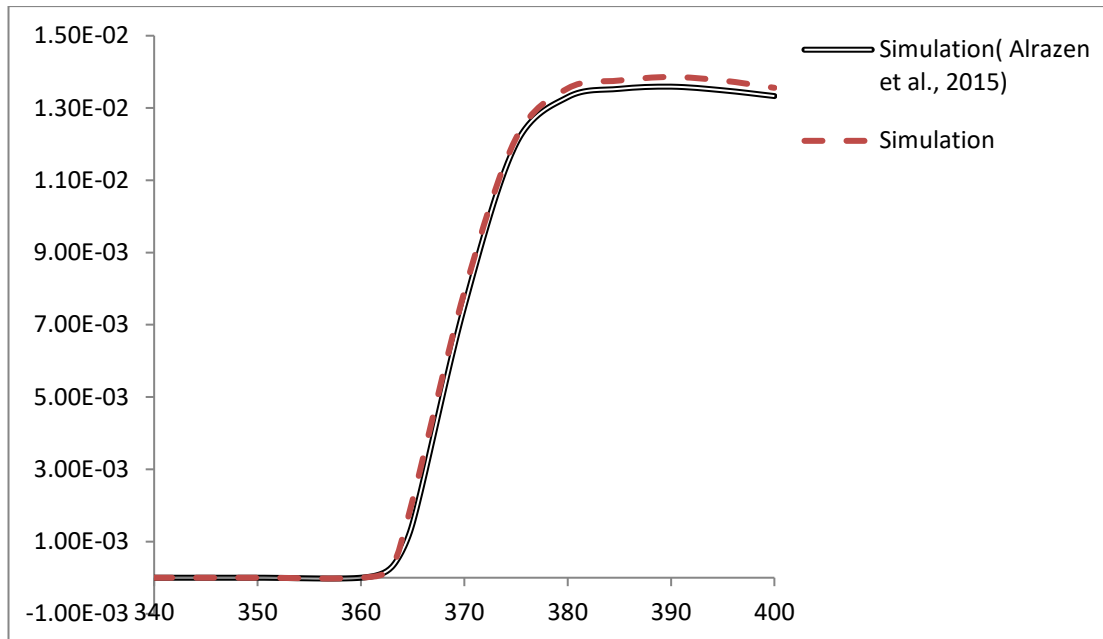


**Figure 4.4: Verification of the NO<sub>x</sub> emission under diesel-H<sub>2</sub> dual fuel engine operation**

#### **4.5 The Effect of LPG and Hydrogen Percentage Variation**

This section explains the effect of variation of gaseous fuel substitution on combustion characteristics (in-cylinder pressure and temperature) and emissions (NO<sub>x</sub>, CO, and CO<sub>2</sub>) of diesel, dual, and tri-fuel operations with a value of different excess air. However, the gaseous fuel percent for LPG and H<sub>2</sub> was illustrated in chapter two in section 3.2, Table 3.3.

##### **4.5.1. Combustion Characteristics**

###### **A. In-Cylinder Pressure**

Figure 4.5, shows the peak in-cylinder pressure for the different gaseous fuel additions under the four excess air ( $\lambda$ ) state. It was discovered that an increase in the value of the excess air led to a decrease in the peak in-cylinder pressure upon addition of every gaseous fuel.

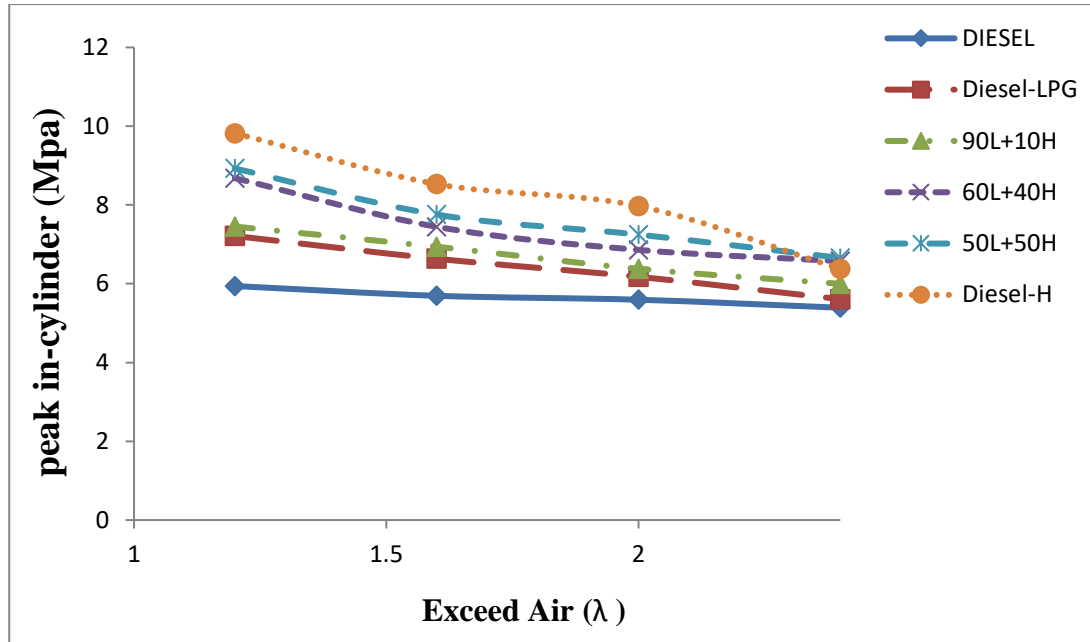


**Figure 4.5: Effect of different ratio of gaseous fuel on peak in-cylinder pressure**

Figures 4.6 a-d show the computed pressure cycles for the various numerical test cases. The crank angle degree was used to represent the results in the Figures 4.6 a-d as well as those for the later ones. The solid black line represents the first case without the gaseous supply for the engine functioning in the diesel fuel mode.

However, increasing the amount of hydrogen means that the peak pressure positions, the pressure cycle shapes, and peak pressure levels need to be modified as well due to the differences in combustion developments. As previously demonstrated, an increase in hydrogen content causes higher flame speeds for the gaseous/air mixture. This also results in the faster pressure rise that is depicted in Figures 4.6 a-d. For diesel-H<sub>2</sub>-LPG operations, the peak in-cylinder pressure gradually increased when the H<sub>2</sub> quantity was increased in LPG. Lata et al., (2012) stated that the addition of hydrogen into the LPG led to the linear increase in the speed of the laminar flame along with the increasing amounts of hydrogen in the fuel mixture. Thus, there is a gradual increase in the in-cylinder pressure as the fraction of H<sub>2</sub> increases in LPG.

Under lower excess air values, there was an increase in a peak in-cylinder pressure because both the in-cylinder gas pressure and temperature were higher. As seen in Figure 4.6-a, at 1.2 excess air and compared to diesel, dual and tri-fuel operations, the peak in-cylinder pressure rose from 5.94 to 7.21, 7.45, 8.68, 8.93, and 9.81 MPa for using diesel, LPG, and the following amounts 90L-10H, 60L-40H, 50L-50H, and H<sub>2</sub>, were added respectively. Hence, H<sub>2</sub> has a higher flame speed and rapid combustion as compared with LPG and diesel fuel.

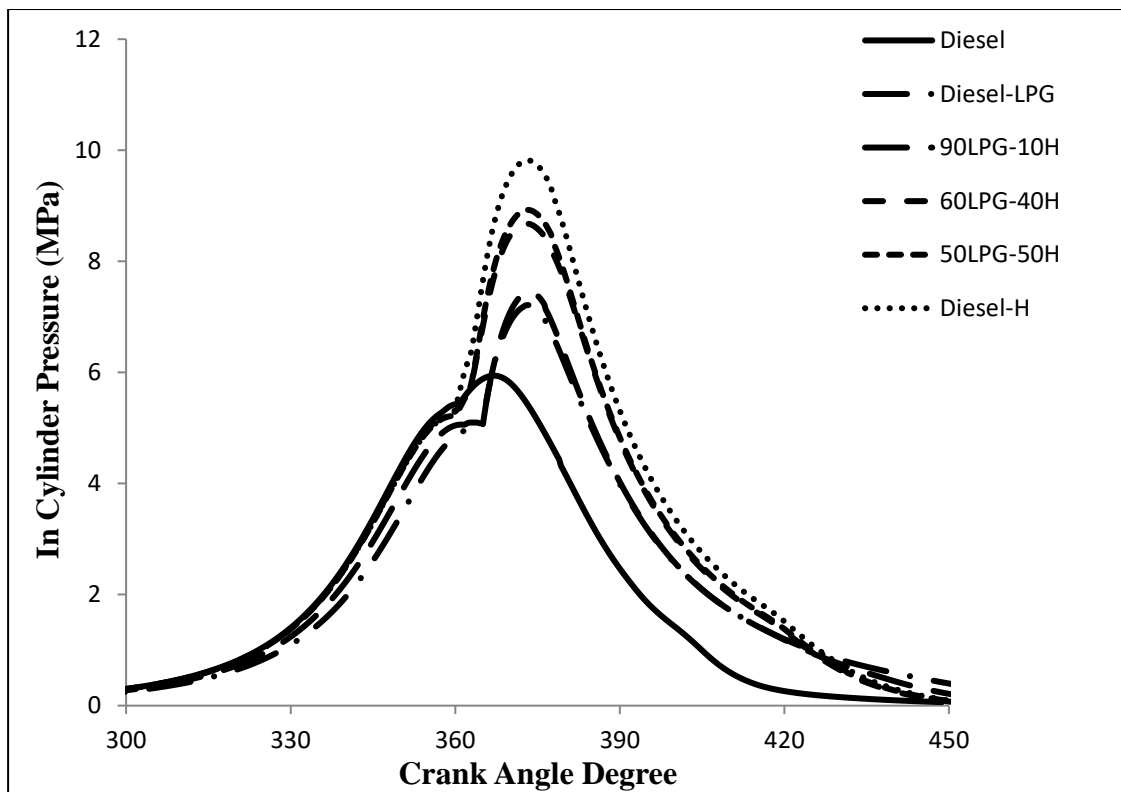


**Figure 4.6-a: in-cylinder pressure curves at 1.2 excess air and different ratio of gaseous fuel**

In this context as shown in Figure 4.6-b, at 1.6 excess air, as compared with diesel fuel, dual and tri-fuel operations, the peak in-cylinder pressure increases from 5.69 to 6.64, 6.9, 7.45, 7.75, and 8.5 MPa for diesel mode, LPG, 90L-10H, L60-H40, L50-

H<sub>2</sub>, and H<sub>2</sub>, respectively. Masood et al., (2007) indicated that the combustion tends to be faster as the percentage of hydrogen rises and thus led to increasing the peak pressure and it is seen more in the dual modes. In addition, enhancement of cylinder pressure in the presence of hydrogen is due to high specific energy content and significantly faster flame (Mansor et al., 2017).

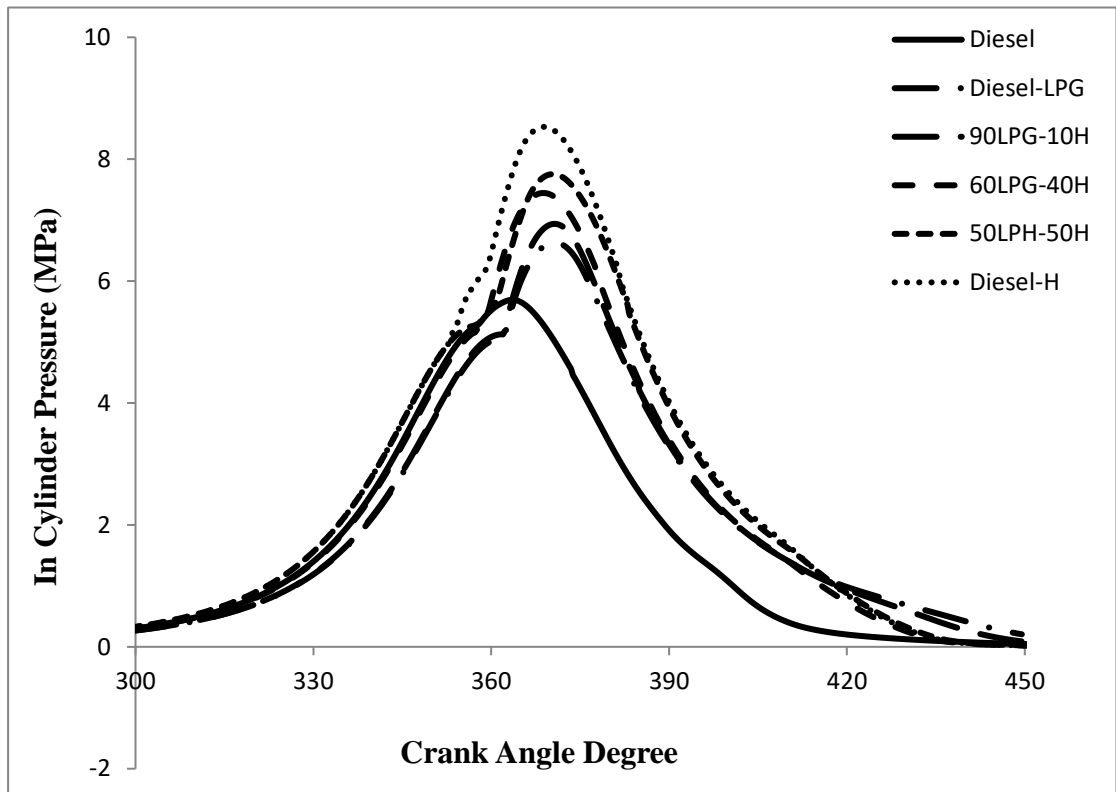


**Figure 4.6-b: in-cylinder pressure curves at 1.6 excess air and different ratio of gaseous fuel**

Similarly, in case 2 excess air, it is obvious that increasing hydrogen fraction the fuel blend results in the increase of in-cylinder pressure and also lead to advancing the occurrence of peak pressure. As shown in Figure 4.6-d, at 2 excess air, as compared with diesel fuel, dual and tri-fuel modes, the peak in-cylinder pressure increased from 5.59 to 6.185, 6.378, 6.86, 7.25, and 7.97 MPa for diesel mode, LPG, 90L-10H, L60-H40, L50-H50, and H<sub>2</sub>, respectively.

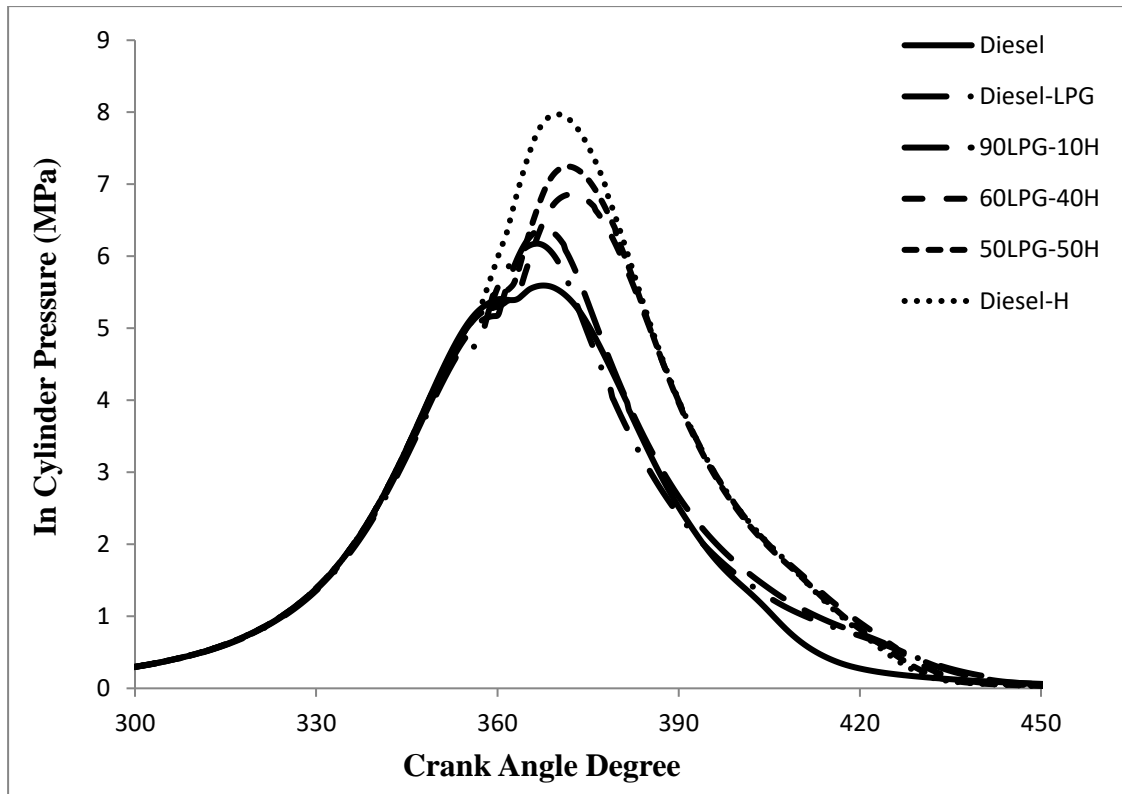


**Figure 4.6-c: in-cylinder pressure curves at 2 excess air and different ratio of gaseous fuel**

On the contrary of hydrogen addition, Qi et al., (2007) mentioned that the in-cylinder pressure peak decreases when the LPG mass fraction increases. In other words, increasing the LPG mass fraction increases the ignition delay, lowers the cetane number of the blended fuels, and leads to an increase in the amount of fuel that is burned during the premixed burning phase. Another important cause for this is the difference in flame propagation speeds between hydrogen and LPG. LPG having much lower flame propagation speed leads to reduced effect on in-cylinder pressure and consequently the heat release rate, and this behavior is more obvious at Figures 4.6 a-d.

Conversely, as seen in Figure 4.6-d, the peak pressure rose when the limit value of hydrogen was added at 2.4 excess air. For example, the increase was observed for

50L-50H, and 60L-40H to LPG, but it began to decrease under diesel-H<sub>2</sub> operations. This might be a result of the low amount of fuels in the air when compared to other similar cases and lean burn operation engine (Jafarmadar, 2014). The value for the peak in-cylinder pressure rose from 6.57 to 6.65 MPa when 60L-40H, and 50L-50H were added, respectively. However, it went down to 6.37 MPa for diesel-H<sub>2</sub>.

Generally, the diesel fuel is the ignition source in a gas-diesel dual fuel engine. Moreover, the succeeding flame propagation has its basis on the combustion of the premixed gaseous fuel-air mixture. Diesel-H<sub>2</sub> and diesel-LPG have different combustions because both H<sub>2</sub> and LPG possess varying flame propagation speeds. Such lower flame propagation speed of LPG leads to a slighter in-cylinder pressure impact. A lengthy ignition delay has been observed for diesel-LPG at all excess air. Zhou et al., (2014) suggested that the longer ignition delay is due to the higher values of reduced partial oxygen pressure and gaseous fuel in the air.

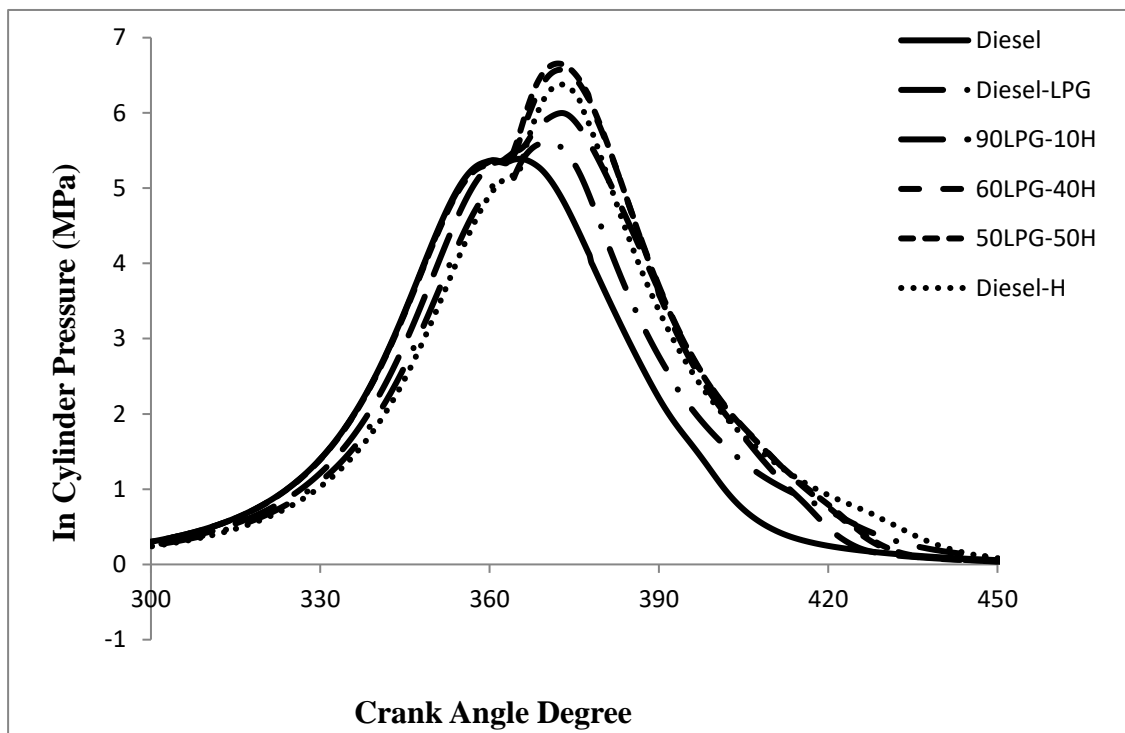


**Figure 4.5-d: in-cylinder pressure curves at 2.4 excess air and different ratio of gaseous fuel**

## B. Temperature

Figure 4.7 show the histories for the in-cylinder temperature for the various gaseous fuel additions under different excess air ( $\lambda$ ). It was noted that when each gaseous fuel was added, the in-cylinder temperature was lowered when the value of excess air rose. For example, the in-cylinder temperature with diesel-H<sub>2</sub> operation clearly decreased from 2632 to 2118, 1955, and 1928 K when operating at excess air values of 1.2, 1.6, 2, and 2.4, respectively. Additionally, for diesel-LPG operation, there was a clear decrease in the cylinder temperature values from 2263 to 1594, 1483, and 1394 K when operating under excess air values of 1.2, 1.6, 2, and 2.4, respectively. For lower excess air ratios the in-cylinder temperature increases noticeably during the combustion and power strokes, due to the advancing of the combustion process and lower combustion duration (Jafarmadar, 2014).

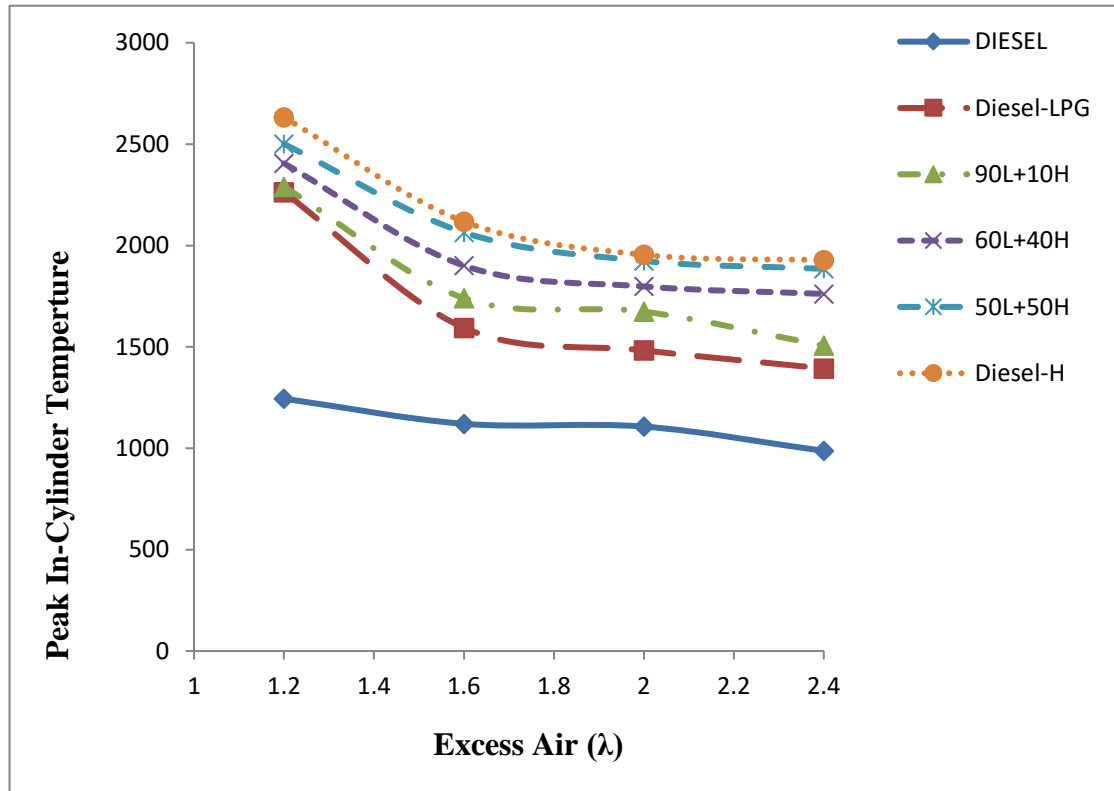


Figure 4.7: Effect of different ratio of gaseous fuel on peak in-cylinder temperature

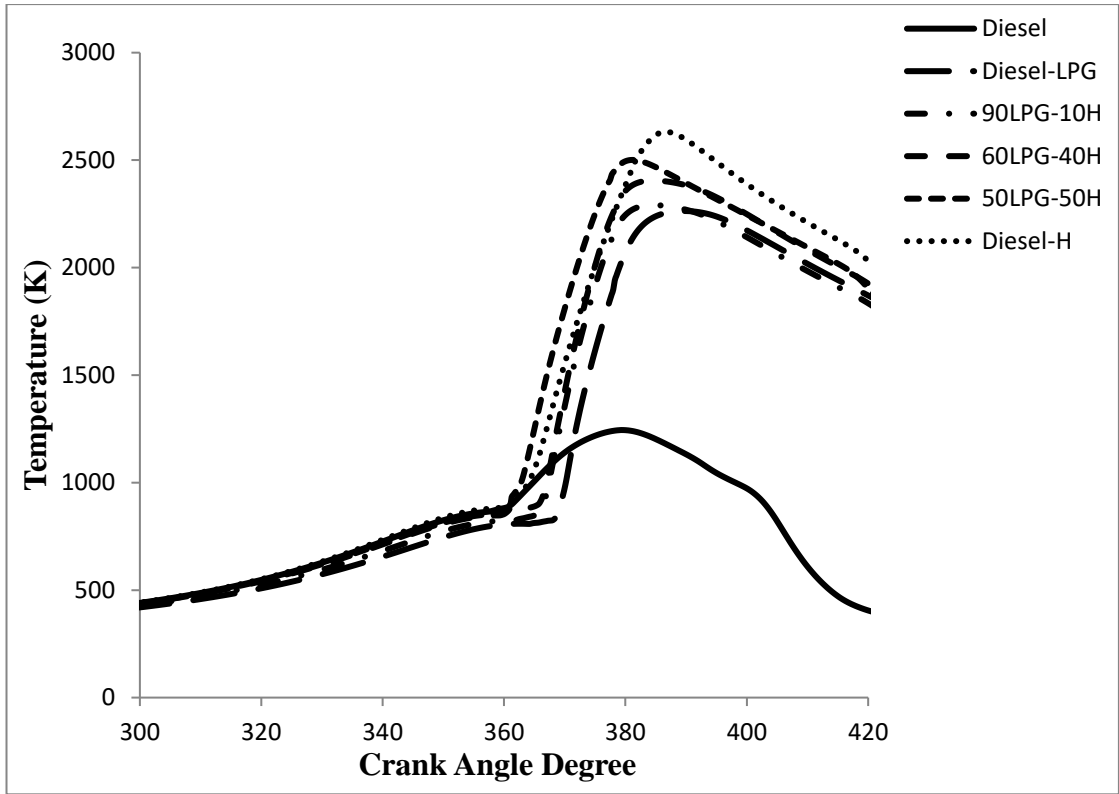


Figures 4.8 a-d, show the in-cylinder temperature rises with the increase of H<sub>2</sub> fraction in LPG throughout the processes of combustion and expansion strokes. The in-cylinder temperature was still relatively high even if excess air's ultra-value was measured with H<sub>2</sub> because of hydrogen's fast burning level, led to the high combustion temperature and higher flame propagation speed. Thus, the temperature values under the diesel-90L-10H operation were still lower compared to operations for diesel-50L-50H, diesel-60L-40H, and diesel-H<sub>2</sub> under all excess air values (1.2, 1.6, 2, and 2.4). Hence, increasing the mass fraction of LPG rise in the heat of evaporation value for diesel-LPG. As a result, decrease the temperature of the cylinder gasses (Qi et al., 2007).

At 1.2 excess air as illustrated in Figure 4.8-a, the in-cylinder temperature is enhanced with the presence of each gaseous fuel and is more apparent with higher hydrogen fraction. The values increase from 1245 to 2263, 2290, 2406, 2501, and 2632 K when using diesel, LPG, 90L-10H, 60L-40H, 50L-50H and H<sub>2</sub>, respectively. The same results were observed with excess air values of 1.6, 2 and 2.4. The rise observed for the in-cylinder temperature can be attributed to several factors, such as the burning of the fuel mixture during the diffusion phase and the propagation of the flame could have affected the reaction. Moreover, it could be due to the premixed mixture's burning as mentioned by Jafarmadar (2014). Consequently, a rise in the peak temperature of the high excess air of 2.4 as shown in Figure 4.8-d was measured when the amount of hydrogen was increased for all gaseous fuel and when compared to diesel fuel and LPG. The values rose from 987 to 1394, 1507, 1761, 1885, and 1928 K for diesel, LPG, 90L-10H, 60L-40H, 50L-50H and H<sub>2</sub>.

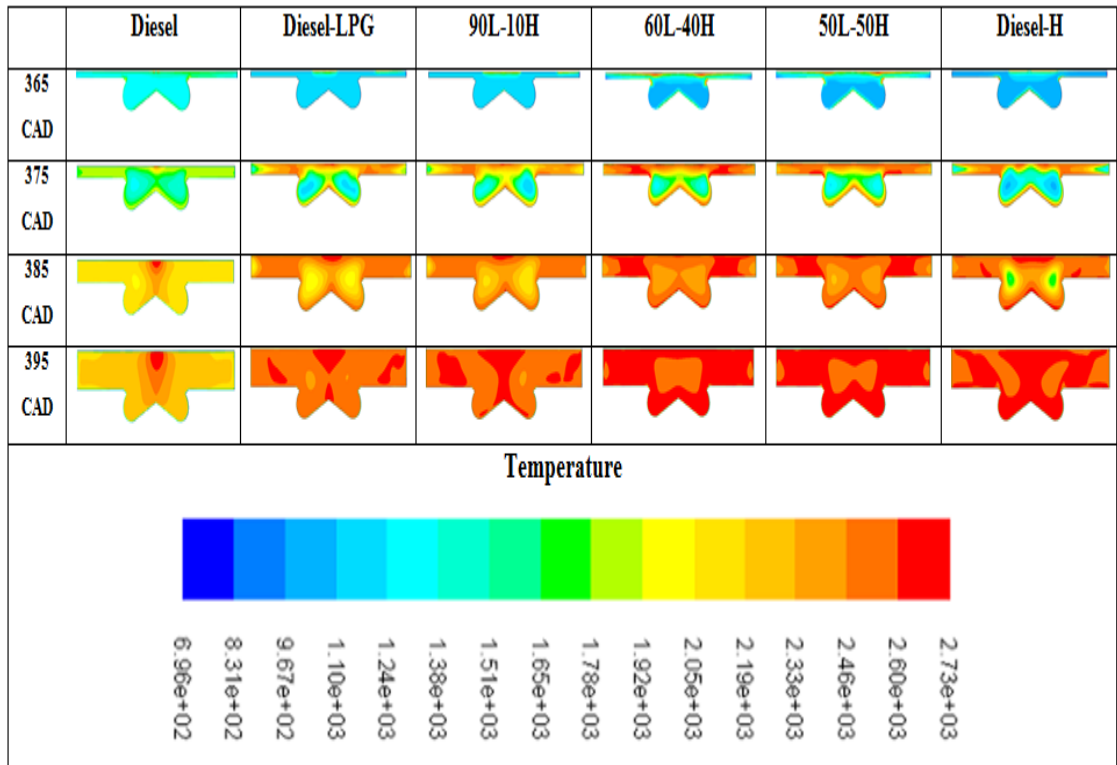
In general, Figures 4.8 a-d depicts the effect of different mixture blends on the in-cylinder temperature. The difference in the combustion of diesel-H<sub>2</sub> and diesel-LPG, under the same energy substitution ratio, is large because of different flame propagation speeds of hydrogen and LPG. The flame propagation speed of LPG is much lower, leading to its smaller impact on in-cylinder pressure and temperature rate. As well as, for diesel-LPG, longer ignition delay is observed at all engine operation conditions.

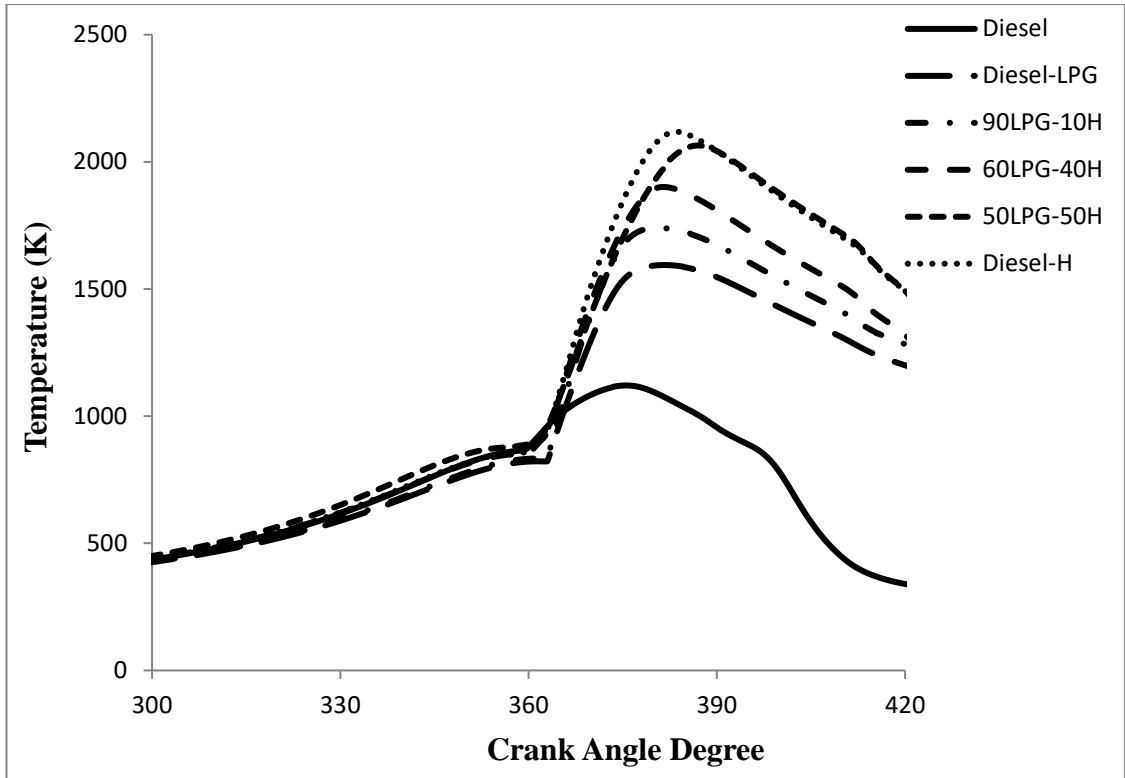
Table 4.1-a present the contours of temperature distribution at several crank angle degrees (CAD) at 1.2 values of excess air under varying gaseous addition ratios. It can be seen that the temperature distribution and formation region reduced when LPG addition to diesel comparing with H<sub>2</sub> addition. Increasing the mass fraction of LPG rise in the heat of evaporation value for diesel-LPG. As well, the flame propagation speed of LPG is also much lower, leading to its smaller impact on temperature rate. As a result, lower distribution temperature as shown in 375, 385, and 395 CAD. In contrast, the temperature distribution is expanded when the H<sub>2</sub> mass fraction increased in diesel-LPG. Higher hydrogen content resulted in a bigger fraction of higher temperature concentration zone (red). Likewise, it is more obvious at 385, and 395 CAD, for 60L-40H, 50L-50H under tri-fuel modes and it reaches the maximum value at diesel-H<sub>2</sub> for dual operation. The same result can observe for the temperature distribution contours with less noticeable effect at 1.6, 2, and 2.4 excess air. Hence, the amount of the gaseous fuel is less with increased the value of excess air as illustrated in Appendix B.



**Figure 4.8-a: Temperature curves under 1.2 excess air and different ratio of gaseous fuel**

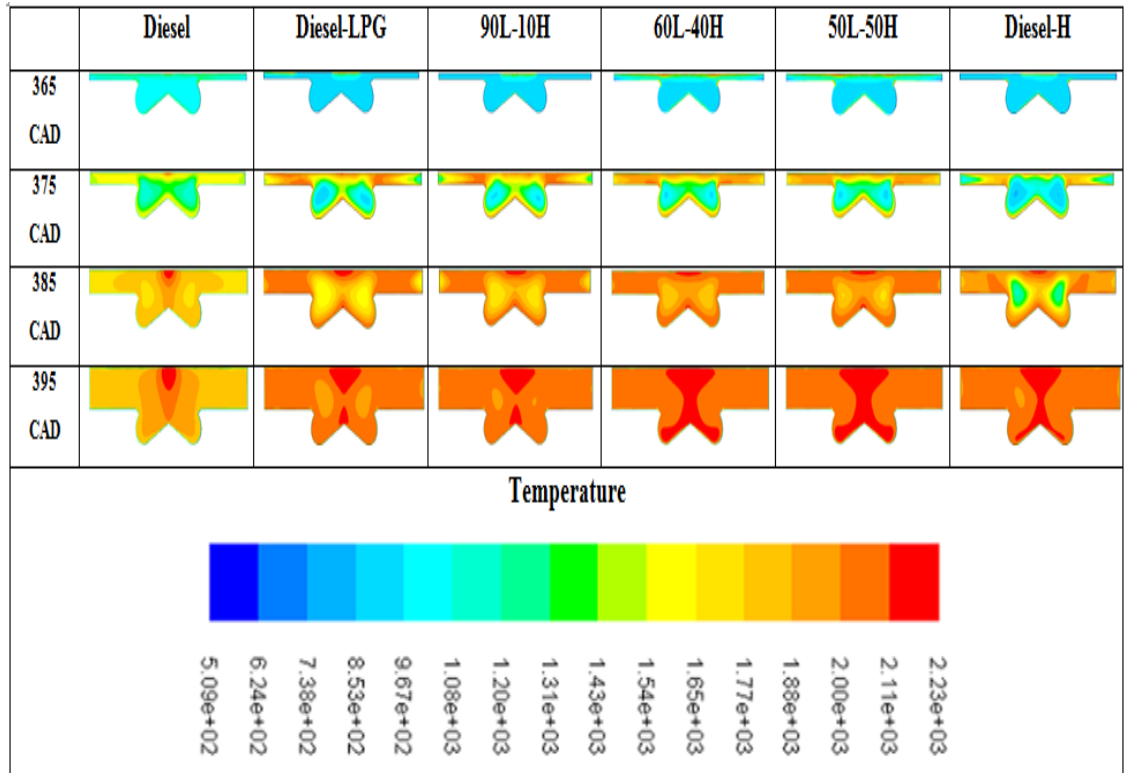
**Table 4.1-a: The development of average temperature under 1.2 excess air and different ratio of gaseous fuel**





**Figure 4.8-b: Temperature curves under 1.6 excess air and different ratio of gaseous fuel**

**Table 4.1-b: The development of average temperature under 1.6 excess air and different ratio of gaseous fuel**



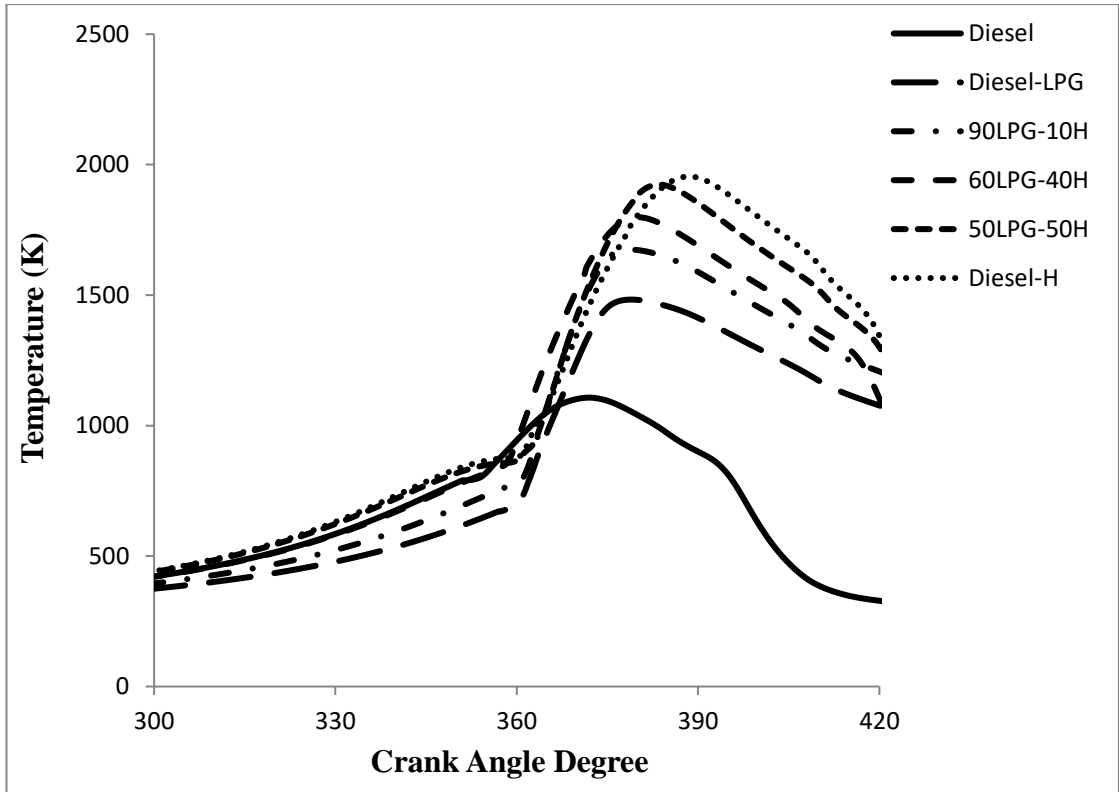


Figure 4.8-c: Temperature curves under 2 excess air and different ratio of gaseous fuel

Table 4.1-c: The development of average temperature under 2 excess air different ratio of gaseous fuel

	Diesel	Diesel-LPG	90L-10H	60L-40H	50L-50H	Diesel-H
365 CAD						
375 CAD						
385 CAD						
395 CAD						
Temperature						
	5.06e+02	6.15e+02	7.23e+02	8.31e+02	9.40e+02	1.05e+03
						1.16e+03
						1.26e+03
						1.37e+03
						1.48e+03
						1.59e+03
						1.70e+03
						1.81e+03
						1.91e+03
						2.02e+03
						2.13e+03

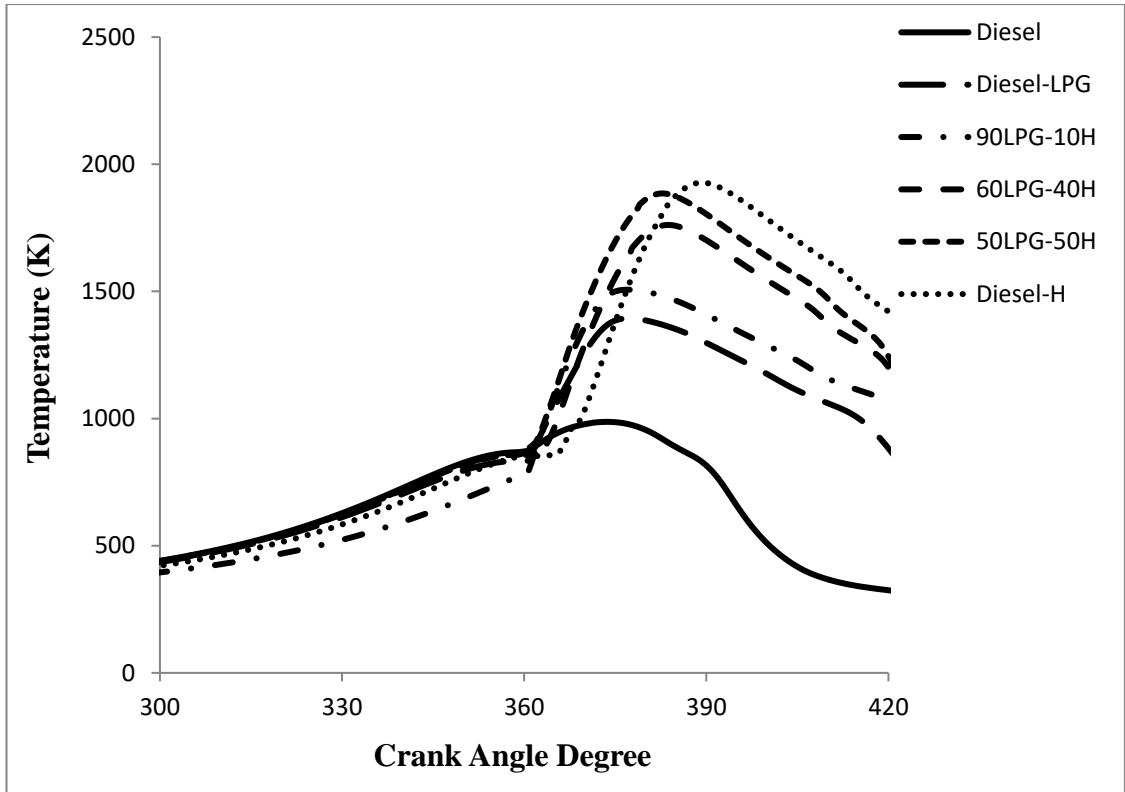


Figure 4.8-d: Temperature curves under 2.4 excess air and different ratio of gaseous fuel

Table 4.1-d: The development of average temperature under 2.4 excess air different ratio of gaseous fuel

	Diesel	Diesel-LPG	90L-10H	60L-40H	50L-50H	Diesel-H
365 CAD						
375 CAD						
385 CAD						
395 CAD						
Temperature						
	4.77e+02	5.77e+02	6.78e+02	7.78e+02	8.79e+02	9.79e+02
			1.08e+03	1.18e+03	1.28e+03	1.38e+03
				1.48e+03	1.58e+03	1.68e+03
					1.78e+03	1.88e+03
						1.98e+03

## 4.5.2. Emissions

### A. Nitrogen Oxides (NO<sub>x</sub>)

The nitrogen oxides are generally made up of nitrogen dioxide (NO<sub>2</sub>) in small amounts and nitric oxide (NO). Generally, these are formed when the atmospheric nitrogen is oxidised in the combustion chamber. When gaseous fuel is combusted, the formation of NO<sub>x</sub> takes place behind the flame front. The oxygen availability and combustion temperatures mainly influence NO formation. On the other hand, NO<sub>x</sub> formation in the dual fuel engine is generally reliant on the diesel pilot spray zone. NO<sub>x</sub> formation decreases when the quantity and size of the pilot diesel fuel increase as well. Additionally, a rise in the nitrogen oxide emission was observed when the oxygen concentration, cylinder temperature, and combustion duration were all increased (Lata et al., 2012). Figure 4.9 demonstrates the variation of nitrogen oxides with excess air ( $\lambda$ ). There was a decrease in NO<sub>x</sub> emission when the excess air was increased.

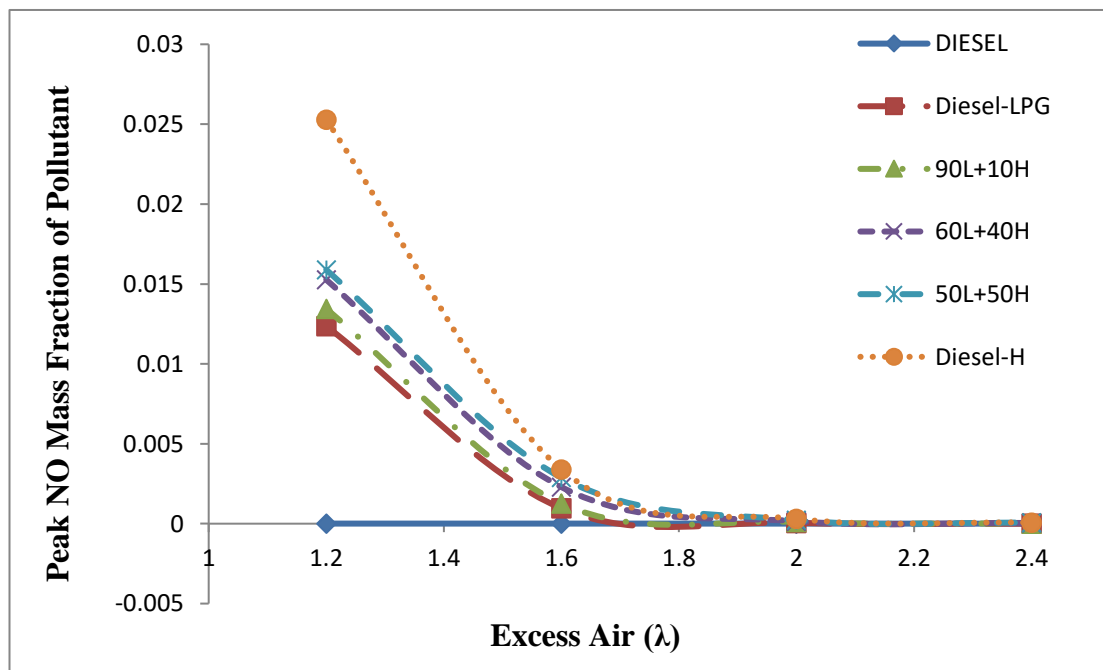


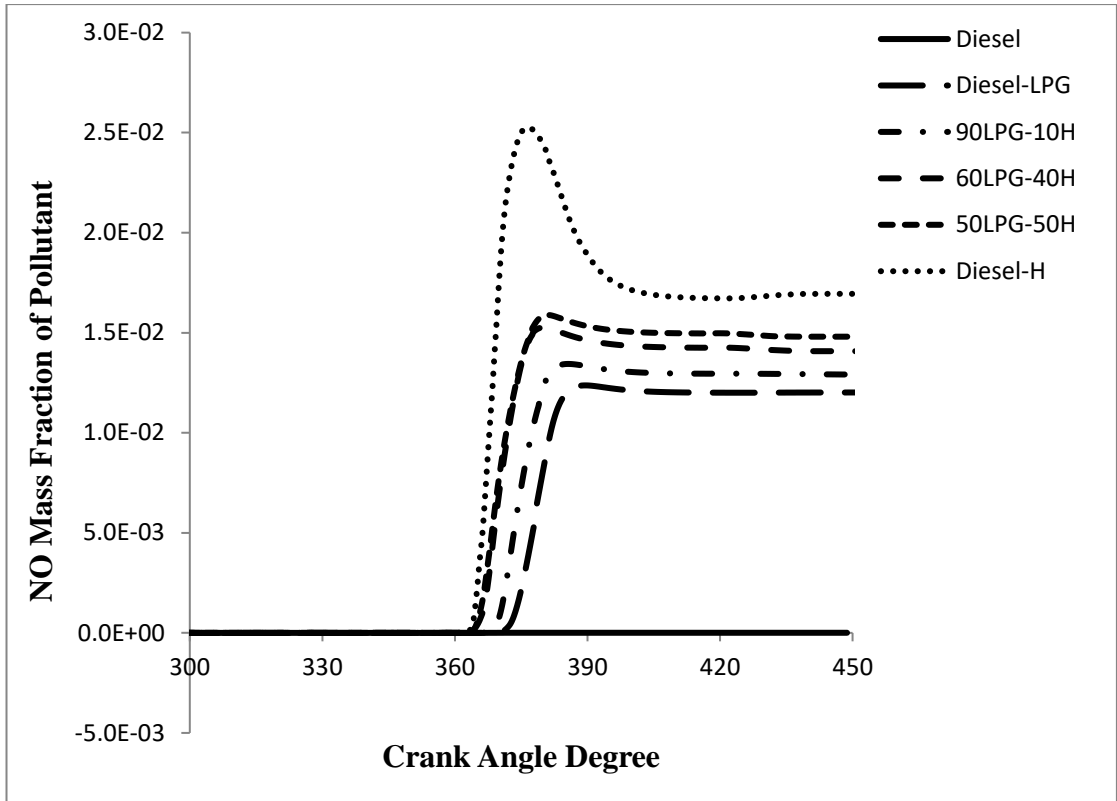
Figure 4.9: Effect of different ratio of gaseous fuel on peak NO emissions

This study used three mixtures of H<sub>2</sub>-LPG under tri-fuel operation. The best for the decrease in NO<sub>x</sub> emission was studied using the highest LPG or the lowest H<sub>2</sub> values. Qi et al., (2007) suggested that a decrease in the concentration of NO<sub>x</sub> is observable when the mass fraction of LPG in the blended fuels is increased. This is due to the fact that a rise in the heat of evaporation values for the diesel-LPG blended fuels, coupled with the increase of the mass fraction of LPG in hydrogen revealed the best effect towards NO<sub>x</sub> emission reduction and lowers the temperature of the cylinder gasses. Thus, for the operation using diesel-90L-10H, the lowest NO<sub>x</sub> emissions were recorded than using the diesel-60L-40H and diesel-50L-50H operations under all excess air values.

Results from 1.2 excess air can be seen in Figure 4.10-a. It was noted that the addition of H<sub>2</sub> fraction to LPG increased the NO<sub>x</sub> mass fraction in comparison to the diesel and LPG, with values rising from  $5.18 \times 10^{-6}$  to  $1.24 \times 10^{-2}$ ,  $1.34 \times 10^{-2}$ ,  $1.53 \times 10^{-2}$ ,  $1.59 \times 10^{-2}$ , and  $2.53 \times 10^{-2}$  when using diesel, LPG, L90-H10, L50-H50, L60-H40, and H<sub>2</sub> respectively. This phenomenon is explained by the fast hydrogen fuel combustion, higher pressure and temperature compared to diesel and LPG combustion (Lim et al., 2015). In addition, according to Choi et al., (2005), the rise in NO<sub>x</sub> emissions that was observed when H<sub>2</sub> was added was dependent on hydrogen fuel's flame temperature, which is higher compared to that of the LPG fuel. However, Figures 4.10 a-d show that increasing diesel content suppresses NO<sub>x</sub> formation due to the low combustion temperature of diesel while increasing hydrogen content rise NO<sub>x</sub> formation due to higher flame temperature (Mansor et al., 2017). For example, at 2.4 excess air, the NO<sub>x</sub> emission increased from  $9.56 \times 10^{-7}$  to  $6.69 \times 10^{-5}$  for diesel case and hydrogen addition respectively.

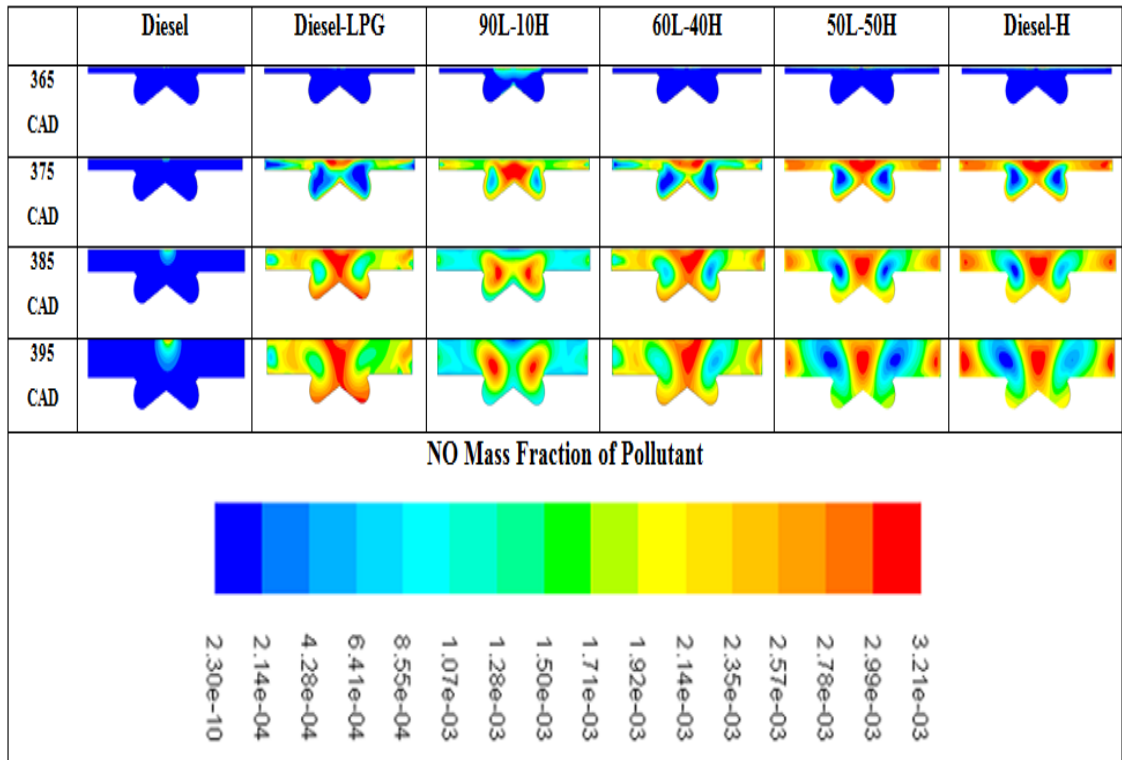


Table 4.2-a illustrated the contours of the  $\text{NO}_x$  emission and its formation region at 1.2 value of excess air under varying gaseous addition ratios at several crank angle degrees (CAD). However, the  $\text{NO}_x$  formation region was expanded with rising the  $\text{H}_2$  mass fraction in the fuel mixture as presented in the Table 4.2-a, at 375, 385, and 395 CAD for diesel- $\text{H}_2$ , 50L-50H, and 60L-40H and reached to maximum region formation at diesel- $\text{H}_2$  under dual fuel operation, also revealed higher concentration zone (red) for diesel-L50-H50 under tri-fuel operation. Thus,  $\text{H}_2$  addition to LPG can increase the velocity of combustion as well as temperatures of combustion that in turn increases  $\text{NO}_x$  emission. Oppositely, the formation region of  $\text{NO}_x$  decrease when the LPG mass fraction increased in the blended fuels as shown at 375, 385, and 395 CAD for LPG, and 90L-10H tables. Hence, increasing the mass fraction of LPG in the blend led to rising in the heat of evaporation values and lower the temperature of the cylinder gasses. Besides, the flame propagation speed of LPG is much lower, leading to smaller impact on temperature rate. As a result reduced the formation region of  $\text{NO}_x$  emission. The same result can be observed for the  $\text{NO}_x$  formation contours with less noticeable effect at 1.6, 2, and 2.4 excess air.



**Figure 4.10-a: NO emissions curves under 1.2 excess air and different ratio of gaseous fuel**

**Table 4.2-a: The development of NO mass fraction of pollutant under 1.2 excess air and different ratio of gaseous fuel**



Similarly, Figure 4.10-b at 1.6 excess air when adding an H<sub>2</sub> fraction to LPG the NO mass fraction was increased as compared with diesel and LPG fuel from  $5.04 \times 10^{-6}$  to  $9.62 \times 10^{-4}$ ,  $1.26 \times 10^{-3}$ ,  $2.29 \times 10^{-3}$ ,  $2.88 \times 10^{-3}$ , and  $3.4 \times 10^{-3}$  for diesel, LPG, L90-H10, L60-H40, L50-H50, and H<sub>2</sub> respectively. In addition, Table 4.2-b represented that the NO mass formation region with different gaseous substitution at various excess air and it reached its maximum rate at the diesel-H<sub>2</sub> operation.

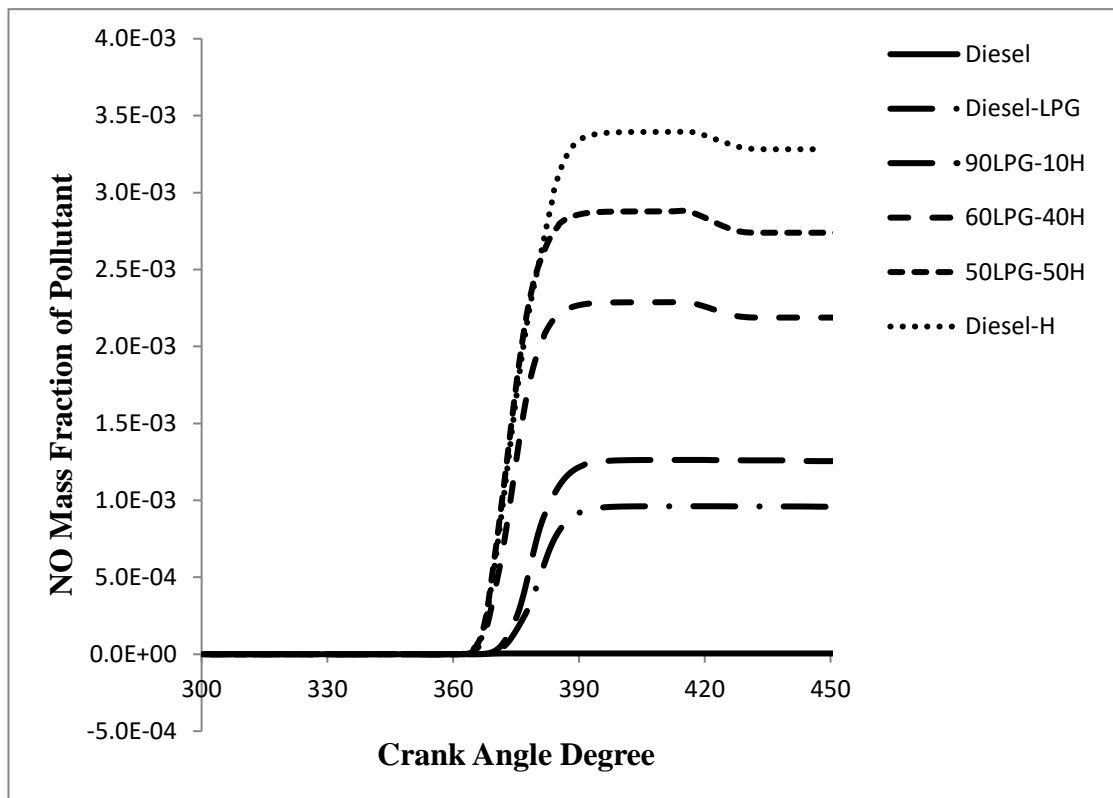
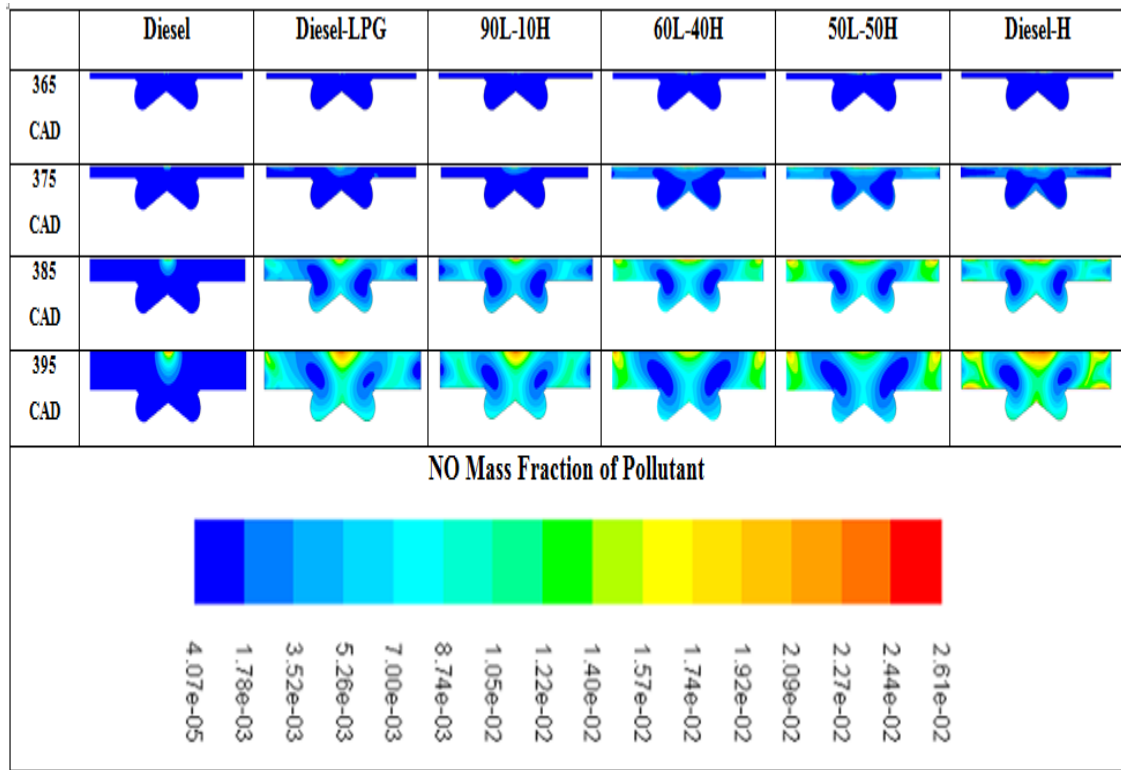


**Figure 4.10-b: NO emissions curves under 1.6 excess air and different ratio of gaseous fuel**

**Table 4.2-b: The development of NO mass fraction of pollutant under 1.6 excess air and different ratio of gaseous fuel**



Likewise, at 2 excess air as shown in Figure 4.10-c, when adding an H<sub>2</sub> fraction to LPG the NO mass fraction was increased as compared with diesel and LPG fuel from  $4.39 \times 10^{-6}$  to  $5.64 \times 10^{-5}$ ,  $1.09 \times 10^{-4}$ ,  $1.51 \times 10^{-4}$ ,  $2.25 \times 10^{-4}$ , and  $3.03 \times 10^{-4}$  for diesel, LPG, L90-H10, L60-H40, L50-H50, and H<sub>2</sub> respectively. Increasing the mass fraction of the H<sub>2</sub> in fuel blend will lead to a rise in combustion temperature and rise the NO emission. Table 4.2-c presented that the NO mass fraction of pollutant and its formation region increased along with the enhancement of H<sub>2</sub> addition to LPG and it reached its maximum rate at the diesel-H<sub>2</sub> operation for dual fuel and 50L-50H for tri-fuel operation.

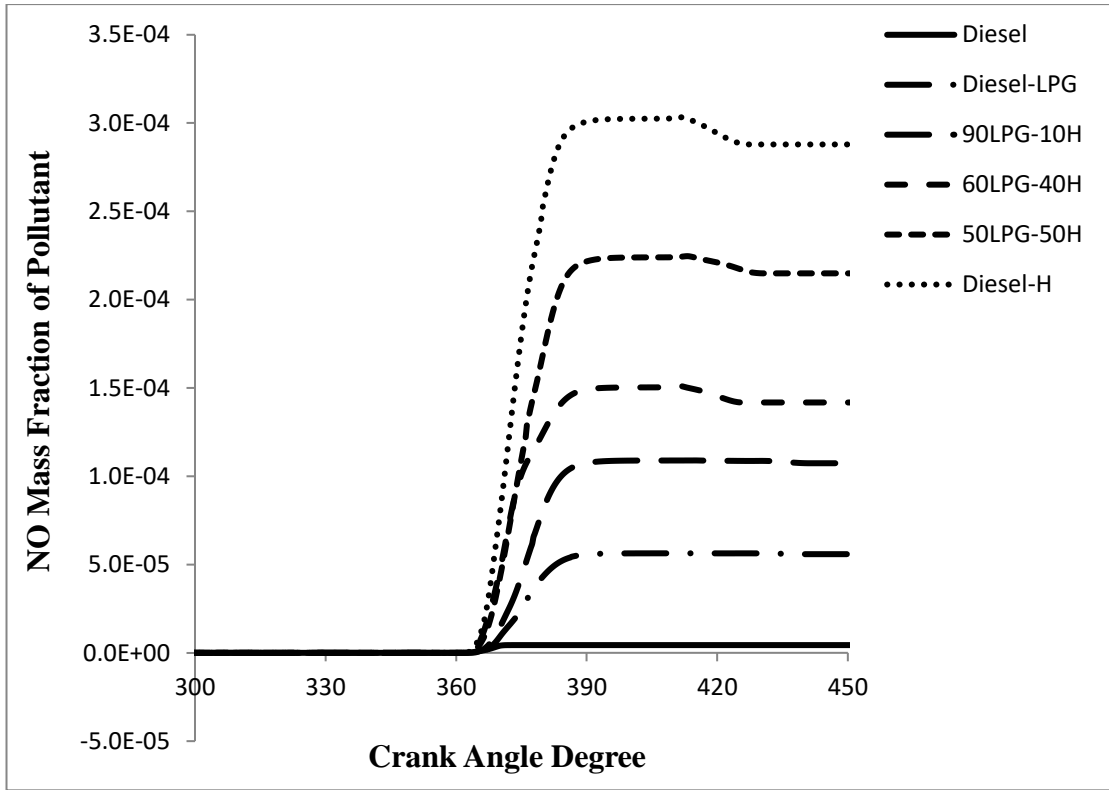
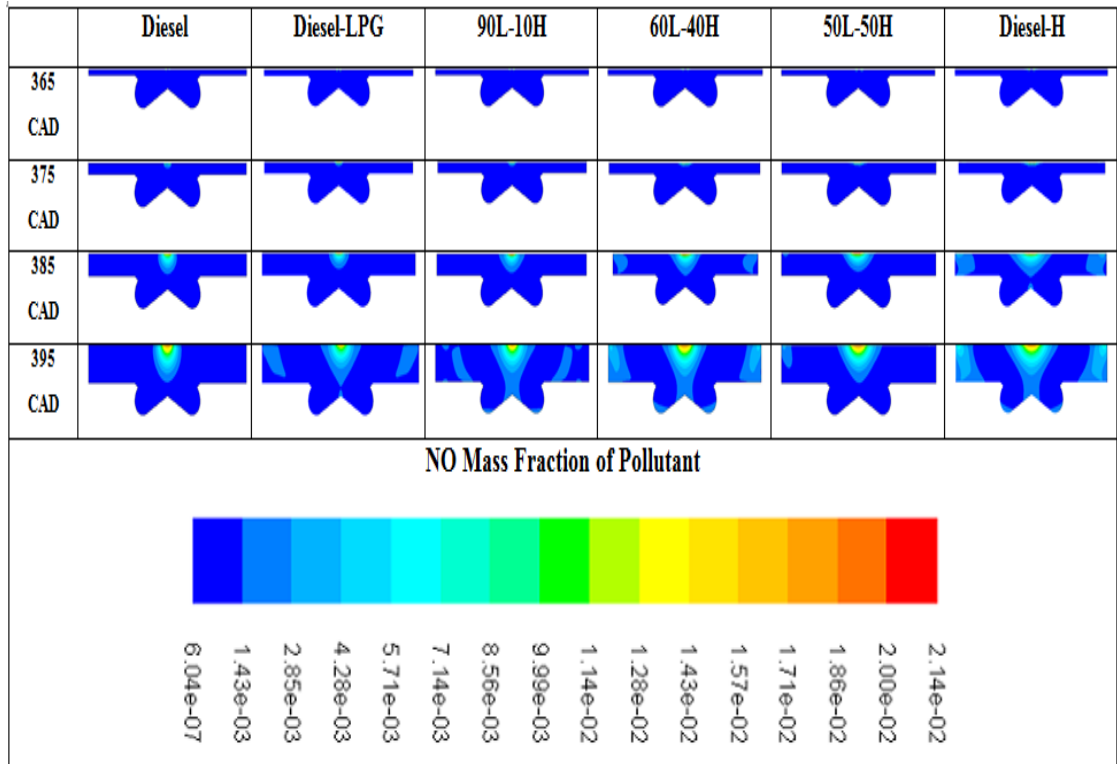


**Figure 4.10-c: NO emission curves under 2 excess air and different ratio of gaseous fuel**

**Table 4.2-c: The development of NO mass fraction of pollutant under 2 excess air and different ratio of gaseous fuel**



In the end, at 2.4 excess air as shown in Figure 4.10-d, when adding an H<sub>2</sub> fraction to LPG the NO mass fraction was increased compared with diesel and LPG from  $9.56 \times 10^{-7}$  to  $2.92 \times 10^{-6}$ ,  $8.01 \times 10^{-6}$ ,  $4.31 \times 10^{-5}$ ,  $5.91 \times 10^{-5}$ , and  $6.69 \times 10^{-5}$ , for using diesel, LPG, 90L-10H, 60L-40H, 50L-50H and H<sub>2</sub>, respectively.

Tables 4.2-d showed the formation region of NO at 2.4 excess air value at several crank angle degrees (CAD) under various ratios of gaseous fuel addition. The H<sub>2</sub> addition to LPG increased the velocity of combustion as well as temperatures of combustion that in turn increases NO emission as shown at 395CAD for 50L-50H, and H<sub>2</sub> compared with increasing the value LPG gaseous at the same excess air ratio.

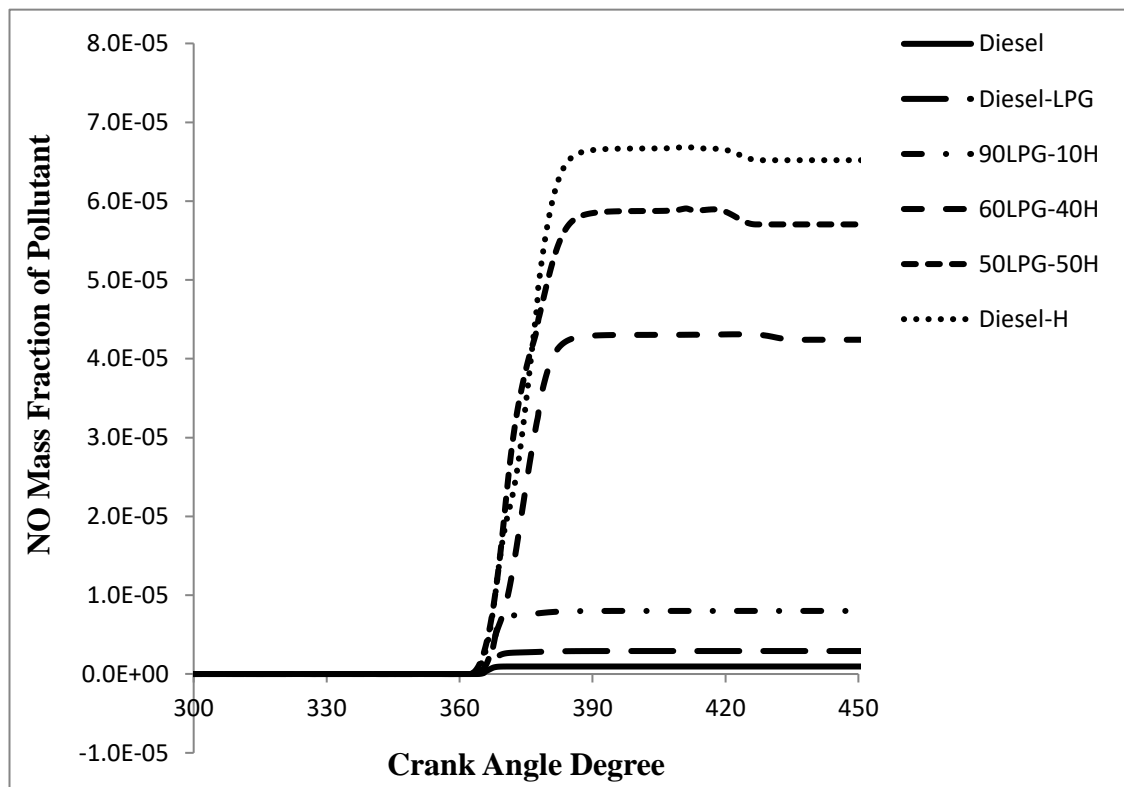
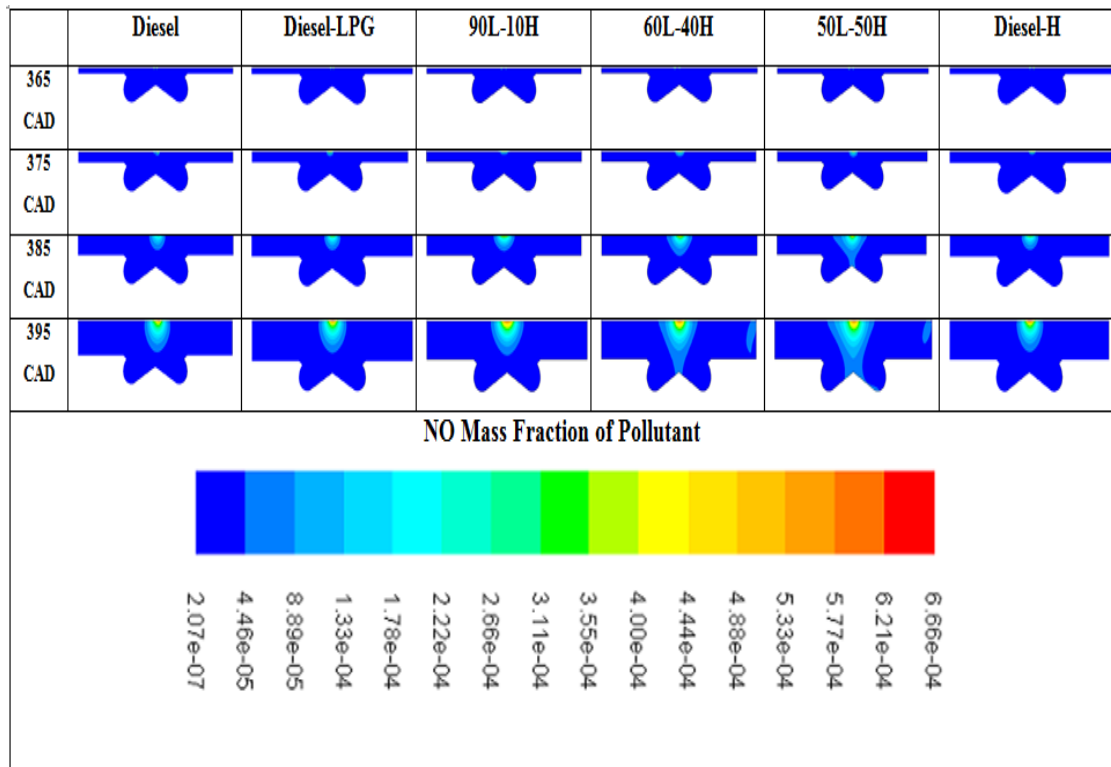


**Figure 4.9-d: NO emission curves under 2.4 excess air and different ratio of gaseous fuel**

**Table 4.2-d: The development of NO mass fraction of pollutant under 2.4 excess air and different ratio of gaseous fuel**



### B. Carbon Monoxide (CO)

CO emissions are strongly affected with the relative air-fuel ratio ( $\lambda$ ) and also by the C/H ratio of the fuels. Moreover, incomplete combustion is the main cause of most CO emissions. Incomplete combustion occurs because of low gas temperatures and the lack of oxidants (Cinar et al., 2016; Gatts et al., 2012). Figure 4.11, shows the CO levels when the values of excess air ( $\lambda$ ) vary. There was an observed decrease in CO emission when the excess air was increased. For example, under diesel-H<sub>2</sub> operation, there was a clear decrease in CO mass fraction values from  $5.7 \times 10^{-3}$  to  $3.5 \times 10^{-3}$ ,  $2.95 \times 10^{-3}$ , and  $2.52 \times 10^{-3}$  under excess air values of 1.2, 1.6, 2, and 2.4, respectively.

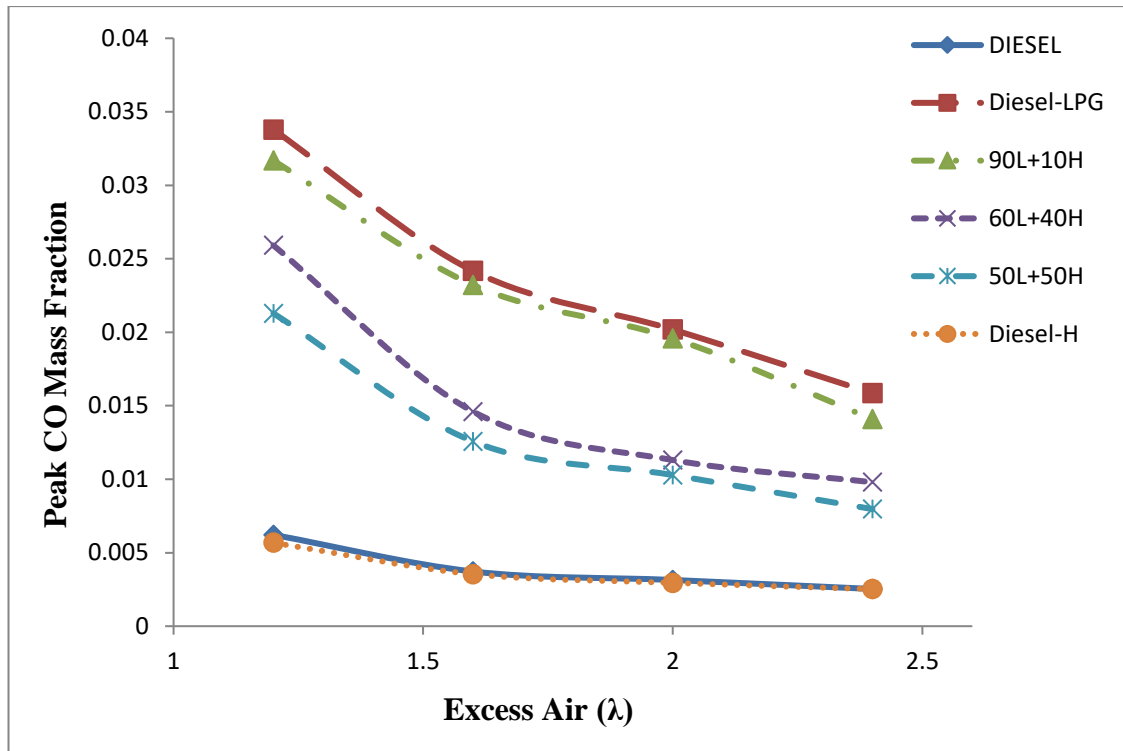


**Figure 4.11: Effect of different ratio of gaseous fuel on peak CO emissions**

Figures 4.12 a-d demonstrate the CO emission variations for operations of the diesel, dual and tri-fuel engines. It was noticed that the fact that higher LPG presence increases the peak value of CO can be attributed to its relatively slow flame speed that leads to incomplete combustion. Thus, an obvious increase in the CO mass fraction was observed, especially when comparing with diesel fuel and H<sub>2</sub> addition to LPG. The values rise from  $6.22 \times 10^{-3}$  to  $2.13 \times 10^{-2}$ ,  $2.59 \times 10^{-2}$ ,  $3.17 \times 10^{-2}$ , and  $3.38 \times 10^{-2}$  for operations under diesel fuel and with the addition of 50L-50H, 60L-40H, 90L-10H, and diesel-LPG, respectively. These were all taken at 1.2 excess air value as seen in Figure 4.12-a and the same result can observe for excess air 1.6, 2, and 2.4. Liquid petroleum gas's high carbon ratio could have led to the increase in carbon monoxide emission. The present study examined the air-fuel ratio ( $\lambda$ ) in LPG.



However, the CO emissions were still high even with the variable value of excess air that was used for the LPG.

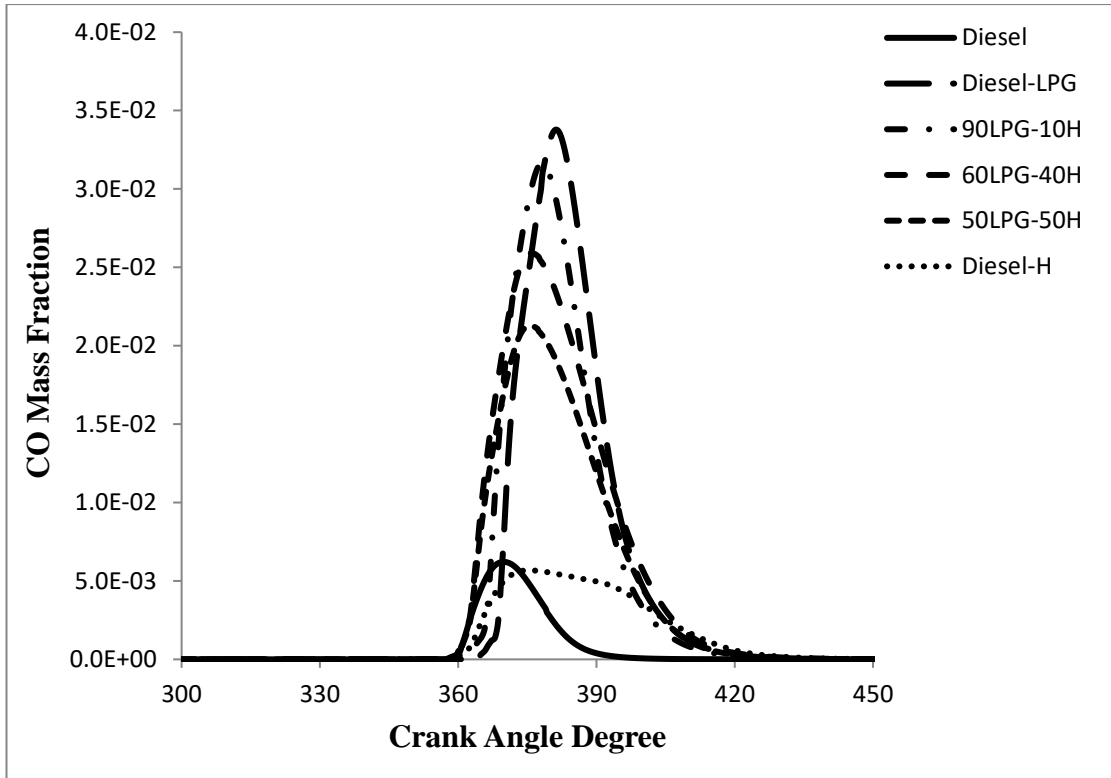
Conversely, the CO emission is lowered when hydrogen's mass fraction in diesel increases. This is in comparison with diesel-LPG fuel operating at all excess air as illustrated in Figures 4.12 a-d. At an excess air value of 2.4, when the amount of hydrogen was increased, a decrease in the CO mass fraction was observed from  $1.41 \times 10^{-2}$  to  $9.79 \times 10^{-3}$ ,  $7.97 \times 10^{-3}$ , and  $2.52 \times 10^{-3}$  for 90L-10H, 60L-40H, 50L-50H, and diesel-H<sub>2</sub> respectively. This is because the gradual lowering of the diesel flow rate takes place simultaneously with the rise in gaseous blends. CO is lowered when the hydrogen energy fraction increases. Hydrogen addition causes enhanced combustion and abundant oxygen is readily accessible for use in the post-oxidation of CO emission. As well as, increasing the hydrogen enrichment fraction allows for the increased formation of O and OH radicals, resulting in a complete combustion (Zhen et al., 2012).

Additionally, hydrogen has a high stoichiometric air-to-fuel ratio and flame speed, which allow its fast combustion and quick consumption of the adjacent air. These reactions could lead to the formation of a couple of lean-oxygen zones in the cylinder and even hinder the oxidation of CO in these areas. Compared to diesel, a shorter post-combustion period is produced. Thus, the necessary cylinder temperature and time for CO oxidation reaction are not easily achieved. This leads to slower reaction kinetics of CO into CO<sub>2</sub>. This effect is investigated in this study as shown in Figures 4.12 a-d. It was observed that CO emission was significantly lowered when hydrogen addition was performed. Therefore, using 50L-50H can lower CO emission compared to the two other H<sub>2</sub>-LPG mixtures under tri-fuel operation. Choi et al., (2005) have suggested that CO emissions could possibly decrease when hydrogen

was added since the amount of oxygen decreases in the rich and stoichiometric areas because of the increase in hydrogen supplement rate.

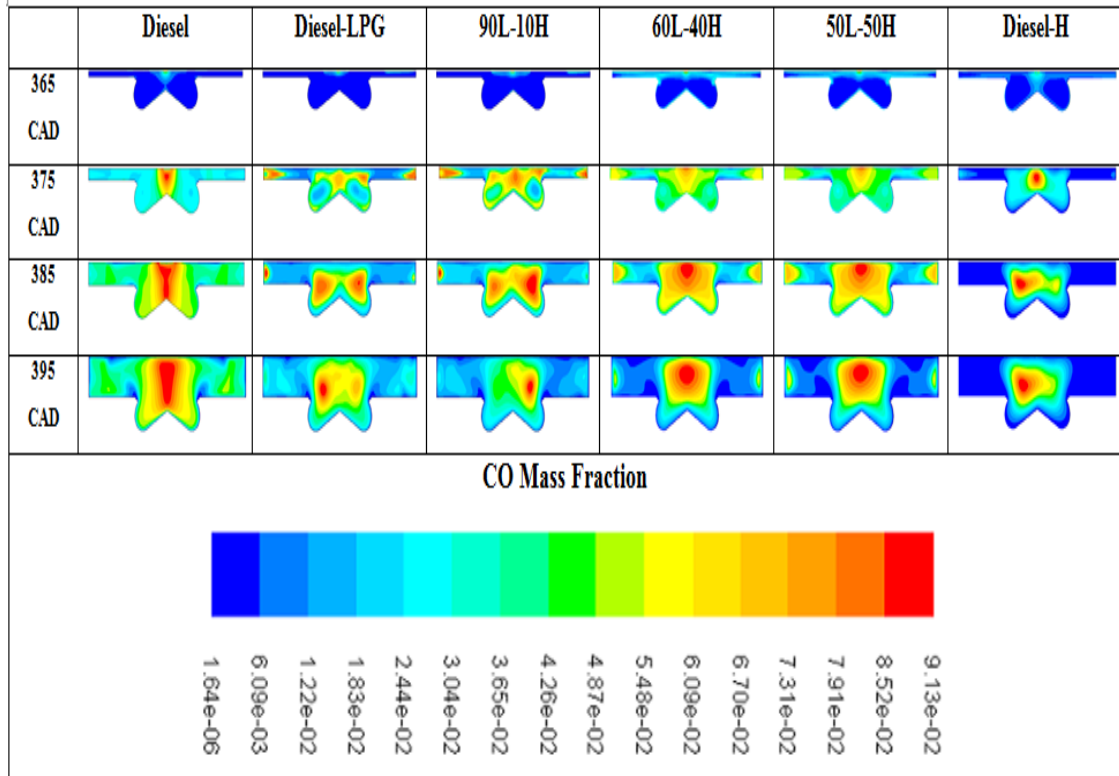
However, the CO emission decreased for diesel-H<sub>2</sub> at a value of 1.2 excess air to  $5.68 \times 10^{-3}$  when compared to the diesel fuel mode value of  $6.22 \times 10^{-3}$ . The same result also can be observed for excess air 1.6, 2, and 2.4. It is quite established that diesel combustion results in low CO combustion. With the introduction of H<sub>2</sub> in diesel, the reduction is further reduced (Mansor et al., 2017).

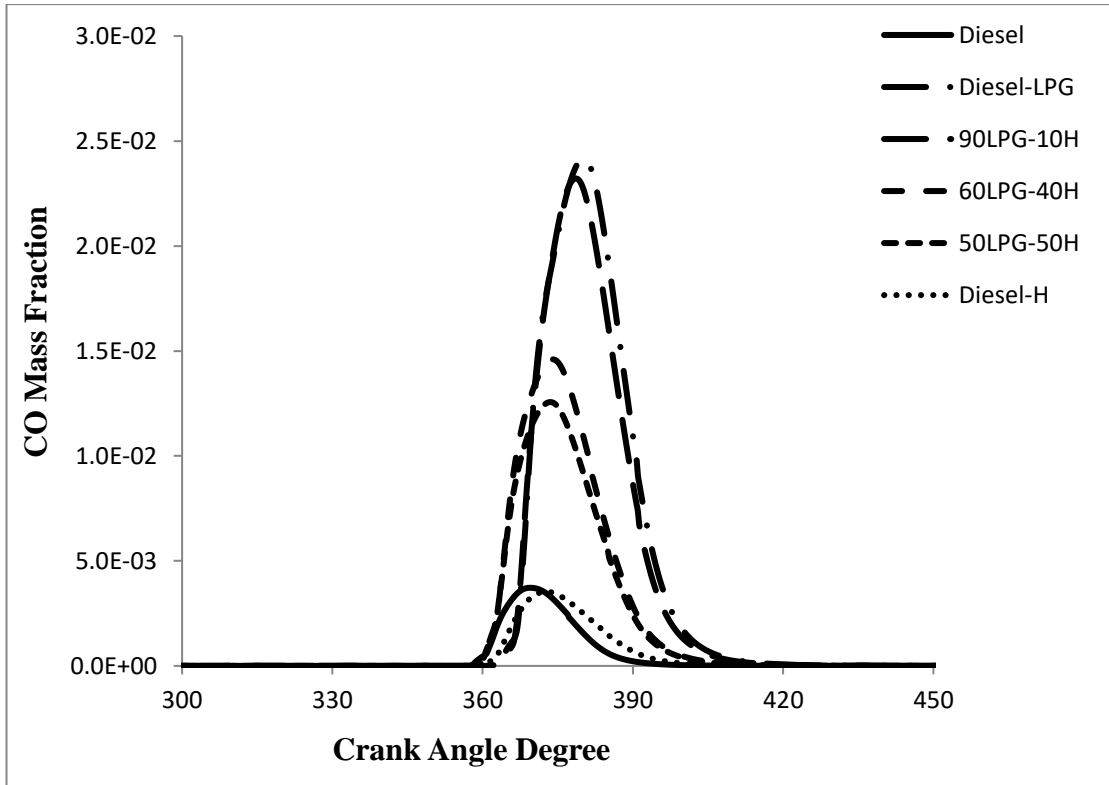
Table 4.3-a showed the formation region of carbon monoxide at 1.2 values of excess air under various ratios of gaseous addition. These contours show at 375, 385, and 395 CAD for H<sub>2</sub> addition, as compared with diesel and LPG. The CO formation region decreases when the H<sub>2</sub> mass fraction addition to the gaseous and this seem obviously at H<sub>2</sub> and 50L-50H tables. This is due to the high flame velocity of hydrogen and resulting in a complete combustion in diesel-H<sub>2</sub> dual fuel operation. In contrast, the formation region of CO emissions was increased as illustrated at 375, 385, and 395 CAD for LPG, 90L-10H, and 60L-40H tables. Thus, the LPG has a higher carbon ratio and helps to produce CO emission. The maximum rate of CO was achieved at the diesel-LPG operation. Furthermore, the same result can be observed for the CO formation contours with less noticeable effect at 1.6, 2, and 2.4 excess air. Thus, the amount of the gaseous fuel is less with increased the excess air as illustrated in Appendix B.



**Figure 4.12-a: CO emissions curves under 1.2 excess air and different ratio of gaseous fuel**

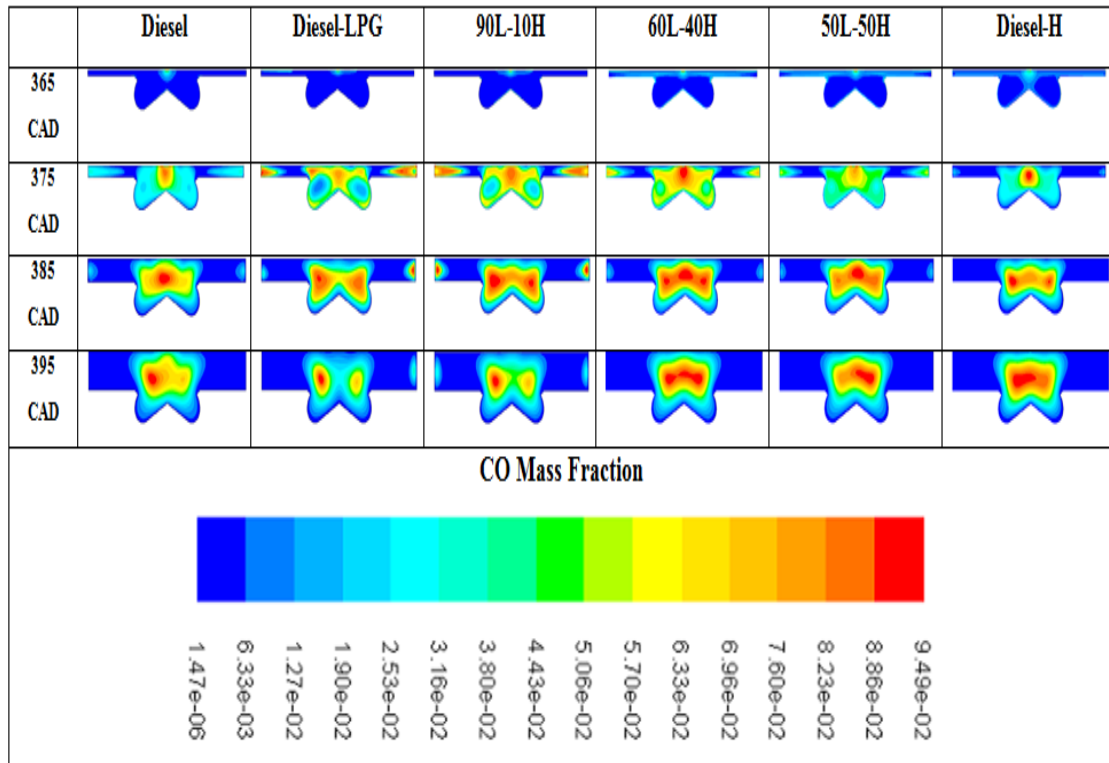
**Table 4.3-a: The development of CO mass fraction under 1.2 excess air and different ratio of gaseous fuel**

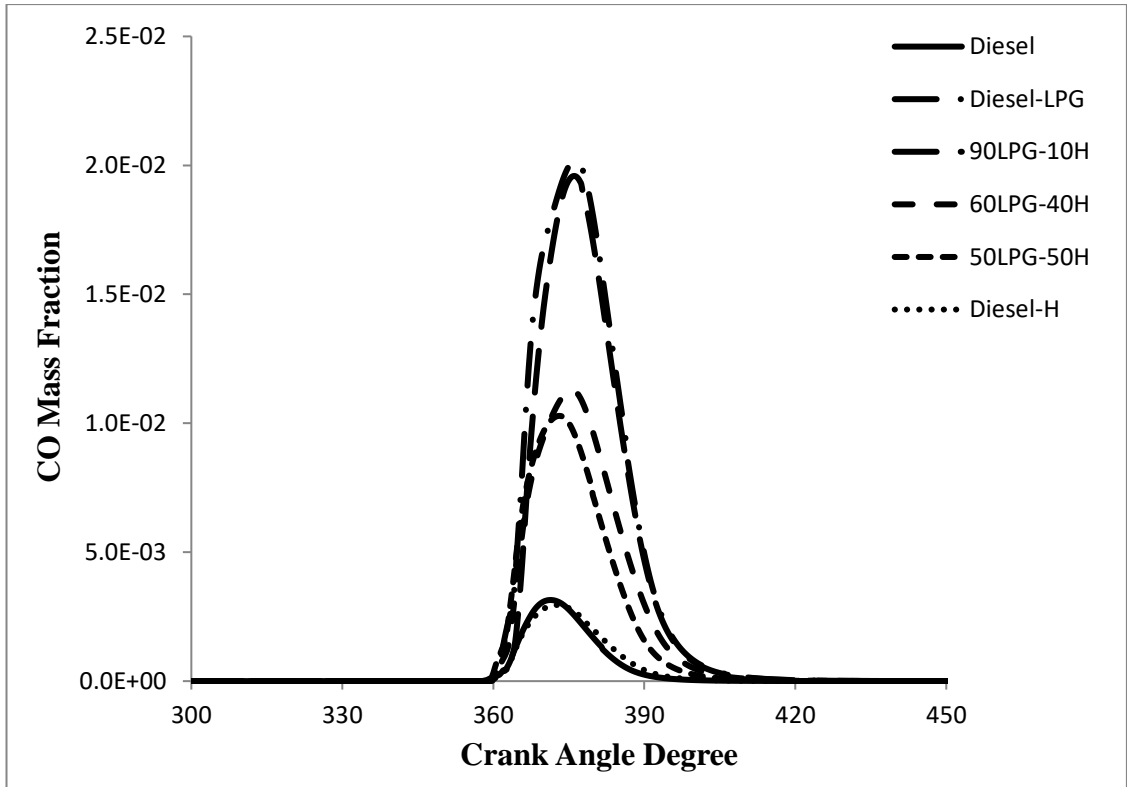




**Figure 4.12-b: CO emissions curves under 1.6 excess air and different ratio of gaseous fuel**

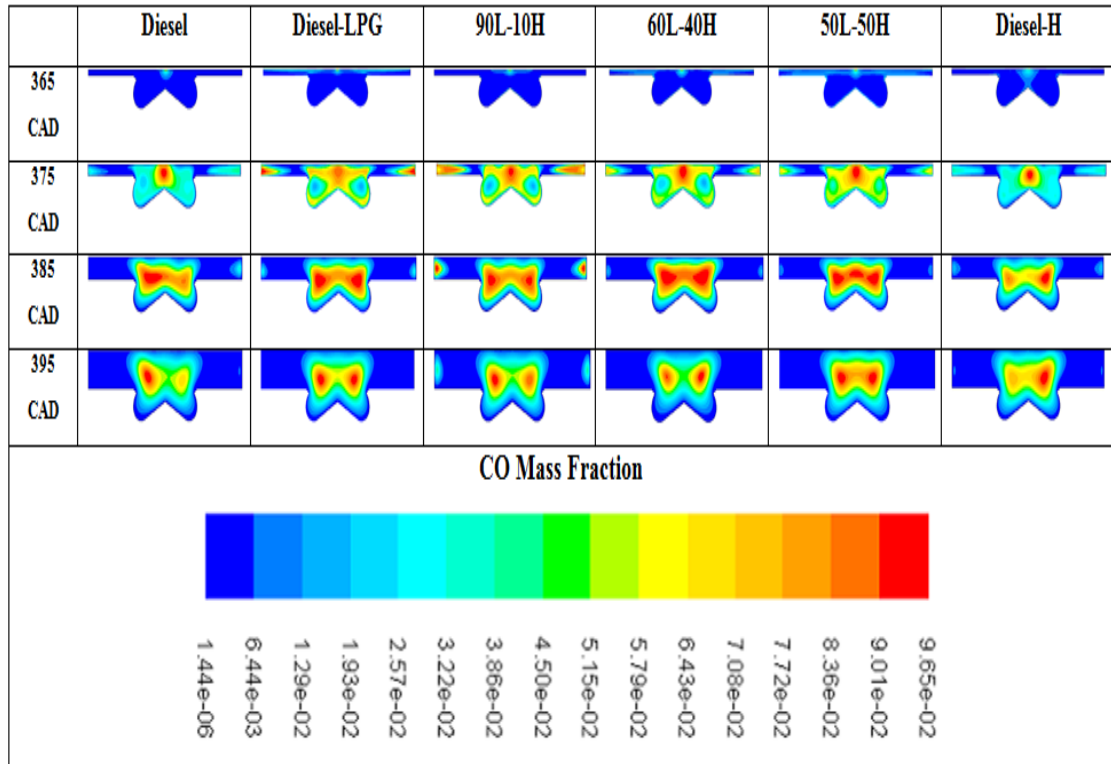
**Table 4.3-b: The development of CO mass fraction under 1.6 excess air and different ratio of gaseous fuel**





**Figure 4.12-c: CO emissions curves under 2 excess air and different ratio of gaseous fuel**

**Table 4.3-c: The development of CO mass fraction under 2 excess air and different ratio of gaseous fuel**



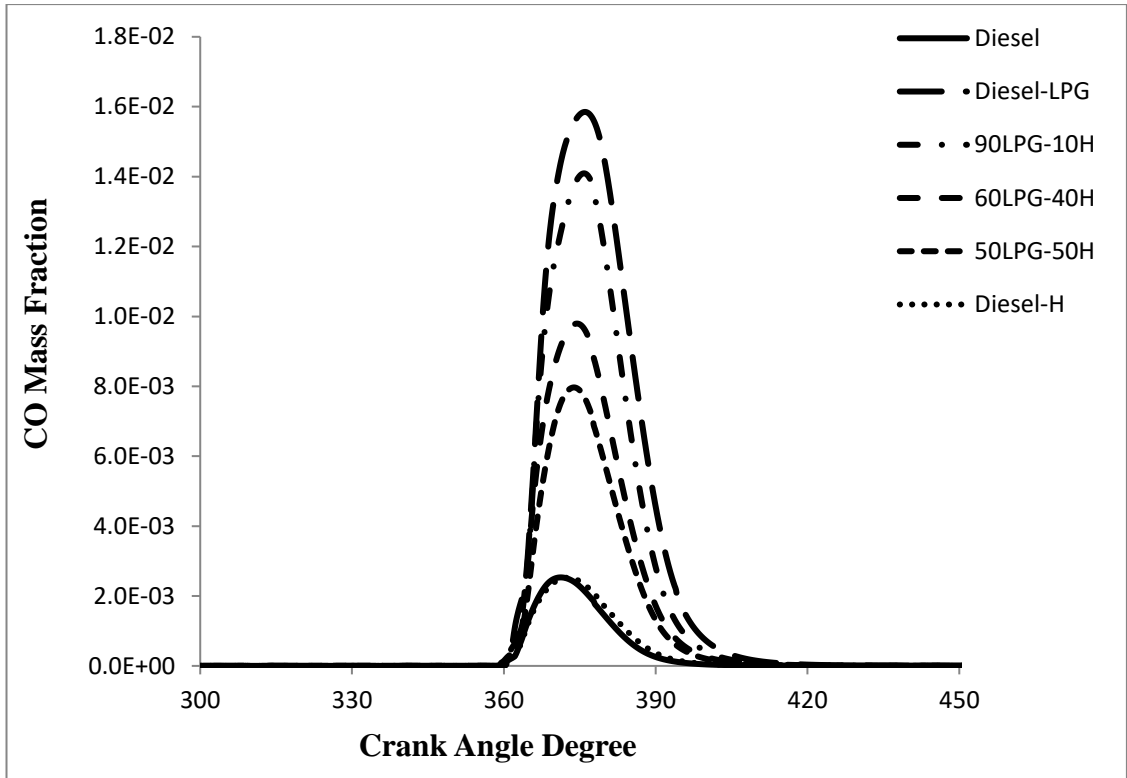
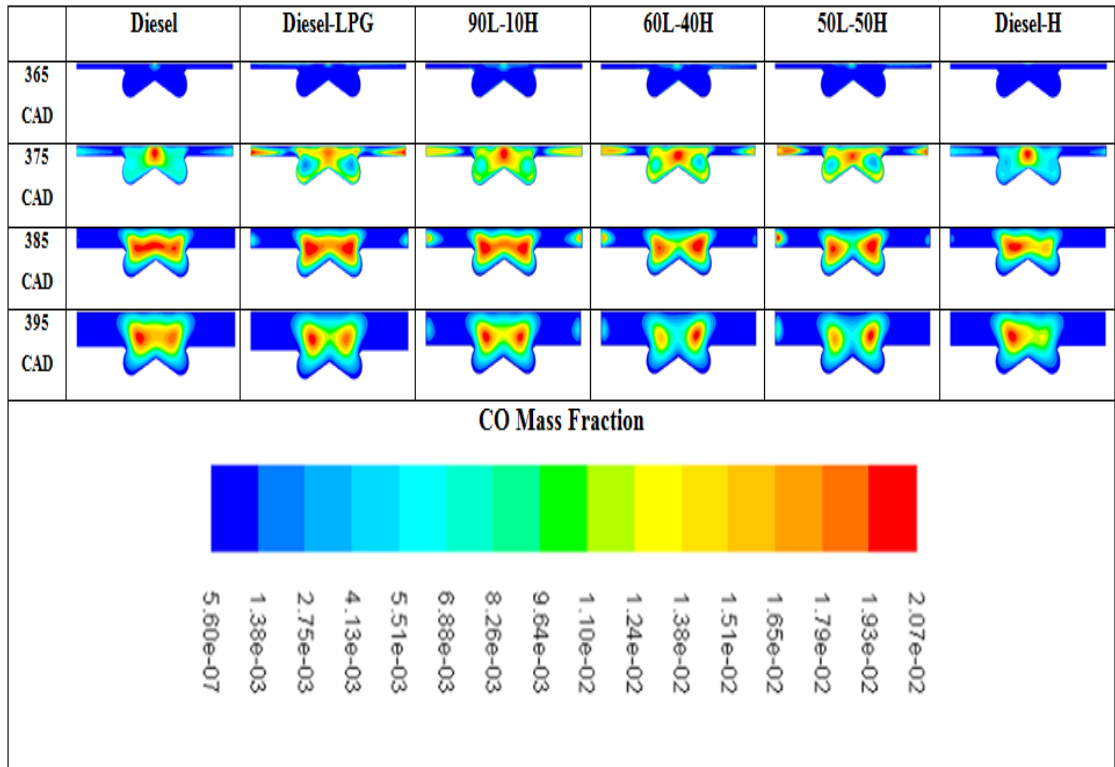


**Figure 4.12-d: CO emissions curves under 2.4 excess air and different ratio of gaseous fuel**

**Table 4.3-d: The development of CO mass fraction under 2.4 excess air and different ratio of gaseous fuel**



### C. Carbon Dioxide (CO<sub>2</sub>)

Figure 4.13, illustrate there is a reduction in a CO<sub>2</sub> mass fraction with an increase in excess air, such as, for diesel-H<sub>2</sub> operation from  $1.07 \times 10^{-2}$  to  $1.01 \times 10^{-2}$ ,  $8.96 \times 10^{-3}$ , and  $7.26 \times 10^{-3}$ . This is in comparison to the diesel fuel mode values of  $1.16 \times 10^{-2}$  to  $1.08 \times 10^{-2}$ ,  $9.92 \times 10^{-3}$ , and  $7.64 \times 10^{-3}$ , operating at excess air values of 1.2, 1.6, 2, and 2.4, respectively. It is clearly observed that diesel combustion results in low CO<sub>2</sub> and CO combustion. With the introduction of H<sub>2</sub> in diesel, the reduction is further reduced. Since high H<sub>2</sub> content in gaseous mixture causes CO<sub>2</sub> dissociation to CO. Saravanan and Nagarajan, (2010) conducted an experiment using a diesel-H<sub>2</sub> dual fuel engine. It was noticed that compared with diesel fuel, there was lower CO<sub>2</sub> emission at all hydrogen flow rates and operating under all the load conditions.

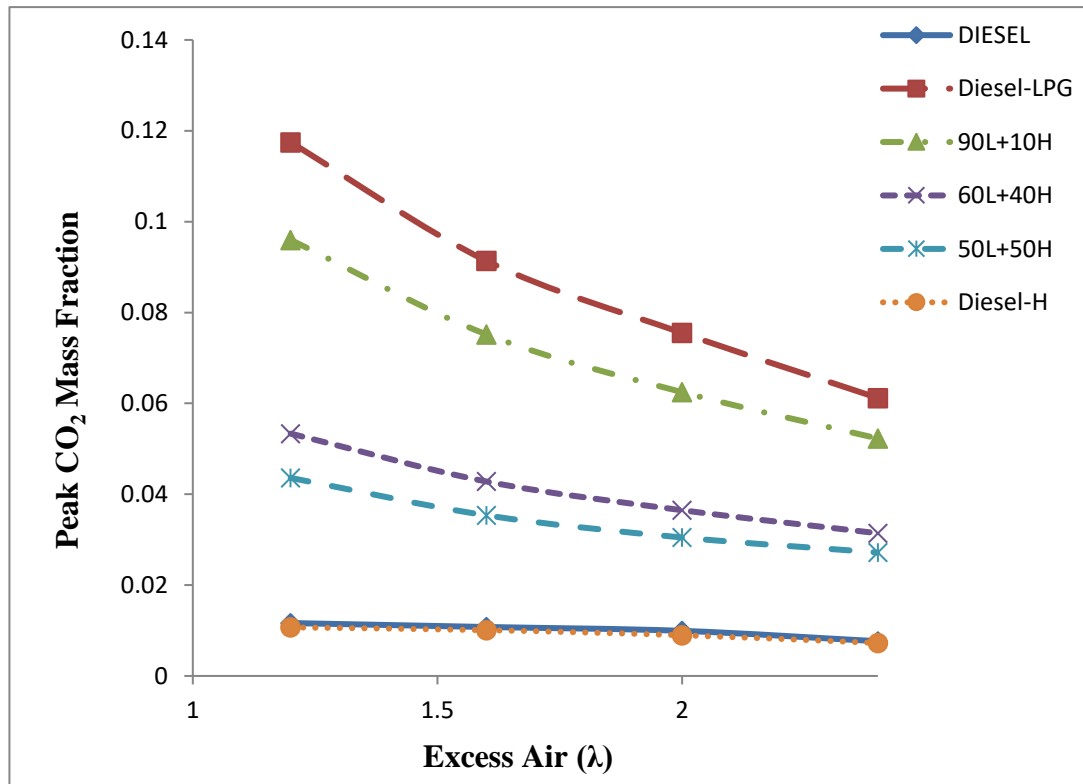


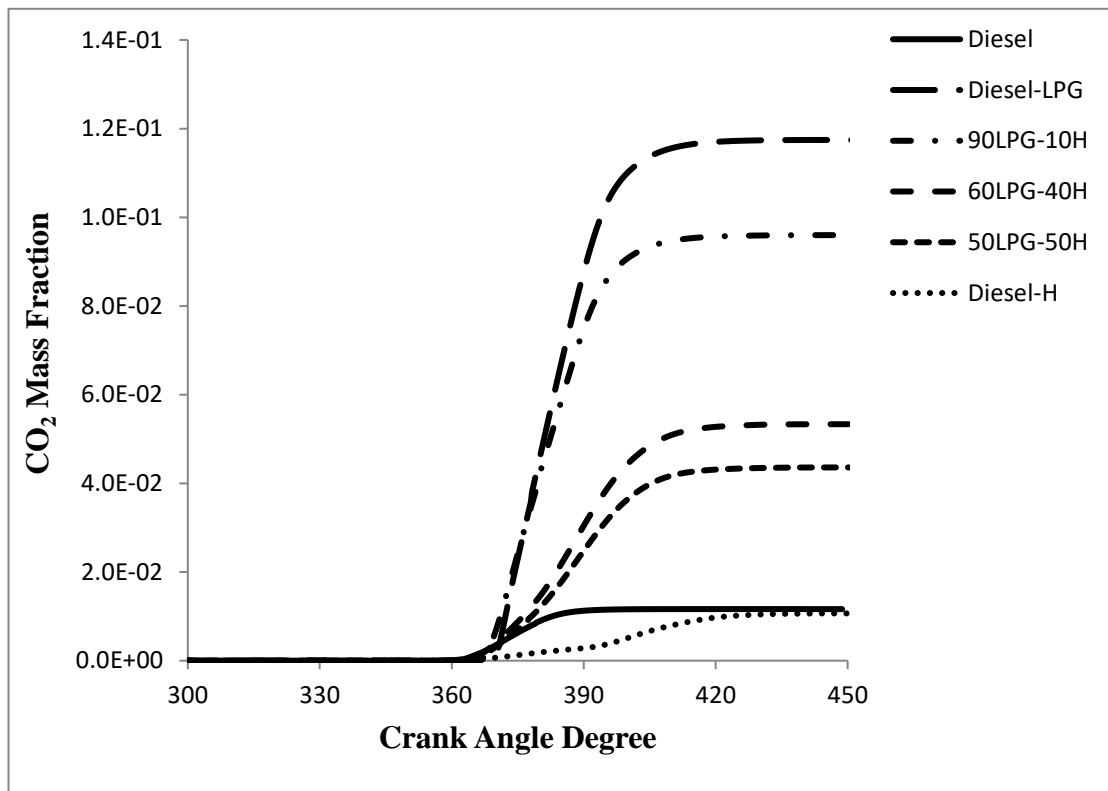
Figure 4.13: Effect of different ratio of gaseous fuel on peak CO<sub>2</sub> emissions

Figures 4.14 a-d demonstrate the CO<sub>2</sub> emission levels when using diesel, dual and tri-fuel operations. When the engine operating under diesel-LPG dual fuel condition, higher LPG presence increases the peak value of CO<sub>2</sub> can be attributed to its relatively slow flame speed that leads to incomplete combustion. Figure 4.14-a shows the increase in the CO<sub>2</sub> mass fraction along with the increase of LPG mass fraction in diesel fuel while operating at all excess air values. At a value of 1.2 excess air, there was an increase in CO<sub>2</sub> value to  $1.17 \times 10^{-1}$  when compared to the normal diesel engine value of  $1.16 \times 10^{-2}$  even when operating at the same excess air. This might be due to the combustion of liquid petroleum gas that aids in the production of CO<sub>2</sub> emissions.

This study shows the variations in value when LPG, 90L-10H, 60L-40H, 50L-50H and hydrogen were added in diesel fuel and how they affected CO<sub>2</sub> mass fraction and lowered the value from  $1.17 \times 10^{-1}$  to  $9.6 \times 10^{-2}$ ,  $5.33 \times 10^{-2}$ ,  $4.36 \times 10^{-2}$ , and  $1.07 \times 10^{-2}$ , respectively. These were all measured at 1.2 excess air. Since the incorporation of hydrogen into LPG broadened the flammability of LPG and reduced CO<sub>2</sub> emission. Köse and Ciniviz, (2013) conduct that the CO<sub>2</sub> emission for all flow rate of hydrogen was decreased compared with diesel fuel. This reduction in CO<sub>2</sub> concentration is because of oxidation reaction reduces with a carbon atom in fuel. The effect is still similar even with 1.6, 2, and 2.4 excess air. For example, at 2.4 excess air, the CO<sub>2</sub> emission decreased from  $7.64 \times 10^{-3}$  to  $7.26 \times 10^{-3}$  for using diesel, and H<sub>2</sub> respectively. Accordingly, it was noted that LPG combustion help in CO<sub>2</sub> production, while H<sub>2</sub> combustion does not. As a result, using the 50L-50H mixture under tri-fuel operation led to lower CO<sub>2</sub> emission compared to the other two of H<sub>2</sub>-LPG mixtures.

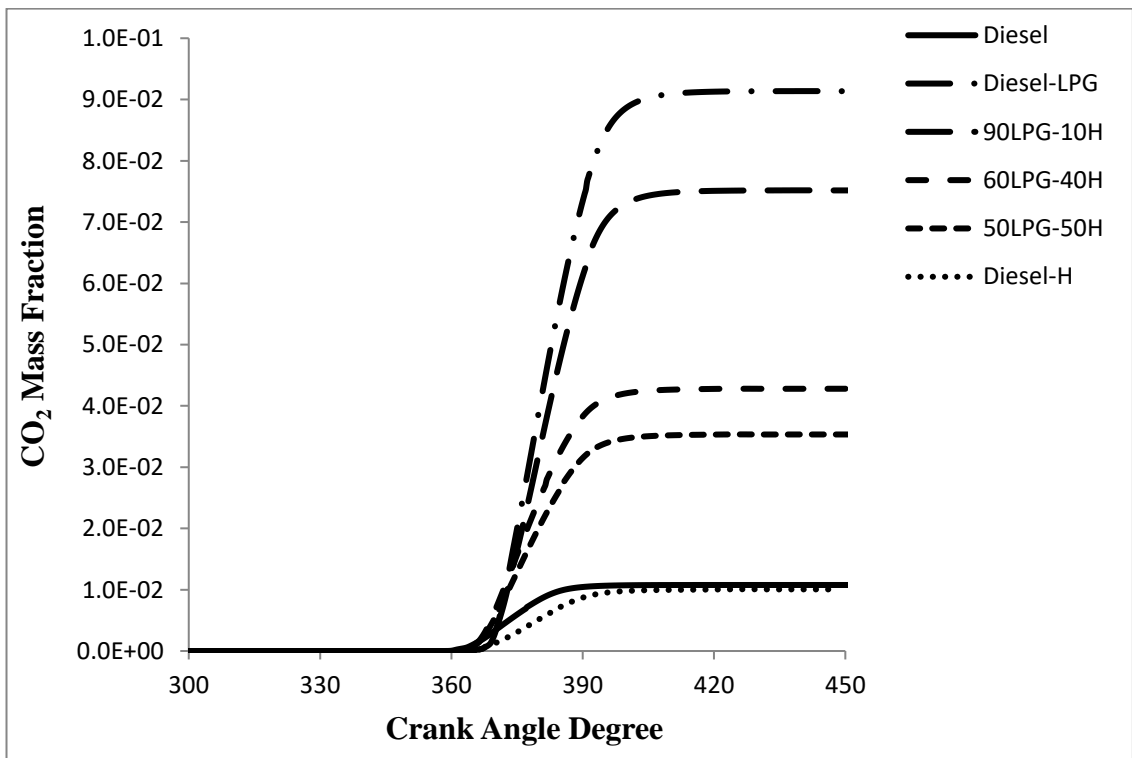
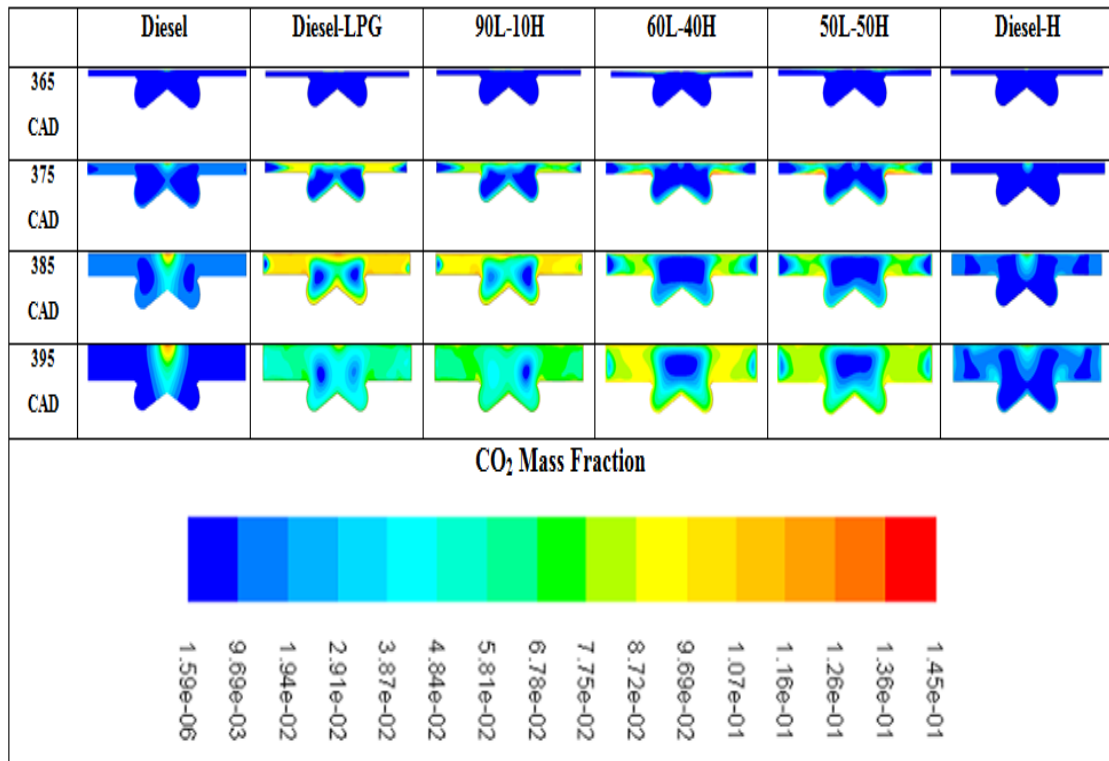


Table 4.4-a shows the distribution of carbon dioxide at 1.2 value of excess under various ratios of gaseous addition. The formation regions of CO<sub>2</sub> were expanded when LPG masses fraction increased in the gaseous fuel and that caused by LPG combustion that helped in the production of CO<sub>2</sub> emissions. As well as, the maximum formation region of carbon dioxide can clearly be observed for LPG, 90L-10H, and 60L-40L at 375, 385, and 395 CAD. On the other hand, for H<sub>2</sub>, and 50L-50H at 375, 385, and 395 CAD the CO<sub>2</sub> formation region decreased clearly when H<sub>2</sub> mass fraction increased. This is due to the high flame velocity and rapid combustion of hydrogen that caused to complete combustion and reduced the CO<sub>2</sub> emission. The same result can observe for the CO<sub>2</sub> distribution contours with less noticeable effect at 1.6, 2, and 2.4 excess air. Hence, the amount of the gaseous fuel less with increased the excess air as illustrated in Appendix B.



**Figure 4.14-a: CO<sub>2</sub> emissions curves under 1.2 excess air and different ratio of gaseous fuel**

**Table 4.4-a: The development of CO<sub>2</sub> mass fraction under 1.2 excess air and different ratio of gaseous fuel**



**Figure 4.14-b: CO<sub>2</sub> emissions curves under 1.6 excess air and different ratio of gaseous fuel**

**Table 4.4-b: The development of CO<sub>2</sub> mass fraction under 1.6 excess air and different ratio of gaseous fuel**

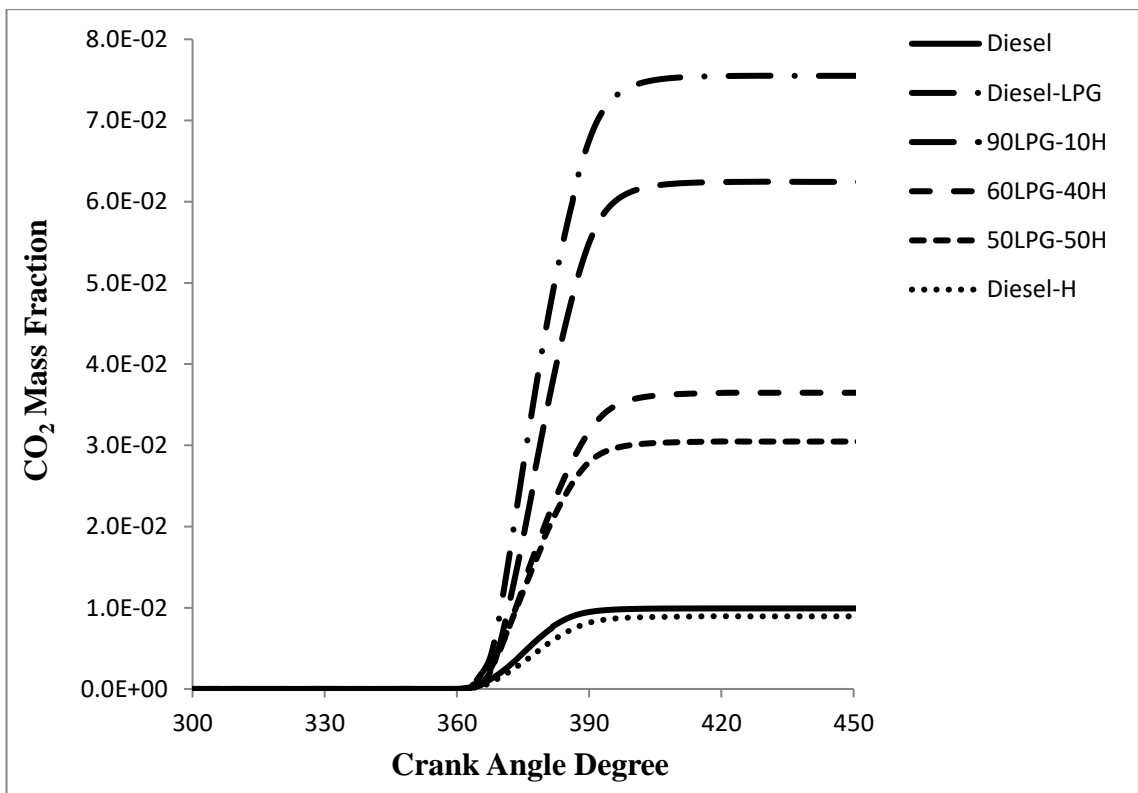
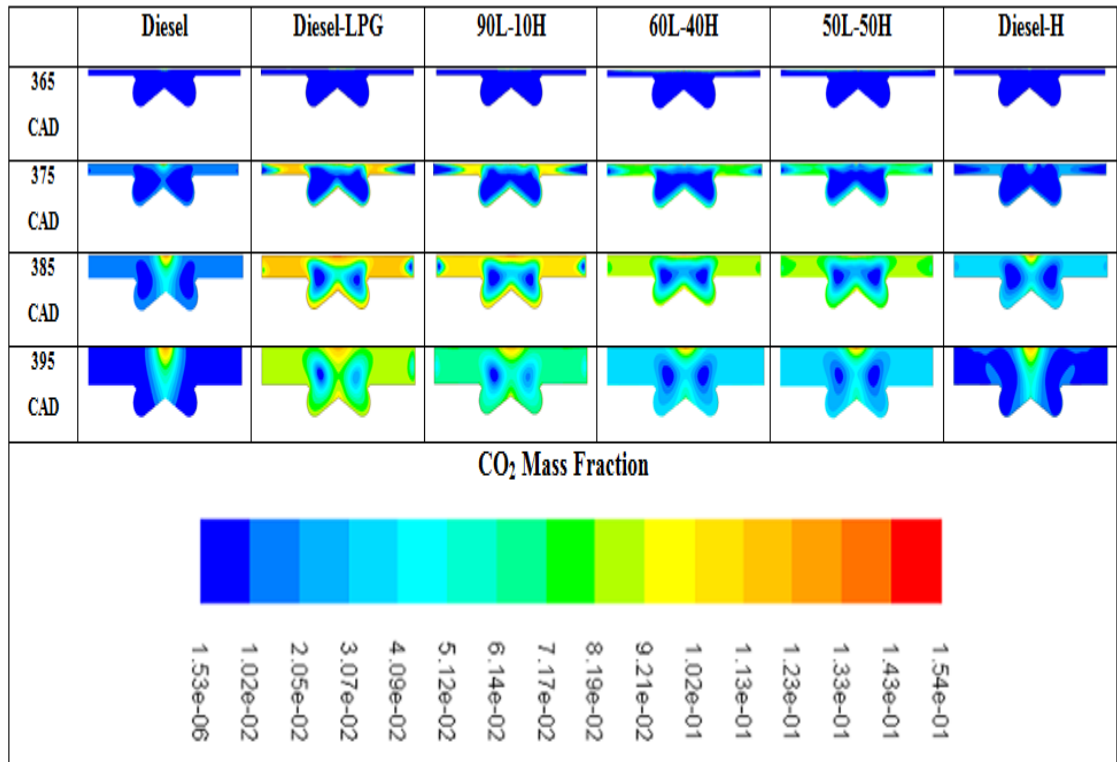


**Figure 4.14-c: CO<sub>2</sub> emissions curves under 2 excess air and different ratio of gaseous fuel**

**Table 4.4-c: The development of CO<sub>2</sub> mass fraction under 2 excess air and different ratio of gaseous fuel**

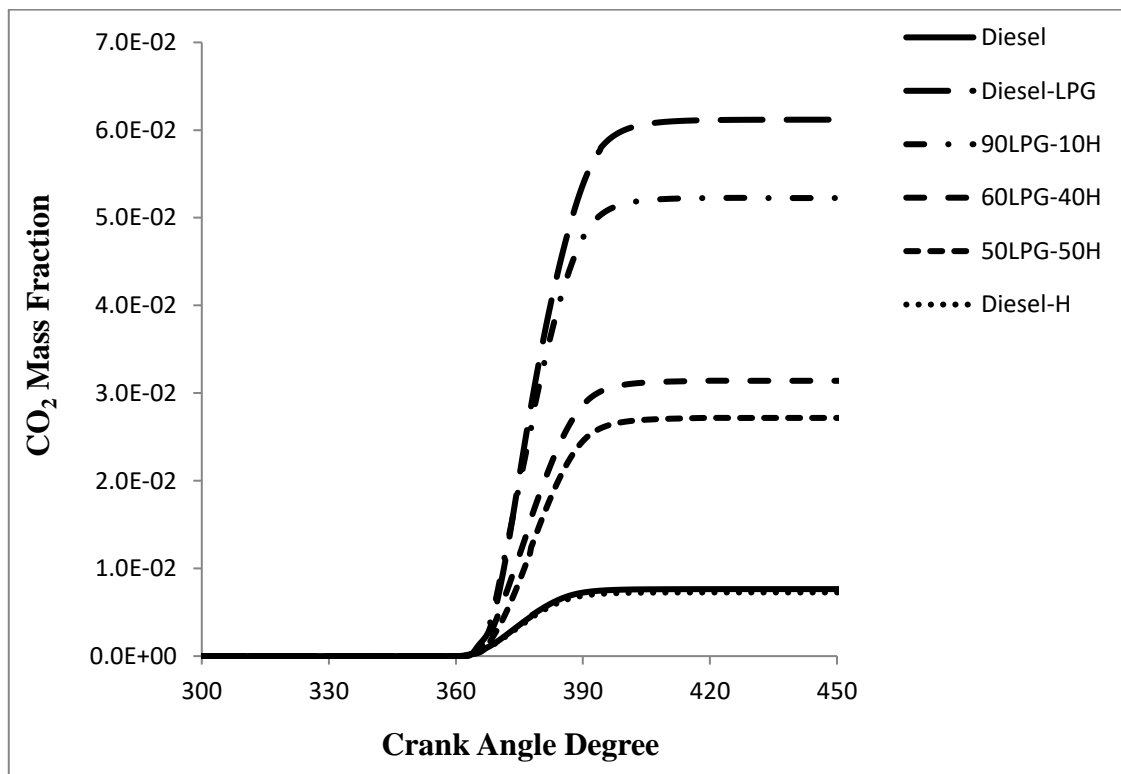
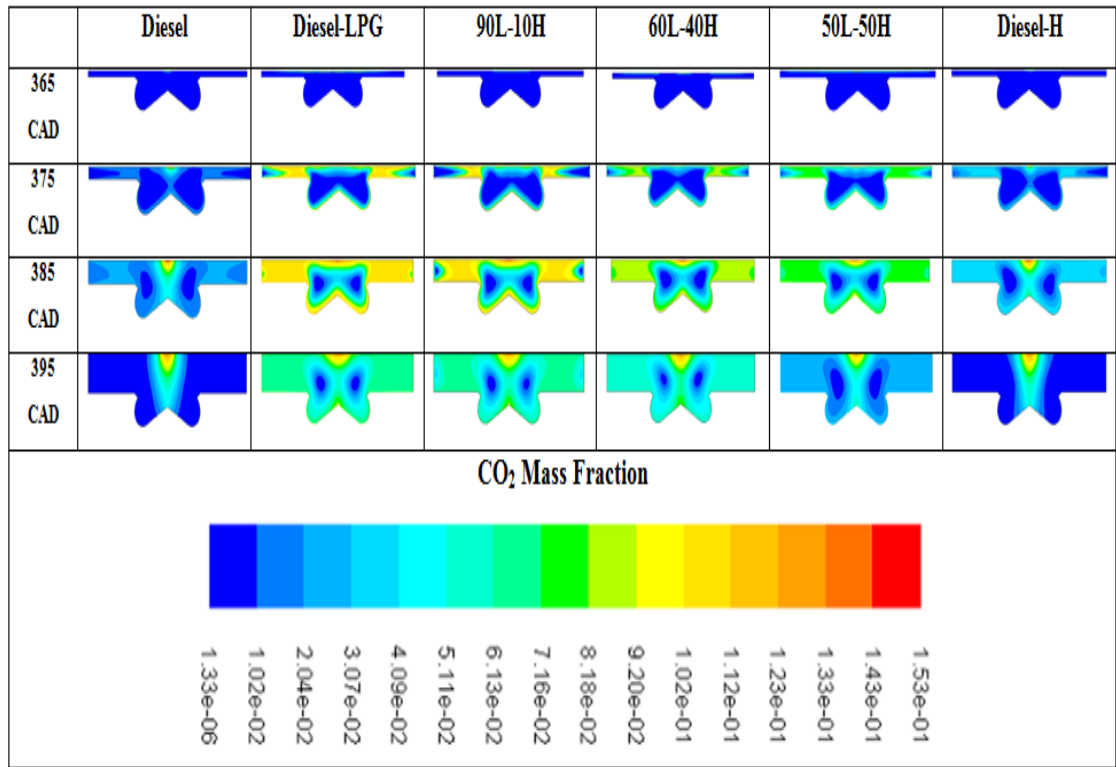
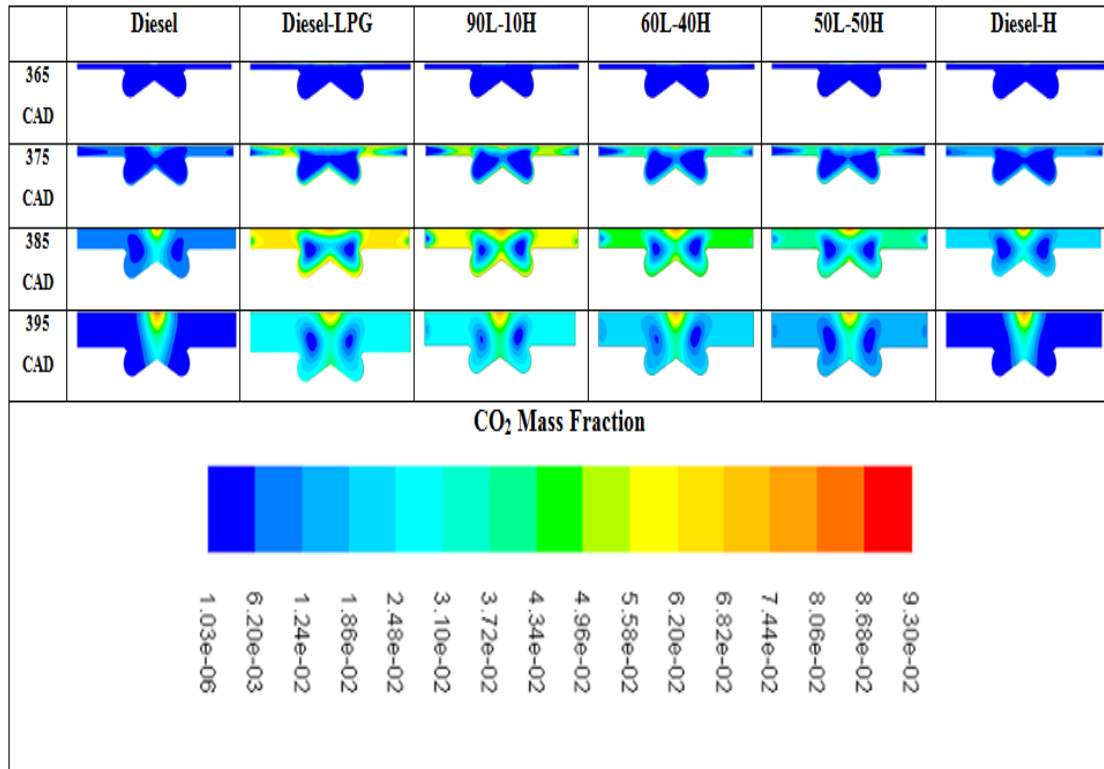


**Figure 4.14-d: CO<sub>2</sub> emissions curves under 2.4 excess air and different ratio of gaseous fuel**

**Table 4.4-d: The development of CO<sub>2</sub> mass fraction under 2.4 excess air and different ratio of gaseous fuel**



#### 4.6 Summary

In the present study, Computational Fluid Dynamic (CFD) approach was used on a Ricardo Hydra diesel engine, a single cylinder that operates using the direct injection method. The simulation data has been validated with experimental data published by Wannatong et al., (2007) in order to get a good accuracy with in-cylinder pressure. Moreover, to verify the accuracy of the emission result from CFD approach, the verification was applied on the NO<sub>x</sub> emission at the same conditions and has been compared with previous work done by Alrazen et al., (2015). The simulation data seems to attain a good agreement with the previous data. Additionally, examined the combustion's characteristic (in-cylinder pressure, temperature), and emissions (NO, CO, CO<sub>2</sub>) of the normal diesel engine, diesel-LPG, diesel-H<sub>2</sub> under dual-fuel, and diesel-LPG-H<sub>2</sub> under tri-fuel operations, with different air-fuel ratios ( $\lambda$ ) such as 1.2,

1.6, 2, and 2.4. However, H<sub>2</sub> addition to LPG will enhance LPG's combustion operation and make it more suitable for application of the diesel modify the engine. Besides that, diesel-LPG-H<sub>2</sub> operations produce lower CO/CO<sub>2</sub> emissions compared to diesel-LPG operation. It also produces lower NO emission compared to diesel-H<sub>2</sub> operation for every value of excess air. In addition, the shortcomings of hydrogen addition are high NO emission at the same excess air ratio compared with operations without hydrogen.

## CHAPTER 5

### CONCLUSION AND RECOMMENDATIONS

#### 5.1 Conclusions

The compression ignition engine of the dual fuel type is a respectable alternative for a conventional diesel engine. The dual fuel engine has many advantages over conventional diesel engine include economical and environmental benefits. Dual fuel engine has been employed in a wide range of applications to utilize various gaseous fuel resources meanwhile exhaust gas emissions are minimized without excessive increase in the engine cost compared to that of conventional diesel engines. Therefore, the employment of alternative gas fuels like Liquefied petroleum gas (LPG), Natural gas (NG), Hydrogen ( $H_2$ ), etc. is a promising technique for reducing the dependence on petroleum-based liquid fuels. For this reason,  $H_2$ , LPG, and mixtures of  $H_2$  and LPG were taken into consideration as an alternative fuel in recent years in order to reduce the pollution of vehicles. Consequently, better engine performance could be obtained when  $H_2$  is added with LPG to make a secondary fuel. As well as, the advantage with LPG presence is to improve hydrogen combustion by avoiding uncontrolled combustion, such as the sharp increase of peak in-cylinder pressure and temperature.

The effect of  $H_2$ , LPG and their mixtures (90L-10H), (60L-40H) and (50L-50H) on the combustion characteristics and emissions of a CI engine under diesel, dual and tri-fuel operations was investigated in this study at four excess air (1.2, 1.6, 2, and 2.4) at (2000 rpm) and five mixing ratios of fuel. This work verified the worth of utilizing the computational fluid dynamics (CFD) process in analyzing the diesel, dual and tri-fuel engine. The utilization of ANSYS design modular was selected to generate the entire

computational domain of the engine. The effects of a number of the cells on the expected result were utilized in order to analyze the most accurate one. The simulation data of in-cylinder pressure and verification of emissions appears to achieve a good agreement with data from previous work. The major conclusions are summarized as following:

- Successfully established a CFD simulation was obtained for predicting the emissions and combustion characteristics on the diesel, dual, and tri-fuel engine operations.
- Knowledge of utilizing the dual and tri-fuel in modify diesel engine and understanding the acceptable values of the mixture to give the best results.
- The addition of gasses fuels increases the peak temperature under all values of excess air. However, the addition of gaseous fuel only increased the in-cylinder pressure for excess air values of 1.2, 1.6, and 2. On the other hand, at 2.4 excess air, the peak pressure increased through the increase of the limit value of H<sub>2</sub>, such as 60L-40H and 50L-50H, when added to LPG. A decrease is then observed with diesel-H<sub>2</sub> modes. This might be due to the lower fuel rates compared with other cases.
- At dual fuel operations, adding H<sub>2</sub> decreases CO and CO<sub>2</sub> emissions when compared with the emission from LPG. Conversely, diesel-LPG-H<sub>2</sub> tri-fuel operations lowered the CO emission when compared to diesel-LPG. It also lowered NO emission when compared to the diesel-H<sub>2</sub> operation for all excess air. In order to lower CO/CO<sub>2</sub> emissions, high H<sub>2</sub> fraction is proposed in LPG (50L-50H). On the other hand, lower H<sub>2</sub> fraction in LPG (90L-10H) can lower the uncontrolled combustion of hydrogen combustion and restrict the increase of NO emission.



## **5.2 Recommendations for future works**

- A. The combustion characteristics and emissions should be examined with various LPG and H<sub>2</sub> substitutions at different engine loads and speeds under tri-fuel operation to be able to see the variations in combustion characteristics and emissions.
- B. The particular geometry should be conducted and retrieved in three-dimensional simulations in order to attain a more actual representation of the reality.

## REFERENCES

- A, D. (2002). Fuel properties of hydrogen, liquefied petroleum gas (LPG), and compressed natural gas (CNG) for transportation. *Energy Sources*, 24(7), 601–610.
- Abagnale, C., Cameretti, M. C., De Simio, L., Gambino, M., Iannaccone, S., & Tuccillo, R. (2014). Numerical simulation and experimental test of dual fuel operated diesel engines. *Applied Thermal Engineering*, 65(1), 403–417.
- Abdullah, S., Kurniawan, W. H., & Shamsudeen, A. (2008). Numerical Analysis of the Combustion Process in a Compressed Natural Gas Direct Injection Engine, 1(2), 65–86.
- Aceves, S. M., Flowers, D. L., Martinez-Frias, J., Smith, J. R., Dibble, R., Au, M., & Girard, J. (2001). HCCI Combustion: Analysis and Experiments. *SAE Technical Paper*, 2077(1), 9.
- Adnan, R., Masjuki, H. H., & Mahlia, T. M. I. (2012). Performance and emission analysis of hydrogen fueled compression ignition engine with variable water injection timing. *Energy*, 43(1), 416–426.
- Agarwal, A. K. (2007). Biofuels (alcohols and biodiesel) applications as fuels for internal combustion engines. *Progress in Energy and Combustion Science*, 33(3), 233–271.
- Ahmad - I, N., Babu, M. K. G., & Ramesh, A. (2005). Experimental Investigations of Different Parameters Affecting the Performance of a CNG - Diesel Dual Fuel Engine.
- Akansu, S. O., Kahraman, N., & Çeper, B. (2007). Experimental study on a spark ignition engine fuelled by methane–hydrogen mixtures. *International Journal of Hydrogen Energy*, 32(17), 4279–4284.
- Alam, M., Goto, S., Sugiyama, K., Kajiwara, M., Mori, M., Konno, M., ... Oyama, K. (2001). Performance and Emissions of a DI Diesel Engine Operated with LPG and Ignition Improving Additives. *SAE Technical Paper*, 3680(1), 11.
- Alkidas, A. C. (2007). Combustion advancements in gasoline engines. *Energy Conversion and Management*, 48(11), 2751–2761.
- Alrazen, H. A., Talib, A. R. A., & Ahmad, K. A. (2015). A two-component CFD studies of the effects of H<sub>2</sub>, CNG, and diesel blend on combustion characteristics and emissions of a diesel engine. *International Journal of Hydrogen Energy*, 41(24), 10483–10495.
- Amarendar Rao, G., C. V. Mohan Rao, and K. G. R. (2008). Experimental investigation of a single-cylinder, four-stroke diesel engine operating on the dual-fuel mode (LPG+ Diesel). *Intl. J. Scientific Computing.*, pp 2.2.
- Anbarasu, A., & Karthikeyan, A. (2014). Performance and Emission Characteristics of Direct Injection Diesel Engine Running On Canola Oil / Diesel Fuel Blend, 15(8), 82–93.

- Aravind, B., Ratna Kishore, V., & Mohammad, A. (2015). Combustion characteristics of the effect of hydrogen addition on LPG-air mixtures. *International Journal of Hydrogen Energy*, 40(46), 16605–16617.
- Ashok, B., Denis Ashok, S., & Ramesh Kumar, C. (2015). LPG diesel dual fuel engine - A critical review. *Alexandria Engineering Journal*, 54(2), 105–126.
- Bora, B. J., Debnath, B. K., Gupta, N., Saha, U. K., & Sahoo, N. (2013). Investigation on the Flow Behaviour of a Venturi Type Gas Mixer Designed for Dual Fuel Diesel Engines, 3(3), 202–209.
- Bression, G., Soleri, D., Savy, S., Dehoux, S., Azoulay, D., Hamouda, H. B.-H., ... Lawrence, N. (2008). A Study of Methods to Lower HC and CO Emissions in Diesel HCCI. *SAE International Journal of Fuels and Lubricants*, 1(1), 2008-01-0034.
- Chaichan, M. T. (2011). Exhaust analysis and performance of a single cylinder diesel engine run on dual fuels mode. *Journal of Engineering*, 17(4).
- Chatlatanagulchai, W., Rhienprayoon, S., Yaovaja, K., & Wannatong, K. (2010). Air/Fuel Ratio Control in Diesel-Dual-Fuel Engine by Varying Throttle, EGR Valve, and Total Fuel. *SAE Technical Paper*, 2200(1).
- Choudhuri, A. R., & Gollahalli, S. R. (2003). Characteristics of hydrogen-hydrocarbon composite fuel turbulent jet flames. *International Journal of Hydrogen Energy*, 28(4), 445–454.
- Cinar, C., Sahin, F., Can, O., & Uyumaz, A. (2016). A comparison of performance and exhaust emissions with different valve lift profiles between gasoline and LPG fuels in a SI engine. *Applied Thermal Engineering*, 107, 1261–1268.
- Díaz, L., Schifter, I., López-Salinas, E., Gamas, E., Rodriguez, R., & Avalos, S. (2000). Optimizing automotive LPG blend for Mexico City. *Fuel*, 79(1), 79–88.
- Donghui, Q., Longbao, Z., & Shenghua, L. (2005). Experimental studies on the combustion characteristics and performance of a naturally aspirated, direct injection engine fuelled with a liquid petroleum gas/diesel blend. *Proceedings of the Institution of Mechanical Engineers, Part D: Journal of Automobile Engineering*, 219(2), 253–261.
- Elnajjar, E., Hamdan, M. O., & Selim, M. Y. E. (2013). Experimental investigation of dual engine performance using variable LPG composition fuel. *Renewable Energy*, 56, 110–116.
- Elnajjar, E., Selim, M., & Hamdan, M. (2011). Effect of Variable LPG Composition Fuel on Dual Fuel Engine Performance (p. 12).
- Elnajjar, E., Selim, M. Y. E., & Hamdan, M. O. (2013). Experimental study of dual fuel engine performance using variable LPG composition and engine parameters. *Energy Conversion and Management*, 76, 32–42.
- Ergenç, A. T., & Koca, D. Ö. (2014). PLC controlled single cylinder diesel-LPG engine. *Fuel*, 130, 273–278.

- Ferguson, C., & Kirkpatrick, A. (2015). *Internal combustion engines: applied thermosciences*.
- Fluent. (2006). FLUENT 6.3 Getting Started Guide, (Fluent Inc.).
- Ganesh, D., Nagarajan, G., & Mohamed Ibrahim, M. (2008). Study of performance, combustion and emission characteristics of diesel homogeneous charge compression ignition (HCCI) combustion with external mixture formation. *Fuel*, 87(17), 3497–3503.
- Gatts, T., Li, H., Liew, C., Liu, S., Spencer, T., Wayne, S., & Clark, N. (2010). An experimental investigation of H<sub>2</sub> emissions of a 2004 heavy-duty diesel engine supplemented with H<sub>2</sub>. *International Journal of Hydrogen Energy*, 35(20), 11349–11356.
- Gatts, T., Liu, S., Liew, C., Ralston, B., Bell, C., & Li, H. (2012). An experimental investigation of incomplete combustion of gaseous fuels of a heavy-duty diesel engine supplemented with hydrogen and natural gas. *International Journal of Hydrogen Energy*, 37(9), 7848–7859.
- Ghazal, O. H. (2013a). A comparative evaluation of the performance of different fuel induction techniques for blends hydrogen–methane SI engine. *International Journal of Hydrogen Energy*, 38(16), 6848–6856.
- Ghazal, O. H. (2013b). Performance and combustion characteristic of CI engine fueled with hydrogen enriched diesel. *International Journal of Hydrogen Energy*, 38(35), 15469–15476.
- Ghiji, M. (2011). *Computational fluid dynamic analysis of knock onset in diesel dual-fuel engine*. University Putra Malaysia (Master Thesis).
- Goldsworthy, L. (2012). Combustion behaviour of a heavy duty common rail marine Diesel engine fumigated with propane. *Experimental Thermal and Fluid Science*, 42, 93–106.
- Gomes Antunes, J. M., Mikalsen, R., & Roskilly, A. P. (2009). An experimental study of a direct injection compression ignition hydrogen engine. *International Journal of Hydrogen Energy*, 34(15), 6516–6522.
- Hairuddin, A. A., Yusaf, T., & Wandel, A. P. (2014). A review of hydrogen and natural gas addition in diesel HCCI engines. *Renewable and Sustainable Energy Reviews*, 32, 739–761.
- Heywood, J. B. (1988). *Internal Combustion Engine Fundamentals. McGrawHill series in mechanical engineering* (Vol. 21).
- Ho Choi, G., Jong Chung, Y., & Han, S. Bin. (2005). Performance and emissions characteristics of a hydrogen enriched LPG internal combustion engine at 1400rpm. *International Journal of Hydrogen Energy*, 30(1), 77–82.
- Jafarmadar, S. (2014). Exergy analysis of hydrogen/diesel combustion in a dual fuel engine using three-dimensional model. *International Journal of Hydrogen Energy*, 39(17), 9505–9514.

- Jayashankara, B., & Ganesan, V. (2010). Effect of fuel injection timing and intake pressure on the performance of a di diesel engine - A parametric study using CFD. *Energy Conversion and Management*, 51(10), 1835–1848.
- Jemni, M. A., Kantchev, G., & Abid, M. S. (2011). Influence of intake manifold design on in-cylinder flow and engine performances in a bus diesel engine converted to LPG gas fuelled, using CFD analyses and experimental investigations. *Energy*, 36(5), 2701–2715.
- Jian, D., Xiaohong, G., Gesheng, L., & Xintang, Z. (2001). Study on Diesel-LPG Dual Fuel Engines. *SAE Technical Paper*, 3679(1), 10.
- Kaario, O., Larmi, M., & Tanner, F. (2002). Relating Integral Length Scale to Turbulent Time Scale and Comparing k- $\epsilon$  and RNG k- $\epsilon$  Turbulence Models in Diesel Combustion Simulation (p. 17).
- Kaleemuddin, S., & Rao, G. A. (2009). Study on Single Cylinder Engine for Performance and Exhaust Emission with Diesel, Bio Diesel, LPG and CNG. *SAE Technical Paper*, 48(32), 9.
- Karamangil, M. I. (2007). Development of the auto gas and LPG-powered vehicle sector in Turkey: A statistical case study of the sector for Bursa. *Energy Policy*, 35(1), 640–649.
- Katinas, V., & Savickas, J. (2012). The analysis of development of gaseous fuel use for transport. *Žemės Ūkio Inžinerija, Mokslo Darbai*, 44(1/3), 144–153.
- Kayes, D., & Hochgreb, S. (1999). Mechanisms of Particulate Matter Formation in Spark-Ignition Engines. 1. Effect of Engine Operating Conditions. *Environmental Science & Technology*, 33(22), 3957–3967.
- Klausmeier, R. F., & Billick, I. F. (1993). Comparative analysis of the environmental impact of alternative transportation fuels. *Energy & Fuels*, 7(1), 27–32.
- Komninos, N. P. (2009). Investigating the importance of mass transfer on the formation of HCCI engine emissions using a multi-zone model. *Applied Energy*, 86(7), 1335–1343.
- Köse, H., & Ciniviz, M. (2013). An experimental investigation of effect on diesel engine performance and exhaust emissions of addition at dual fuel mode of hydrogen. *Fuel Processing Technology*, 114, 26–34.
- Kumar Bose, P., & Banerjee, R. (2012). An Experimental Investigation on the Role of Hydrogen in the Emission Reduction and Performance Trade-Off Studies in an Existing Diesel Engine Operating in Dual Fuel Mode Under Exhaust Gas Recirculation. *Journal of Energy Resources Technology*, 134(1), 12601.
- Kuo, K. K., John, W., & Sons, W. &. (2005). *PRINCIPLES OF COMBUSTION SECOND EDITION*.
- Lata, D. B., & Misra, A. (2010). Theoretical and experimental investigations on the performance of dual fuel diesel engine with hydrogen and LPG as secondary fuels. *International Journal of Hydrogen Energy*, 35(21), 11918–11931.

- Lata, D. B., & Misra, A. (2011). Analysis of ignition delay period of a dual fuel diesel engine with hydrogen and LPG as secondary fuels. *International Journal of Hydrogen Energy*, 36(5), 3746–3756.
- Lata, D. B., & Misra, A. (2012). Experimental Investigations on the Performance of a Dual Fuel Diesel Engine with Hydrogen and LPG as Secondary Fuels (pp. 119–128). Springer Berlin Heidelberg.
- Lata, D. B., Misra, A., & Medhekar, S. (2011). Investigations on the combustion parameters of a dual fuel diesel engine with hydrogen and LPG as secondary fuels. *International Journal of Hydrogen Energy*, 36(21), 13808–13819.
- Lata, D. B., Misra, A., & Medhekar, S. (2012). Effect of hydrogen and LPG addition on the efficiency and emissions of a dual fuel diesel engine. *International Journal of Hydrogen Energy*, 37(7), 6084–6096.
- Lee, J., Choi, S., Kim, H., Kim, D., Choi, H., & Min, K. (2013). Reduction of emissions with propane addition to a diesel engine. *International Journal of Automotive Technology*, 14(4), 551–558.
- Leermakers, C., & Berge, B. Van den. (2011). Direct Injection of Diesel-Butane Blends in a Heavy Duty Engine. *SAE International Journal of Fuels and Lubricants*, 4(2), 2011-01–2400.
- Liew, C., Li, H., Liu, S., Besch, M. C., Ralston, B., Clark, N., & Huang, Y. (2012). Exhaust emissions of a H<sub>2</sub>-enriched heavy-duty diesel engine equipped with cooled EGR and variable geometry turbocharger. *Fuel*, 91(1), 155–163.
- Liew, C., Li, H., Nuskowski, J., Liu, S., Gatts, T., Atkinson, R., & Clark, N. (2010). An experimental investigation of the combustion process of a heavy-duty diesel engine enriched with H<sub>2</sub>. *International Journal of Hydrogen Energy*, 35(20), 11357–11365.
- Lilik, G. K., Zhang, H., Herreros, J. M., Haworth, D. C., & Boehman, A. L. (2010). Hydrogen assisted diesel combustion. *International Journal of Hydrogen Energy*, 35(9), 4382–4398.
- Lim, C., Kim, D., Song, C., Kim, J., Han, J., & Cha, J.-S. (2015). Performance and emission characteristics of a vehicle fueled with enriched biogas and natural gases. *Applied Energy*, 139, 17–29.
- Mansor, M. R. A., Abbood, M. M., & Mohamad, T. I. (2017). The influence of varying hydrogen-methane-diesel mixture ratio on the combustion characteristics and emissions of a direct injection diesel engine. *Fuel*, 190, 281–291.
- Mansour, C., Bounif, A., Aris, A., & Gaillard, F. (2001). Gas–Diesel (dual-fuel) modeling in diesel engine environment. *International Journal of Thermal Sciences*, 40(4), 409–424.
- Masood, M., Ishrat, M. M., & Reddy, A. S. (2007). Computational combustion and emission analysis of hydrogen–diesel blends with experimental verification. *International Journal of Hydrogen Energy*, 32(13), 2539–2547.

- Miao, J., Leung, C. W., Huang, Z., Cheung, C. S., Yu, H., & Xie, Y. (2014). Laminar burning velocities, Markstein lengths, and flame thickness of liquefied petroleum gas with hydrogen enrichment. *International Journal of Hydrogen Energy*, 39(24), 13020–13030.
- Miller Jothi, N. K., Nagarajan, G., & Renganarayanan, S. (2007). *Experimental studies on homogeneous charge CI engine fueled with LPG using DEE as an ignition enhancer. Renewable Energy* (Vol. 32).
- Miyamoto, T., Hasegawa, H., Mikami, M., Kojima, N., Kabashima, H., & Urata, Y. (2011). Effect of hydrogen addition to intake gas on combustion and exhaust emission characteristics of a diesel engine. *International Journal of Hydrogen Energy*, 36(20), 13138–13149.
- Mousavi, S. M., Saray, R. K., Poorghasemi, K., & Maghbouli, A. (2016). A numerical investigation on combustion and emission characteristics of a dual fuel engine at part load condition. *Fuel*, 166(x), 309–319.
- Murthy, K., Madhwesh, N., & Shrinivasarao, B. R. (2012). Influence of Injection Timing on the Performance of Dual Fuel Compression Ignition Engine with Exhaust Gas Recirculation. *International Journal of Engineering Research and Development*, 1(11), 36–42.
- Najjar, Y. S. H. (2013). Hydrogen safety: The road toward green technology. *International Journal of Hydrogen Energy*, 38(25), 10716–10728.
- Ng, H. K., Gan, S., Ng, J.-H., & Pang, K. M. (2013). Simulation of biodiesel combustion in a light-duty diesel engine using integrated compact biodiesel–diesel reaction mechanism. *Applied Energy*, 102, 1275–1287.
- Ogawa, H., Miyamoto, N., Li, C., Nakazawa, S., & Akao, K. (2001). Low Emission and Knock-Free Combustion with Rich and Lean Biform Mixture in a Dual-Fuel CI Engine with Induced LPG as the Main Fuel. *SAE Technical Paper*, 9.
- Oilgae – Glossary. (2014). Retrieved from [http://www.oilgae.com/ref/glos/nox\\_emissions.html](http://www.oilgae.com/ref/glos/nox_emissions.html)
- Pal, A., & Tiwari, A. (2013). An Investigation of the Combustion and Emission Characteristics of Compression Ignition Engines in Dual- Fuel Mode. *International Journal of Advance Research and Innovation*, 3(3), 98–106.
- Pal, A., & Tiwari, A. (2013). An investigation of the combustion and emission characteristics of compression ignition engines in dual-fuel mode.
- Papagiannakis, R. G., Rakopoulos, C. D., Hountalas, D. T., & Rakopoulos, D. C. (2010). Emission characteristics of high speed, dual fuel, compression ignition engine operating in a wide range of natural gas/diesel fuel proportions. *Fuel*, 89(7), 1397–1406.
- Paykani, A. (2011). Performance and Emission Characteristics of Dual Fuel Engines at Part Loads Using Simultaneous Effect of Exhaust Gas Recirculation and Pre-Heating of Inlet Air. *International Journal of Automotive Engineering*, 1(2), 53–67.

- Pirouzpanah, V., Khoshbakhti Saray, R., Sohrabi, A., & Niaei, A. (2007). Comparison of thermal and radical effects of EGR gases on combustion process in dual fuel engines at part loads. *Energy Conversion and Management*, 48(7), 1909–1918.
- Poonia, M. P., Bhardwaj, A., Jethoo, A. S., & Pandel, U. (2011). Experimental Investigations on Engine Performance and Exhaust Emissions in an LPG Diesel Dual Fuel Engine, 2(6), 2–6.
- Poonia, M. P., Ramesh, A., & Gaur, R. R. (1999). Experimental Investigation of the Factors Affecting the Performance of a LPG - Diesel Dual Fuel Engine. *SAE Technical Papers*, 1123(1), 12.
- Qi, D. H., Bian, Y. Z., Ma, Z. Y., Zhang, C. H., & Liu, S. Q. (2007). Combustion and exhaust emission characteristics of a compression ignition engine using liquefied petroleum gas–Diesel blended fuel. *Energy Conversion and Management*, 48(2), 500–509.
- Ramos da Costa, Y. J., Barbosa de Lima, A. G., Bezerra Filho, C. R., & de Araujo Lima, L. (2012). Energetic and exergetic analyses of a dual-fuel diesel engine. *Renewable and Sustainable Energy Reviews*, 16(7), 4651–4660.
- Rao, G. A., Raju, A. V. S., Rajulu, K. G., & Rao, C. V. M. (2010). Performance Evaluation of a Dual Fuel Engine (Diesel + LPG). *Indian Journal of Science and Technology*, 3(3), 235–237.
- Rao, G., Raju, A., Rao, C., & Rajulu, K. (2011). Effect of LPG Content on the Performance and Emissions of A Diesel-LPG Dual-Fuel Engine. *Bangladesh Journal of Scientific and Industrial Research*, 46(2), 195–200.
- Raslavičius, L., Keršys, A., Mockus, S., Keršienė, N., & Starevičius, M. (2014). Liquefied petroleum gas (LPG) as a medium-term option in the transition to sustainable fuels and transport. *Renewable and Sustainable Energy Reviews*, 32, 513–525.
- Rosha, P., Bharj, R. S., & Gill, K. J. S. (2014). Performance and emission characteristics of Diesel + LPG dual fuel engine with exhaust gas recirculation, 3(10), 2570–2574.
- S Ganesan, A. R. (2002). Experimental investigations on a LPG-diesel dual fuel engine. *Journal of the Institution of Engineers(India), Part MC, Mechanical Engineering Division*, 83(3), 105–111.
- Sahoo, B. B., Sahoo, N., & Saha, U. K. (2009). Effect of engine parameters and type of gaseous fuel on the performance of dual-fuel gas diesel engines—A critical review. *Renewable and Sustainable Energy Reviews*, 13(6), 1151–1184.
- Saleh, H. E. (2008). Effect of variation in LPG composition on emissions and performance in a dual fuel diesel engine. *Fuel*, 87(13), 3031–3039.
- Saravanan, N., & Nagarajan, G. (2008). An experimental investigation of hydrogen-enriched air induction in a diesel engine system. *International Journal of Hydrogen Energy*, 33(6), 1769–1775.



- Saravanan, N., & Nagarajan, G. (2009). An insight on hydrogen fuel injection techniques with SCR system for NOX reduction in a hydrogen–diesel dual fuel engine. *International Journal of Hydrogen Energy*, *34*(21), 9019–9032.
- Saravanan, N., & Nagarajan, G. (2010). Performance and emission studies on port injection of hydrogen with varied flow rates with Diesel as an ignition source. *Applied Energy*, *87*(7), 2218–2229.
- Saravanan, N., Nagarajan, G., & Narayanasamy, S. (2008). An experimental investigation on DI diesel engine with hydrogen fuel. *Renewable Energy*, *33*(3), 415–421.
- Saravanan, N., Nagarajan, G., Sanjay, G., Dhanasekaran, C., & Kalaiselvan, K. M. (2008). Combustion analysis on a DI diesel engine with hydrogen in dual fuel mode. *Fuel*, *87*(17), 3591–3599.
- Selim, M. Y. E., Al-Omari, S. B., & Al-Aseery, A. A. J. (2009). Effects of Steam Injection to Dual Fuel Engine on Performance, Noise and Exhaust Emission.
- Sh Yasiry, A., & Shahad, H. A. (2016). An experimental study of the effect of hydrogen blending on burning velocity of LPG at elevated pressure. *International Journal of Hydrogen Energy*, *41*(42), 19269–19277.
- Shojaeefard, M., & N. (2008). Flow simulation in engine cylinder with spring mesh. *American Journal of Applied Sciences*, *1336–1343*, 5(10).
- Sjöberg, M., & Dec, J. E. (2005). An investigation into lowest acceptable combustion temperatures for hydrocarbon fuels in HCCI engines. *Proceedings of the Combustion Institute*, *30*(2), 2719–2726.
- Soni, D. K., & Gupta, R. (2016). Optimization of methanol powered diesel engine: A CFD approach. *Applied Thermal Engineering*, *106*, 390–398.
- Sproat, R., Hassan, A. M., Waldie, A., Jay, G., & Holland, D. (2006). The Risk Posed to Vehicle Occupants and Rescue Personnel by Dual-Fuelled Vehicles Fitted with Liquid Petroleum Gas (LPG) Tanks. *SAE Technical Papers*, *1274*(1), 9.
- Stavinoha, L. L., Alfaro, E. S., Dobbs, H. H., Villahermosa, L. A., & Heywood, J. B. (2000). Alternative Fuels: Gas to Liquids as Potential 21st Century Truck Fuels. *SAE Technical Papers*, *3422*(1), 18.
- Stewart, J., Clarke, A., & Chen, R. (2007). An experimental study of the dual-fuel performance of a small compression ignition diesel engine operating with three gaseous fuels. *Proceedings of the Institution of Mechanical Engineers, Part D: Journal of Automobile Engineering*, *221*(8), 943–956.
- Stone, R. (1999). *Solutions Manual for Introduction to Internal Combustion Engines*. London: Macmillan Education UK.
- Surawski, N. C., Miljevic, B., Bodisco, T. A., Situ, R., Brown, R. J., & Ristovski, Z. D. (2014). Performance and gaseous and particle emissions from a liquefied petroleum gas (LPG) fumigated compression ignition engine. *Fuel*, *133*, 17–25.

- Szwaja, S., & Grab-Rogalinski, K. (2009). Hydrogen combustion in a compression ignition diesel engine. *International Journal of Hydrogen Energy*, 34(10), 4413–4421.
- Thomas Renald, R. C., & Somasundaram, P. (2012). Experimental investigation on attenuation of emission with optimized LPG jet induction in a dual fuel diesel engine and prediction by ANN model. *Energy Procedia*, 14, 1427–1438.
- Ugurlyu, A., & Oztuna, S. (2015). A comparative analysis study of alternative energy sources for automobiles. *International Journal of Hydrogen Energy*, 40(34), 11178–11188.
- Verhelst, S., & Wallner, T. (2009). Hydrogen-fueled internal combustion engines. *Progress in Energy and Combustion Science*, 35(6), 490–527.
- Vijayabalan, P., & Nagarajan, G. (2009). Performance , Emission and Combustion of LPG Diesel Dual Fuel. *Jordan Journal of Mechanical and Industrial Engineering*, 3(2), 105–110.
- Wannatong, K., Akarapanyavit, N., Siengsanorh, S., & Chanchaona, S. (2007). Combustion and Knock Characteristics of Natural Gas Diesel Dual Fuel Engine. *SAE Technical Paper*, 1, 1894–1899.
- Wattanavichien, K. (2011). Spray and Combustion Visualization of LPG-PME Dual Fuelling an IDI Compression Ignition Engine. In *3rd Regional Conference on Mechanical and Aerospace Technology* (p. 15).
- Xu, G.-L., Yao, C.-D., & Rutland, C. J. (2014). Simulations of diesel-methanol dual-fuel engine combustion with large eddy simulation and Reynolds-averaged Navier-Stokes model. *International Journal of Engine Research*, 15(6), 751–769.
- Xu, J., Zhang, X., Liu, J., & Fan, L. (2010). Experimental study of a single-cylinder engine fueled with natural gas–hydrogen mixtures. *International Journal of Hydrogen Energy*, 35(7), 2909–2914.
- Yamık, H. (2002). Dizel Motorlarda Alternatif Yakıt Olarak Yağ Esterlerinin Kullanılma İmkanlarının Araştırılması.". *Doktora Tezi, Gazi Üniversitesi Fen Bilimleri Enstitüsü, Ankara*, 71–90.
- Yang, Z., Chu, C., Wang, L., & Huang, Y. (2015). Effects of H<sub>2</sub> addition on combustion and exhaust emissions in a diesel engine. *Fuel*, 139, 190–197.
- Yap, D., Peucheret, S. M., Megaritis, A., Wyszynski, M. L., & Xu, H. (2006). Natural gas HCCI engine operation with exhaust gas fuel reforming. *International Journal of Hydrogen Energy*, 31(5), 587–595.
- Zhen, H. S., Cheung, C. S., Leung, C. W., & Choy, Y. S. (2012). Effects of hydrogen concentration on the emission and heat transfer of a premixed LPG-hydrogen flame. *International Journal of Hydrogen Energy*, 37(7), 6097–6105.
- Zhou, J. H., Cheung, C. S., & Leung, C. W. (2014). Combustion, performance and emissions of a diesel engine with H<sub>2</sub>, CH<sub>4</sub> and H<sub>2</sub>–CH<sub>4</sub> addition. *International Journal of Hydrogen Energy*, 39(9), 4611–4621.

Zhu, L., Cheung, C. S., Zhang, W. G., & Huang, Z. (2010). Emissions characteristics of a diesel engine operating on biodiesel and biodiesel blended with ethanol and methanol. *Science of the Total Environment*, 408(4), 914–921.

## **APPENDICES**

## APPENDIX A

**Table A.1-Gaseous Fuel Properties**

	LPG	90L-10H	50L-50H	60L-40H	Hydrogen
Density/(kg/m <sup>3</sup> )	1.882	1.7022	0.9829	1.1627	0.0837
LHV/(MJ/kg)	46.3	53.663	83.115	75.752	119.93
Stoichiometric AFR/(kg/kg)	15.8	17.659	25.095	23.236	34.39
Flammability limits/(Vol.% in air)	2.1-10.1	---	---	---	4.0-75.0
Boiling point (°C)	-42.1	---	---	---	-252.8
Latent heat of vaporization at 15.6 °C (kJ/kg)	358.2				454.3
Laminar burning velocity/(m/s)	0.45	---	---	---	2.8
Auto ignition temperature/(K)	768	---	---	---	858

## APPENDIX B

### MASS FRACTION OF INPUT GASEOUS

#### Mass Fraction of LPG, H<sub>2</sub>, O<sub>2</sub>, and N<sub>2</sub>

Ratio of gaseous blend		Mass fraction of LPG%	Mass fraction of H <sub>2</sub> %	Mass flow rate of diesel fuel	Mass fraction of O <sub>2</sub> %	Mass fraction of N <sub>2</sub> %
<b>Diesel-H<sub>2</sub></b>	1.2	0.0	1.1082	0.0	22.75	76.146
	1.6	0.0	0.8335	0.0	22.8	76.369
	2	0.0	0.668	0.0	22.8455	76.485
	2.4	0.0	0.5572	0.0	22.872	76.571
<b>Diesel-LPG</b>	1.2	3.58	0.0	0.0	22.2	74.24
	1.6	2.7079	0.0	0.0	22.37	74.898
	2	2.178	0.0	0.0	22.4998	75.323
	2.4	1.8217	0.0	0.0	22.581	75.5973
<b>Diesel+90L+10H</b>	1.2	2.86	0.3183	0.0	22.68	74.55
	1.6	2.165	0.241	0.0	22.446	75.15
	2	1.74069	0.19340965	0.0	22.5552	75.5106
	2.4	1.45526	0.1616959	0.0	22.628099	75.755
<b>Diesel+60L+40H</b>	1.2	1.432	0.955	0.0	22.45	75.2
	1.6	1.08	0.72	0.0	22.6	75.6
	2	0.0869	0.57923	0.0	22.6669	75.88486
	2.4	0.7259267	0.483859	0.0	22.7217548	76.06846
<b>Diesel+50L+50H</b>	1.2	1.1037	1.1037	0.0	22.5	75.3
	1.6	0.83	0.83	0.0	22.64	75.7
	2	0.6682	0.6682	0.0	22.693	75.971
	2.4	0.55804	0.55804	0.0	22.743	76.141
<b>Diesel kg/hr.</b>	1.2	0.0	0.0	1.11	23.2	76.8
	1.6	0.0	0.0	0.8325333	23.2	76.8
	2	0.0	0.0	0.6660266	23.2	76.8
	2.4	0.0	0.0	0.5550223	23.2	76.8

## **BIODATA OF STUDENT**

Radhwan Ali Abd Alreda was born in Maysan, Iraq on 4 September 1987. He completed his primary and secondary school in Maysan then al Thawra was the high school for him. The period of study was from 1993-1994 until 2004-2005, respectively.

He started his B.Sc. Degree in Automotive Technologies Engineering of Baghdad Technical College in 2006 and graduated in 2009.

In 22<sup>th</sup> Jun 2014, he traveled to Malaysia and joined ELS Institute in UPM for six months. Then he obtained permeation to continue his study in Master of since in Mechanical Engineering at Universiti Putra Malaysia on February 2015.

## **LIST OF PUBLICATIONS**

Radhwan Ali, Nuraini Abdul Aziz, and Abdul Aziz Hairuddin. A Review of effect the LPG fuels addition on the emissions and performance in compression ignition engine accepted in the Journal of Engineering and Applied Sciences.

Radhwan Ali, Nuraini Abdul Aziz, and Abdul Aziz Hairuddin. Numerical simulation of effect the mixing LPG, hydrogen, and diesel fuel on combustion characteristic and emission in compression-ignition engine submitted to the Fuel journal / Elsevier.